Return to Royce Lummus

C 2

RM L7B17 C 2

RESEARCH MEMORANDUM

WIND-TUNNEL DEVELOPMENT OF OPTIMUM DOUBLE-SLOTTED-FLAP CONFIGURATIONS FOR SEVEN THIN NACA AIRFOIL SECTIONS

By

Jones F. Cahill and Stanley F. Racisz

Langley Memorial Aeronautical Laboratory
Langley Field, Va.

RM L7B17

NATIONAL ADVISORY COMMITTEE
FOR AERONAUTICS
WASHINGTON
April 28, 1947

NATIONAL ADVISORY COMMITTEE FOR AEROANUTICS

RESEARCH MEMORANDUM

WIND-TUNNEL DEVELOPMENT OF OPTIMUM DOUBLE-SLOTTED-FLAP CONFIGURATIONS FOR SEVEN THIN NACA AIRFOIL SECTIONS

By Jones F. Cahill and Stanley F. Racisz

SUMMARY

An investigation has been made in the Langley two-dimensional low-turbulence tunnels to develop optimum double-slotted-flap configurations for seven thin NACA airfoil sections. The airfoils tested were the NACA 63-210, 64-208, 64-210, 64_1-212, 65-210, 66-210, and 1410 airfoil sections. Each of the airfoil sections tested was equipped with a flap of 0.25 chord and a fore flap of 0.075 chord. In addition, the NACA 66-210 and the NACA 64-208 airfoil sections were also tested with a 0.100-chord and a 0.056-chord fore flap, respectively. Lift measurements were made at a Reynolds number of 2.4×10^6 to obtain the configuration giving the highest maximum section lift coefficient for each of the airfoil sections tested. The lift characteristics were measured for Reynolds numbers up to 9.0×10^6 in order to obtain an indication of the scale effects. The section pitching-moment characteristics and the effect of leading-edge roughness on the lift characteristics were measured for the best double-slotted-flap configuration for each of the airfoil sections at a Reynolds number of 6.0×10^6.

The best fore-flap locations were generally found to be about 1-percent chord forward and about 2-percent chord below the slot lip. The best flap positions varied considerably. The deflections for which the highest maximum lift coefficients were measured were about 50° to 55° for the flap and about 25° to 30° for the fore flap.

The maximum section lift coefficient of the airfoil section with either a split or double slotted flap decreased as the position of minimum pressure was moved to the rear or as the airfoil thickness was decreased to 0.08 chord. In all cases, the maximum section lift coefficient increased as the Reynolds number was increased from 2.4×10^6 to 6.0×10^6 but generally decreased or remained constant as the Reynolds number was increased from 6.0×10^6 to 9.0×10^6. Increasing the fore-flap chord provided increases in the maximum section lift coefficients of both the NACA 64-208 and the NACA 66-210 airfoil sections with double slotted flaps. The addition of standard

roughness to the leading edges of the airfoils equipped with double slotted flaps generally decreased the maximum section lift coefficient by amounts slightly less than those obtained with the flaps retracted, decreased the variation of the maximum section lift coefficient with position of minimum pressure and with airfoil thickness, and caused the stall to be less abrupt than that for the smooth condition. The ratio of increment of section pitching-moment coefficient to increment of section lift coefficient at a section angle of attack of 0° $\left(\frac{\Delta c_m}{\Delta c_l}\right)_{\alpha_0=0^\circ}$ based on the total chord of the airfoil with the double slotted flap extended was approximately the same as that obtained for the airfoil with the split flap. An unstable pitching-moment break is encountered at the stall for each of the airfoils when equipped with the double slotted flaps and seems to be peculiar to double slotted flaps.

INTRODUCTION

The use of thin wing sections to increase the critical speeds of high-speed, highly loaded airplanes has been accompanied by the need for suitable high-lift devices to be used for take-off and landing. An investigation has been made in the Langley two-dimensional low-turbulence tunnels to develop high-lift trailing-edge flaps suitable for use on thin wing sections that are most likely to be used on high-speed aircraft. The first part of this investigation, reported in reference 1, covered the development of four types of flap for the NACA 65-210 airfoil section. The double slotted flap, discussed in reference 1, gave maximum lift coefficients higher than any one of the three single slotted flaps tested. The second part of this investigation, reported herein, covers the development of similar double-slotted-flap configurations for six other thin NACA airfoil sections. Data from reference 1 on the NACA 65-210 airfoil section with a double slotted flap have been included to complete the comparison of the results obtained.

The seven thin NACA airfoil sections tested with double slotted flaps in the Langley two-dimensional low-turbulence tunnels are as follows: NACA 63-210, 64-208, 64-210, 64_1-212, 65-210, 66-210, and 1410 airfoil sections. Profiles of the plain airfoil sections are shown in figure 1.

The best maximum lift configurations were developed at a Reynolds number of 2.4×10^6 for each of the double slotted flaps which consisted of a 0.250-chord main flap and a 0.075-chord fore flap.

The section lift and pitching-moment characteristics were then measured at higher Reynolds numbers up to 9.0×10^6 for configurations that not only approximated the best maximum lift configurations but that also allowed the flap and fore flap to retract as a unit within the airfoil contour. The effects of leading-edge roughness on the section lift characteristics were determined at a Reynolds number of 6.0×10^6.

Data on the lift and pitching-moment characteristics of these airfoil sections equipped with 0.20-chord split flaps deflected 60° are included to show a comparison between the effects of the two types of flap.

SYMBOLS

α_o	section angle of attack, degrees
c	airfoil chord with flap retracted
c_l	section lift coefficient
$c_{l_{max}}$	maximum section lift coefficient
$c_{m_{c/4}}$	section pitching-moment coefficient about quarter-chord point
δ_f	flap deflection measured between flap chord line and its position when retracted, degrees
δ_{ff}	fore-flap deflection measured between fore-flap chord line and airfoil chord line, degrees
x/c	distance along airfoil chord line, fraction of c
t/c	airfoil thickness, fraction of c
x_1, y_1	horizontal and vertical positions, respectively, of the fore-flap reference point measured from trailing edge of slot lip, percent c, positive forward and down, respectively, (fig. 2)
x_2, y_2	horizontal and vertical positions, respectively, of flap reference point measured from trailing edge of fore flap, percent c, positive forward and down, respectively, (fig. 2)

R Reynolds number

Δc_m increment of section pitching-moment coefficient

Δc_l increment of section lift coefficient

MODELS

Each of the models tested had a chord of 24 inches and completely spanned the 3-foot-wide test sections of the two tunnels. The main part of each model ahead of the flap was constructed of laminated mahogany, and the flaps were constructed of steel. A typical airfoil and double slotted flap, including the essential dimensions, is shown in figure 2. Ordinates for the plain airfoil sections are given in tables 1 to 7.

Each of the main flaps was of 0.250 chord and was developed by scaling the ordinates of the main flap tested on the NACA 65-210 airfoil section (reference 1) in proportion to the airfoil thickness at each station along the chord. Ordinates of the flaps tested are given in tables 8 to 14. Each of the flaps was tested in combination with the 0.075c fore flap used in reference 1. In addition, the NACA 64-208 airfoil was tested with a 0.056c fore flap and the NACA 66-210 airfoil was tested with a 0.100c fore flap. Sketches of the three fore flaps are presented as figure 3, and their ordinates are given in tables 15 to 17. The flaps and fore flaps were attached to the main portions of the models at the ends in such a manner that they could be set at any desired positions and deflections. The flap and fore-flap positions were measured from their reference points, which are defined as the intersection of their chord lines with their leading edges. (See fig. 2.)

For tests of each model in the smooth condition, the model was sanded with no. 400 carborundum paper to produce aerodynamically smooth surfaces. For tests of the airfoil with leading-edge roughness, the surfaces were the same as for the smooth condition except that 0.011-inch carborundum grains were applied over a surface length of 0.16 chord centered at the chord line. This leading-edge-roughness condition corresponds to the standard roughness described in reference 2.

APPARATUS AND TESTS

The investigation was made in the Langley two-dimensional low-turbulence tunnel (LTT) and the Langley two-dimensional low-turbulence pressure tunnel (TDT).

IDEAL & OPTIMUM POSITIONS

Section lift characteristics were obtained from static pressure measurements along the floor and ceiling of the tunnel test section, and section pitching-moment characteristics were determined from deflections of a torque tube. Details of the test methods and the methods used in correcting the data to free-air conditions are given in reference 2.

Lift measurements were made at a Reynolds number of 2.4×10^6 in the LTT to obtain the ideal configurations. The ideal configurations (those giving the highest maximum lift coefficients) were determined by first determining the ideal position of the flap relative to the fore flap for several combinations of flap and fore-flap deflections. The configuration giving the highest maximum lift was, if necessary, altered slightly to allow the flap and fore flap to be retracted as a unit within the wing contour. With the position of the flap thus fixed relative to the fore flap, lift measurements were made to obtain the best position of the flap and fore-flap combination. This resulting position is called the optimum position. The optimum positions developed in the LTT at each of several deflections were then tested in the TDT at a Reynolds number of 6.0×10^6. For the configuration giving the highest maximum lift coefficient at a Reynolds number of 6.0×10^6, pitching-moment characteristics and the effect of leading-edge roughness on the lift characteristics were also determined at a Reynolds number of 6.0×10^6, and the lift characteristics were determined at Reynolds numbers of 3.0×10^6 and 9.0×10^6. The maximum free-stream Mach number attained during any of these tests was less than 0.18.

PRESENTATION OF RESULTS

The data obtained for the airfoil section with a double slotted flap at a Reynolds number of 2.4×10^6 are presented as contours of maximum lift coefficient for various flap and fore-flap positions. These data indicate the maximum section lift coefficient that may be obtained for a given flap location and deflection,or the loss in maximum section lift coefficient that may result if flap locations other than the ideal are selected.

The lift characteristics at a Reynolds number of 6.0×10^6 are presented for several of the more promising double-slotted-flap configurations for each airfoil section. The section pitching-moment characteristics for the smooth condition and also the lift characteristics for the condition with leading-edge roughness are presented for the configuration having the highest maximum lift coefficient at a Reynolds number of 6.0×10^6. Additional data are presented showing the lift and pitching-moment characteristics of the plain airfoil section at several Reynolds numbers and the lift and pitching-moment characteristics at a Reynolds number of 6.0×10^6 for the airfoil section with a 0.20-chord split flap deflected 60°. The data for the plain airfoil section and the airfoil with a split flap were obtained from reference 2. In some cases, data for the airfoil section with a split flap were available for several additional Reynolds numbers and are also included.

The figures in which the data are presented for each of the airfoil sections tested are listed in the following table:

Airfoil section / Data	63-210	64-208	64-210	65-210	66-210	1410	64_1-212
	Figure						
Plain airfoil and split flaps	4	8	13	19	20	27	31
Contours of flap location for $c_{l_{max}}$	5	9	14	17	21 [b]24	28	32
Contours of fore-flap location for $c_{l_{max}}$	6	10	15	18	22 [b]25	29	33
Characteristics for optimum configuration	7	11 [a]12	16	19	23 [b]26	30	34

[a]0.056c fore flap.

[b]0.100c fore flap.

DISCUSSION

Maximum Lift

Effect of flap and fore-flap location.- The variation of the section lift characteristics of the flapped airfoil section as the flap location varies is primarily a result of changes in the slot shapes. A secondary effect, resulting from the change in airfoil chord as the flap is moved chordwise, also exists; but within the range of positions for these tests, this effect is small. The ideal configurations are therefore the ones for which the best slot shapes are formed at the flap and fore-flap leading edges. The data shown on the contours of flap and fore-flap location indicate that the ideal flap and fore-flap configuration for maximum lift is one that forms converging nozzles and directs the air flow downward over both the flap and fore flap.

For most of the ideal configurations with the 0.075c fore flap, the fore flap was located approximately 1-percent c forward of the slot lip and approximately 2-percent c below the slot lip. For the NACA 63-210 airfoil section, however, (fig. 6) the ideal fore-flap location was approximately 1-percent c farther forward than the average. Although the best position of the fore flap for the NACA 64_1-212 airfoil is actually behind the slot lip (fig. 33) there is little difference between the maximum lift coefficients obtained at the ideal position and at the position corresponding to the average of the others. The flap locations for the ideal configurations varied considerably for each of the airfoil and flap combinations tested, as would probably be expected inasmuch as each airfoil section was tested with the flap designed for that airfoil. An indication of the ideal double-slotted-flap configurations for airfoils and flaps similar to those tested in this investigation may be obtained from the contours of flap location. These configurations, however, should not be applied to airfoil-flap combinations having shapes radically different from those tested. In addition, an indication of the loss in maximum section lift coefficient which may be caused by structural deflections of the flap or by construction errors may be obtained from the contours. For example, in the case of the NACA 63-210 airfoil section (fig. 5(a)), a departure of 0.01c from the ideal flap location can decrease the maximum section lift coefficient by as much as 0.3. For most of the optimum configurations, the flap deflection was 50° or 55° and the fore-flap deflection was 25° or 30°, although there was little difference in the maximum lift coefficients measured for these deflections. Increasing the deflection of the fore-flap aids both in forming a converging slot and in directing the air flow downward over the flap. A limit is reached in these effects, however, when the fore-flap deflection becomes high enough to cause the flow over the upper surface of the fore flap itself to separate. The use of the optimum flap positions rather than the ideal positions in the tests which followed resulted in a maximum decrease in the maximum lift coefficient of 0.07.

Effect of fore-flap chord.- The data presented in figures 23 and 26 show that increasing the fore-flap chord from 0.075c to 0.100c increased the maximum section lift coefficient of the NACA 66-210 airfoil section by approximately 0.1 at a Reynolds number of 6.0×10^6. A comparison of the data presented in figures 11 and 12 indicates that decreasing the fore-flap chord from 0.075c to 0.056c results in a slight decrease in the maximum section lift coefficient of the NACA 64-208 airfoil section with a double slotted flap. The data presented in reference 3 also show that increasing the fore-flap chord may be beneficial in increasing the maximum section lift coefficient. The increase in maximum section lift coefficient obtained by the use of larger fore flaps may be attributed to a combination of the increased area of the lifting surface and better slot shapes.

Effect of position of minimum pressure.- The variation of $c_{l_{max}}$ with the position of minimum pressure for several NACA 6-series airfoils of 10-percent thickness is presented in figure 35 for a Reynolds number of 6.0×10^6. Data presented in reference 2 indicate that for airfoil sections of thicknesses less than about 0.12c, the stall usually begins at the leading edge. Since the leading-edge radii of NACA 6-series airfoils decrease as the position of minimum pressure moves to the rear, this type of stall becomes more pronounced. The decrease in maximum lift coefficient with rearward movement of the position of minimum pressure, shown on figure 35, is therefore probably caused principally by the decrease in leading-edge radius. It is expected that for thicker airfoil sections, where the stall begins over some rear portion of the airfoil instead of near the leading edge, the decrease in the leading-edge radius with rearward movement of the position of minimum pressure would have a smaller effect on the maximum section lift coefficient. The increment in section lift coefficient caused by the addition of the double slotted flap to the NACA 6-series plain airfoil section having a maximum thickness of 10-percent c remained substantially constant (approx. 1.4) over the range of minimum pressure positions tested.

Effect of airfoil thickness.- The variation of maximum lift coefficient with airfoil thickness for the three NACA 64-series airfoils tested is shown in figure 35. The data in figure 35 show that for airfoil thicknesses between 0.12c and 0.08c the maximum lift coefficients of the plain airfoils and the airfoils with both split and double slotted flaps decrease as the airfoil thickness is decreased, although not all in the same manner. The increment of maximum lift coefficient caused by the double slotted flap decreases at a nearly constant rate as the thickness is decreased, while the increment in maximum lift coefficient caused by the split flap decreases as the thickness is decreased from 0.12c to 0.10c and then increases again as the thickness is further decreased to 0.08c.

Data in reference 2 have shown that the maximum lift coefficients of most airfoil sections decrease as the airfoil thickness is increased above about 0.12c although the maximum lifts of these same airfoils when equipped with split flaps continue to increase up to a thickness as high as 0.16c or 0.18c. Previous scattered data have shown that the maximum lift coefficients of airfoil sections equipped with double slotted flaps follow the same general trend. The data in figure 35 extend these previous results down to a thickness of 0.08c.

The maximum lift coefficient of the NACA 1410 airfoil, also shown in figure 35, is approximately the same as the maximum lift coefficient for the NACA 64_1-212 airfoil section.

Reynolds number effect.- The variation of maximum section lift coefficient with Reynolds number is shown in figure 36. In all cases, increasing the Reynolds number from 2.4×10^6 to 6.0×10^6 resulted in large increases in the maximum section lift coefficients. However, increasing the Reynolds number from 6.0×10^6 to 9.0×10^6 caused slight decreases or no change in the maximum lift coefficients of each of the airfoil sections except the NACA 64-210 section. Figure 11 indicates that the NACA 64-208 section followed the same trend as the NACA 64-210 section.

An explanation of scale effect on the maximum lift of airfoil sections is given in reference 4, and this explanation is usually applicable to airfoils with flaps. Generally, variations of the lift with Reynolds number are apparent only in regions of incipient stall (high angles of attack), but for these thin airfoil sections with double slotted flaps the lift decreases with increase in Reynolds number in the linear portion of the lift curve (low angles of attack). This decrease in lift coefficient is probably caused by changes in the flow conditions through the slots as the Reynolds number is varied. It is, therefore, probable that a new ideal configuration could be developed at higher Reynolds numbers, and slightly higher maximum lifts might be obtained.

Effect of flap on angle of attack for maximum lift.- A comparison of the data for the plain airfoil sections and that for the airfoils with flaps deflected shows that the stall occurs at a considerably lower angle of attack when the flap is deflected. The deflection of a trailing-edge flap causes an incremental load distribution which consists of an incremental basic load distribution and an incremental additional load distribution. (See reference 5.) The decrease in the angle of attack at which the stall occurs is attributed to the fact that the additional load, which comprises a large part of the incremental load distribution, increases the adverse pressure gradient in the vicinity of the airfoil leading edge; and, therefore, the critical pressure gradient is attained at a lower angle of attack.

Effect of leading-edge roughness.- The addition of standard roughness to the leading edge of the airfoil decreased the maximum lift coefficients of all the airfoil configurations in such a way that there was only a slight variation of maximum lift coefficient with position of minimum pressure (fig. 35).

The maximum lift coefficients of the plain airfoil and the airfoil with either of the flaps in the rough condition, increased as the airfoil thickness was increased but not so rapidly as in the smooth condition. For the airfoil with either a split or a double slotted flap, the decrement in maximum section lift coefficient caused by leading-edge roughness was less than that obtained for the plain airfoil section with the exception of the NACA 1410 and the NACA 64_1-212 airfoils which gave slightly higher decrements with the double slotted flap deflected.

A comparison of the lift curves for the smooth condition with those for the condition with leading-edge roughness indicates that for thin airfoil sections, leading-edge roughness tends to give a less abrupt stall than that obtained for the smooth condition. This can be attributed to the manner in which the stall occurs. For a smooth thin airfoil section, the stall first occurs in the vicinity of the leading edge, whereas with leading-edge roughness the stall occurs over some rear portion of the airfoil and progresses forward.

Pitching Moments

Glauert has shown in reference 5 that for plain trailing-edge hinged flaps, the incremental pitching moment caused by the deflection of a flap is a linear function of the incremental lift coefficient. The rather meager data in figure 37 show that this is probably also true for airfoils with split or double slotted flaps. If the ratio $\left(\frac{\Delta c_m}{\Delta c_l}\right)_{\alpha_0=0^\circ}$ is calculated on the basis of the total chord of the model with the double slotted flap extended, reasonably good agreement is shown for the double slotted flap and the split flap on these airfoil sections. The total chord with the flap extended is equal to the sum of the flap chord and the distance from the airfoil leading edge to the flap leading edge.

For each of these airfoil sections equipped with the double slotted flap, an unstable break in the pitching-moment curve (decrease in negative pitching moment) occurs at the stall. This unstable break seems to be peculiar to the double slotted flaps since it occurs in no case for the plain airfoil or for the airfoil with the split flap. The actual cause of this phenomenon is not clear and an analysis of pressure-distribution data would be required to shown what flow changes determine the stability of the section at the stall.

CONCLUSIONS

Seven thin NACA airfoil sections equipped with double slotted flaps were tested in the Langley two-dimensional low-turbulence tunnels. The airfoils tested were the NACA 63-210, 64-208, 64-210, 64_1-212, 65-210, 66-210, and 1410 airfoil sections. Each airfoil was tested with a double slotted flap consisting of a 0.25-chord main flap and a 0.075-chord fore flap. In addition, the NACA 66-210 airfoil was tested with a 0.100-chord fore flap and the NACA 64-208 airfoil was tested with a 0.056-chord fore flap. The results of the tests provided the following conclusions:

1. The best fore-flap positions for these airfoils were generally about 1-percent chord forward and 2-percent chord below the slot lip. The best flap positions varied considerably. The deflections for which the highest maximum lift coefficients were measured were about 50° to 55° for the flap and about 25° to 30° for the fore flap.

2. For the airfoil section with either a split or double slotted flap, the maximum section lift coefficient decreased as the position of minimum pressure was moved to the rear and as the airfoil thickness was decreased to 0.08 chord.

3. In all cases, the maximum section lift coefficient increased appreciably as the Reynolds number was increased from 2.4×10^6 to 6.0×10^6 but generally decreased or remained constant as the Reynolds number was increased from 6.0×10^6 to 9.0×10^6.

4. Increasing the fore-flap chord provided increases in the maximum section lift coefficients of the NACA 64-208 and the NACA 66-210 airfoil sections with double slotted flaps.

5. The addition of standard roughness to the leading edge of the airfoils equipped with double slotted flaps (a) caused decrements in maximum lift coefficient that were generally slightly less than those with flaps retracted, (b) caused a decrease in the variation of maximum lift coefficient with position of minimum pressure or with airfoil thickness, and (c) caused the stalls to be less abrupt than those for the airfoil in the smooth condition.

6. The ratio of increment of section pitching-moment coefficient to increment of section lift coefficient at a section angle of attack of 0° $\left(\frac{\Delta c_m}{\Delta c_l}\right)_{\alpha_0=0^{\circ}}$ based on the total chord of the airfoil with the double slotted flap extended was approximately the same as that obtained for the airfoil with the split flap.

7. An unstable pitching-moment break is encountered at the stall for each of the airfoils when equipped with the double slotted flaps and seems to be peculiar to double slotted flaps.

Langley Memorial Aeronautical Laboratory
National Advisory Committee for Aeronautics
Langley Field, Va.

REFERENCES

1. Cahill, Jones F.: Two-Dimensional Wind-Tunnel Investigation of Four Types of High-Lift Flaps on an NACA 65-210 Airfoil Section. NACA TN No. 1191, 1947.

2. Abbott, Ira H., von Doenhoff, Albert E., and Stivers, Louis S. Jr.: Summary of Airfoil Data. NACA ACR No. L5C05, 1945.

3. Braslow, Albert L., and Loftin, Lawrence K., Jr.: Two-Dimensional Wind-Tunnel Investigation of an Approximately 14-Percent-Thick NACA 66-Series-Type Airfoil Section with a Double Slotted Flap. NACA TN No. 1110, 1946.

4. Jacobs, Eastman N., and Sherman, Albert: Airfoil Section Characteristics as Affected by Variations of the Reynolds Number. NACA Rep. No. 586, 1937.

5. Glauert, H.: Theoretical Relationships for an Aerofoil with Hinged Flap. R. & M. No. 1095, British A.R.C., 1927.

TABLE 1

ORDINATES FOR NACA 63-210 AIRFOIL

[Stations and ordinates given in percent airfoil chord]

Upper surface		Lower surface	
Station	Ordinate	Station	Ordinate
0	0	0	0
.430	.876	.570	-.776
.669	1.107	.831	-.967
1.162	1.379	1.338	-1.165
2.398	1.939	2.602	-1.567
4.886	2.755	5.114	-2.121
7.382	3.372	7.618	-2.524
9.882	3.877	10.118	-2.843
14.890	4.665	15.110	-3.319
19.902	5.240	20.098	-3.648
24.917	5.647	25.083	-3.857
29.933	5.910	30.067	-3.966
34.951	6.030	35.049	-3.970
39.968	6.009	40.032	-3.867
44.985	5.861	45.015	-3.671
50.000	5.599	50.000	-3.393
55.013	5.235	54.987	-3.045
60.024	4.786	59.976	-2.644
65.032	4.264	64.968	-2.204
70.036	3.684	69.964	-1.740
75.038	3.061	74.962	-1.271
80.036	2.414	79.964	-.822
85.030	1.761	84.970	-.415
90.021	1.121	89.979	-.087
95.010	.530	94.990	.102
100.000	0	100.000	0

L.E. radius: 0.770
Slope of radius through L.E.: 0.084

TABLE 2

ORDINATES FOR NACA 65-210 AIRFOIL

[Stations and ordinates given in percent airfoil chord]

Upper surface		Lower surface	
Station	Ordinate	Station	Ordinate
0	0	0	0
.435	.819	.565	-.719
.678	.999	.822	-.859
1.169	1.273	1.331	-1.059
2.408	1.757	2.592	-1.385
4.898	2.491	5.102	-1.859
7.394	3.069	7.606	-2.221
9.894	3.555	10.106	-2.521
14.899	4.338	15.101	-2.992
19.909	4.938	20.091	-3.346
24.921	5.397	25.079	-3.607
29.936	5.732	30.064	-3.788
34.951	5.954	35.049	-3.894
39.968	6.067	40.032	-3.925
44.984	6.058	45.016	-3.868
50.000	5.915	50.000	-3.709
55.014	5.625	54.986	-3.435
60.027	5.217	59.973	-3.075
65.036	4.712	64.964	-2.652
70.043	4.128	69.957	-2.184
75.045	3.479	74.955	-1.689
80.044	2.783	79.956	-1.191
85.038	2.057	84.962	-.711
90.028	1.327	89.972	-.293
95.014	.622	94.986	.010
100.000	0	100.000	0

L.E. radius: 0.687
Slope of radius through L.E.: 0.084

TABLE 3

ORDINATES FOR NACA 66-210 AIRFOIL

[Stations and ordinates given in percent airfoil chord]

Upper surface		Lower surface	
Station	Ordinate	Station	Ordinate
0	0	0	0
.436	.806	.564	-.706
.679	.980	.821	-.840
1.171	1.245	1.329	-1.031
2.412	1.699	2.588	-1.327
4.902	2.401	5.098	-1.769
7.399	2.958	7.601	-2.110
9.898	3.432	10.102	-2.389
14.903	4.202	15.097	-2.856
19.912	4.796	20.088	-3.204
24.924	5.257	25.076	-3.467
29.937	5.608	30.063	-3.664
34.952	5.862	35.048	-3.802
39.968	6.024	40.032	-3.882
44.984	6.095	45.016	-3.905
50.000	6.074	50.000	-3.868
55.016	5.960	54.984	-3.770
60.030	5.736	59.970	-3.594
65.042	5.332	64.958	-3.272
70.051	4.759	69.949	-2.815
75.056	4.071	74.944	-2.281
80.055	3.289	79.945	-1.697
85.049	2.445	84.951	-1.099
90.037	1.570	89.963	-.536
95.019	.724	94.981	-.092
100.000	0	100.000	0

L.E. radius: 0.662
Slope of radius through L.E.: 0.084

TABLE 4

ORDINATES FOR NACA 1410 AIRFOIL

[Stations and ordinates given in percent airfoil chord]

Upper surface		Lower surface	
Station	Ordinate	Station	Ordinate
0	0	0	0
1.174	1.639	1.326	-1.515
2.398	2.297	2.602	-2.055
4.870	3.194	5.130	-2.726
7.358	3.837	7.642	-3.157
9.854	4.338	10.146	-3.462
14.861	5.062	15.139	-3.844
19.880	5.531	20.120	-4.031
24.907	5.809	25.093	-4.091
29.937	5.940	30.063	-4.064
40.000	5.836	40.000	-3.836
50.025	5.385	49.975	-3.439
60.042	4.692	59.958	-2.914
70.051	3.804	69.949	-2.304
80.049	2.741	79.951	-1.629
90.034	1.513	89.966	-.901
95.021	.832	94.979	-.512
100.000	.105	100.000	-.105

L.E. radius: 1.10
Slope of radius through L.E.: 0.05

NATIONAL ADVISORY COMMITTEE FOR AERONAUTICS

TABLE 5

ORDINATES FOR NACA 64-208 AIRFOIL

[Stations and ordinates given in percent airfoil chord]

Upper surface		Lower surface	
Station	Ordinate	Station	Ordinate
0	0	0	0
.445	.706	.555	-.606
.688	.862	.812	-.722
1.180	1.110	1.320	-.896
2.421	1.549	2.579	-1.177
4.912	2.189	5.088	-1.557
7.410	2.681	7.590	-1.833
9.909	3.089	10.091	-2.055
14.915	3.741	15.085	-2.395
19.924	4.232	20.076	-2.640
24.935	4.598	25.065	-2.808
29.948	4.856	30.052	-2.912
34.961	5.009	35.039	-2.949
39.974	5.063	40.026	-2.921
44.988	4.978	45.012	-2.788
50.000	4.787	50.000	-2.581
55.011	4.506	54.989	-2.316
60.020	4.152	59.980	-2.010
65.027	3.733	64.973	-1.673
70.031	3.263	69.969	-1.319
75.032	2.749	74.968	-.959
80.031	2.200	79.969	-.608
85.027	1.634	84.973	-.288
90.019	1.067	89.981	-.033
95.010	.522	94.990	.110
100.000	0	100.000	0

L.E. radius: 0.550
Slope of radius through L.E.: 0.084

TABLE 6

ORDINATES FOR NACA 64-210 AIRFOIL

[Stations and ordinates given in percent airfoil chord]

Upper surface		Lower surface	
Station	Ordinate	Station	Ordinate
0	0	0	0
.431	.867	.569	-.767
.673	1.056	.827	-.916
1.163	1.354	1.337	-1.140
2.401	1.884	2.599	-1.512
4.890	2.656	5.110	-2.024
7.387	3.248	7.613	-2.400
9.887	3.736	10.113	-2.702
14.894	4.514	15.106	-3.168
19.905	5.097	20.095	-3.505
24.919	5.533	25.081	-3.743
29.934	5.836	30.066	-3.892
34.951	6.010	35.049	-3.950
39.968	6.059	40.032	-3.917
44.985	5.938	45.015	-3.748
50.000	5.689	50.000	-3.483
55.014	5.333	54.987	-3.143
60.025	4.891	59.975	-2.749
65.033	4.375	64.967	-2.315
70.038	3.799	69.962	-1.855
75.040	3.176	74.960	-1.386
80.038	2.518	79.962	-.926
85.033	1.849	84.968	-.503
90.024	1.188	89.977	-.154
95.012	.564	94.988	.068
100.000	0	100.000	0

L.E. radius: 0.720
Slope of radius through L.E.: 0.084

TABLE 7

ORDINATES FOR NACA 64_1-212 AIRFOIL

[Stations and ordinates given in percent airfoil chord]

Upper surface		Lower surface	
Station	Ordinate	Station	Ordinate
0	0	0	0
.418	1.025	.582	-.925
.659	1.245	.841	-1.105
1.147	1.593	1.353	-1.379
2.382	2.218	2.618	-1.846
4.868	3.123	5.132	-2.491
7.364	3.815	7.636	-2.967
9.865	4.386	10.135	-3.352
14.872	5.291	15.128	-3.945
19.886	5.968	20.114	-4.376
24.903	6.470	25.097	-4.680
29.921	6.815	30.079	-4.871
34.941	7.008	35.059	-4.948
39.961	7.052	40.039	-4.910
44.982	6.893	45.018	-4.703
50.000	6.583	50.000	-4.377
55.016	6.151	54.984	-3.961
60.029	5.619	59.971	-3.477
65.039	5.004	64.961	-2.944
70.045	4.322	69.955	-2.378
75.047	3.590	74.953	-1.800
80.045	2.825	79.955	-1.233
85.038	2.054	84.962	-.708
90.027	1.303	89.973	-.269
95.013	.604	94.987	.028
100.000	0	100.000	0

L.E. radius: 1.040
Slope of radius through L.E.: 0.084

NATIONAL ADVISORY
COMMITTEE FOR AERONAUTICS

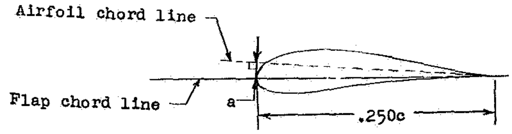

TABLE 8

FLAP ORDINATES FOR 63-210 AIRFOIL

[Stations and ordinates given from flap chord line in percent airfoil chord]

Upper surface		Lower surface	
Station	Ordinate	Station	Ordinate
0	0	0	0
.25	.74	.25	-.35
.50	.95	.50	-.50
1.00	1.24	1.00	-.68
2.00	1.60	2.00	-.83
3.00	1.78	2.50	-.83
4.00	1.88	3.00	-.79
5.00	1.95	6.00	-.56
6.00	1.99	9.00	-.35
7.00	1.99	12.00	-.15
8.00	1.98	15.00	.01
9.00	1.94	18.00	.11
10.00	1.86	21.00	.16
12.00	1.62	24.00	.06
15.00	1.21	25.00	0
18.00	.82		
21.00	.47		
24.00	.12		
25.00	0		

L.E. radius: 0.562
L.E. radius center: 0.201 above flap chord line
Dimension a: 0.200

TABLE 9

FLAP ORDINATES FOR 65-210 AIRFOIL

[Stations and ordinates given from flap chord line in percent airfoil chord]

Upper surface		Lower surface	
Station	Ordinate	Station	Ordinate
0	0	0	0
.28	.92	.28	-.41
.56	1.19	.56	-.62
1.12	1.56	1.12	-.88
1.69	1.83	1.69	-1.00
2.22	1.99	2.48	-1.03
3.38	2.22	4.98	-.83
4.50	2.33	7.48	-.63
5.61	2.38	9.98	-.44
7.00	2.40	12.48	-.27
9.00	2.35	14.98	-.12
11.00	2.16	17.48	.01
12.51	1.91	19.99	.10
15.01	1.50	22.49	.12
17.51	1.10	25.00	0
20.00	.711		
22.50	.341		
25.00	0		

L.E. radius: 0.800
L.E. radius center: 0.240 above flap chord line
Dimension a: 0.400

TABLE 10

FLAP ORDINATES FOR 66-210 AIRFOIL

[Stations and ordinates given from flap chord line in percent airfoil chord]

Upper surface		Lower surface	
Station	Ordinate	Station	Ordinate
0	0	0	0
.25	1.09	.25	-.50
.50	1.35	.50	-.75
1.00	1.76	1.00	-1.03
2.00	2.30	2.00	-1.27
3.00	2.65	2.50	-1.30
4.00	2.84	3.00	-1.26
5.00	2.95	6.00	-.98
6.00	3.00	9.00	-.72
7.00	3.02	12.00	-.46
8.00	3.00	15.00	-.21
9.00	2.94	18.00	-.02
10.00	2.85	21.00	.06
12.00	2.50	24.00	.04
15.00	1.85	25.00	0
18.00	1.25		
21.00	.71		
24.00	.18		
25.00	0		

L.E. radius: 1.207
L.E. radius center: 0.295 about flap chord line
Dimension a: 0.752

TABLE 11

FLAP ORDINATES FOR 1410 AIRFOIL

[Stations and ordinates given from flap chord line in percent airfoil chord]

Upper surface		Lower surface	
Station	Ordinate	Station	Ordinate
0	0	0	0
.25	.89	.25	-.38
.50	1.14	.50	-.62
1.00	1.48	1.00	-.92
2.00	1.93	2.00	-1.14
3.00	2.20	2.50	-1.15
4.00	2.36	3.00	-1.13
5.00	2.48	6.00	-1.01
6.00	2.55	9.00	-.88
7.00	2.59	12.00	-.77
8.00	2.58	15.00	-.63
9.00	2.56	18.00	-.47
10.00	2.50	21.00	-.30
12.00	2.27	24.00	-.14
15.00	1.81	25.00	-.11
18.00	1.33		
21.00	.80		
24.00	.28		
25.00	.11		

L.E. radius: 0.831
L.E. radius center: 0.249 above flap chord line
Dimension a: 0.700

NATIONAL ADVISORY COMMITTEE FOR AERONAUTICS

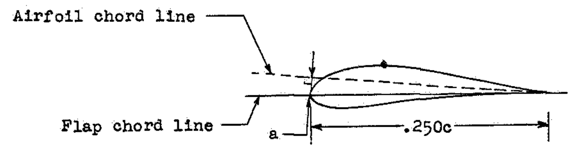

TABLE 12

FLAP ORDINATES FOR 64-208 AIRFOIL

[Stations and ordinates given from flap chord line in percent airfoil chord]

Upper surface		Lower surface	
Station	Ordinate	Station	Ordinate
0	0	0	0
.25	.65	.25	-.27
.50	.78	.50	-.42
1.00	1.06	1.00	-.58
2.00	1.37	2.00	-.71
3.00	1.54	2.50	-.73
4.00	1.67	3.00	-.69
5.00	1.73	6.00	-.48
6.00	1.75	9.00	-.29
7.00	1.75	12.00	-.14
8.00	1.73	15.00	0
9.00	1.70	18.00	.11
10.00	1.64	21.00	.12
12.00	1.45	24.00	.05
15.00	1.10	25.00	0
18.00	.75		
21.00	.43		
24.00	.13		
25.00	0		

L.E. radius: 0.411
L.E. radius center: 0.171 above flap chord line
Dimension a: 0.060

TABLE 13

FLAP ORDINATES FOR 64-210 AIRFOIL

[Stations and ordinates given from flap chord line in percent airfoil chord]

Upper surface		Lower surface	
Station	Ordinate	Station	Ordinate
0	0	0	0
.25	.78	.25	-.34
.50	1.01	.50	-.50
1.00	1.32	1.00	-.70
2.00	1.69	2.00	-.90
3.00	1.89	2.50	-.90
4.00	2.01	4.95	-.70
5.00	2.07	9.96	-.33
6.00	2.09	14.98	-.04
7.00	2.09	19.99	.13
9.00	2.05	25.00	0
11.00	1.88		
15.04	1.30		
20.02	.62		
25.00	0		

L.E. radius: 0.620
L.E. radius center: 0.170 above flap chord line
Dimension a: 0.288

TABLE 14

FLAP ORDINATES FOR 64_1-212 AIRFOIL

[Stations and ordinates given from flap chord line in percent airfoil chord]

Upper surface		Lower surface	
Station	Ordinate	Station	Ordinate
0	0	0	0
.25	.94	.25	-.44
.50	1.18	.50	-.63
1.00	1.53	1.00	-.85
2.00	1.97	2.00	-1.05
3.00	2.21	2.50	-1.03
4.00	2.35	3.00	-1.00
5.00	2.44	6.00	-.74
6.00	2.47	9.00	-.49
7.00	2.47	12.00	-.25
8.00	2.45	15.00	-.08
9.00	2.40	18.00	.09
10.00	2.31	21.00	.14
12.00	2.01	24.00	.05
15.00	1.52	25.00	0
18.00	1.02		
21.00	.58		
24.00	.14		
25.00	0		

L.E. radius: 0.870
L.E. radius center: 0.260 above flap chord line
Dimension a: 0.500

NATIONAL ADVISORY
COMMITTEE FOR AERONAUTICS

TABLE 15

ORDINATES FOR 0.056-CHORD FORE FLAP

[Stations and ordinates given from fore flap chord line in percent airfoil chord]

Station	Upper ordinate	Lower ordinate
0	0	0
.42	.82	----
.83	1.10	----
1.25	1.25	-.85
1.67	1.31	-.59
2.08	1.31	-.33
2.50	1.27	-.15
3.33	1.10	.10
3.75	.97	.16
4.17	.81	.19
4.58	.61	.18
5.00	.40	.13
5.42	.15	.05
5.625	0	0
L.E. radius: 0.90 (on chord line)		

TABLE 16

ORDINATES FOR 0.075-CHORD FORE FLAP

[Stations and ordinates given from fore flap chord line in percent airfoil chord]

Station	Upper ordinate	Lower ordinate
0	0	0
.42	.95	-.93
.83	1.31	-1.14
1.25	1.52	-1.20
1.67	1.62	-1.11
2.08	1.72	-.85
2.92	1.74	-.36
3.75	1.64	-.02
4.58	1.43	.18
5.42	1.13	.27
6.25	.75	.25
7.08	.28	.11
7.50	0	0
L.E. radius: 1.20 (on chord line)		

TABLE 17

ORDINATES FOR 0.100-CHORD FORE FLAP

[Stations and ordinates given from fore flap chord line in percent airfoil chord]

Station	Upper ordinate	Lower ordinate
0	0	0
.50	1.12	-----
1.00	1.53	-----
1.50	1.81	-----
2.00	2.01	-----
2.50	2.14	-1.10
3.00	2.21	-.71
4.00	2.24	-.15
5.00	2.14	.22
6.00	1.94	.44
7.00	1.60	.51
8.00	1.16	.45
9.00	.62	.27
10.00	0	0
L.E. radius: 1.50 (on chord line)		

NATIONAL ADVISORY COMMITTEE FOR AERONAUTICS

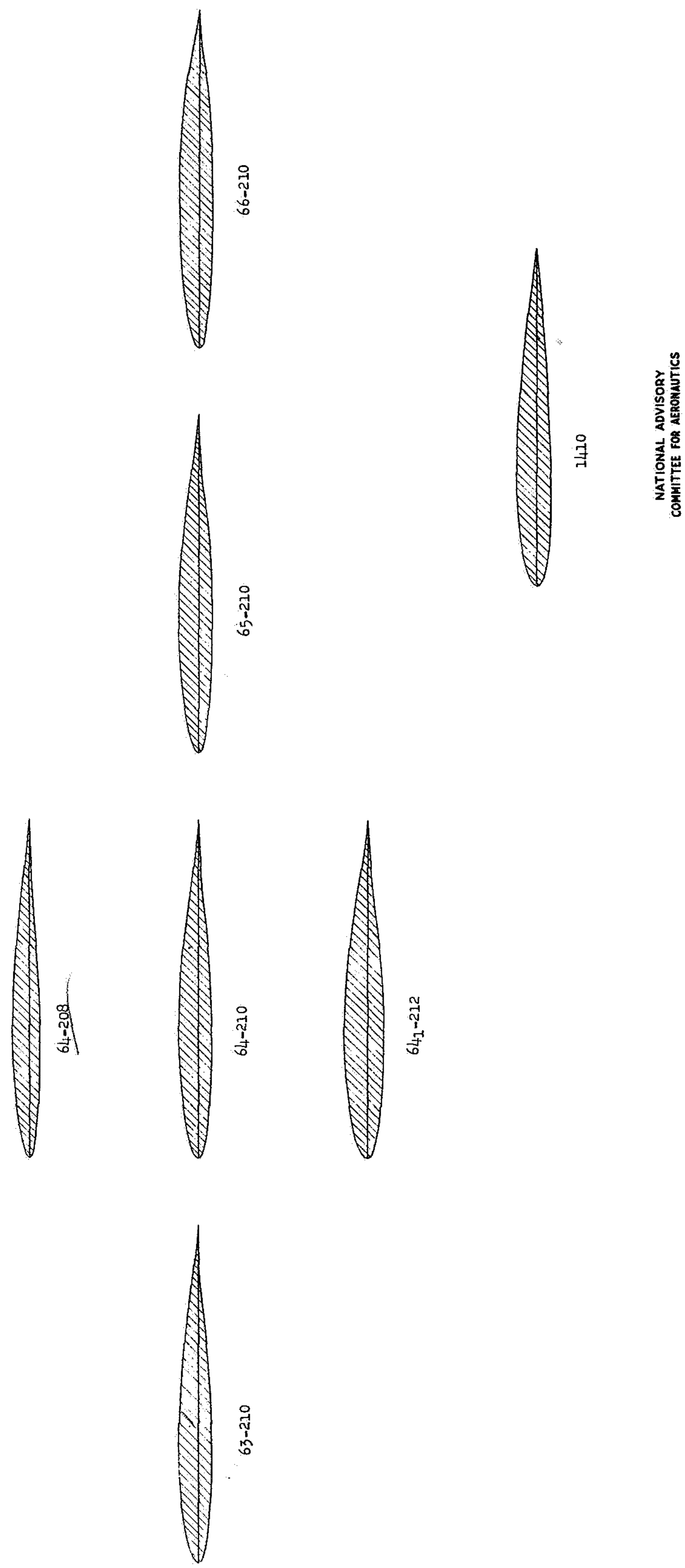

Figure 1.- Profiles of NACA airfoil sections tested with double slotted flaps.

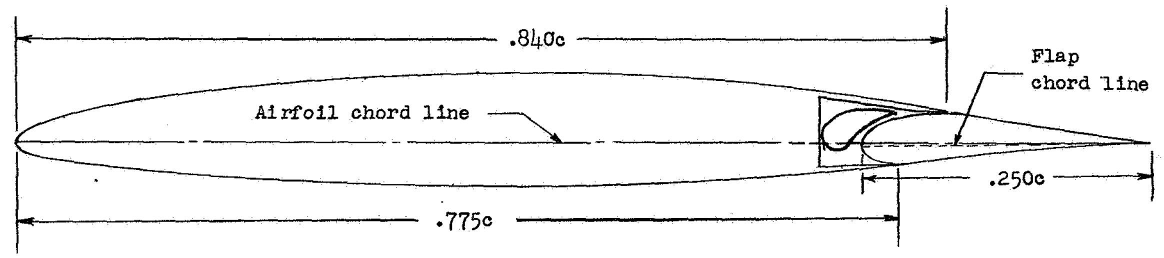

(a) Airfoil with flap.

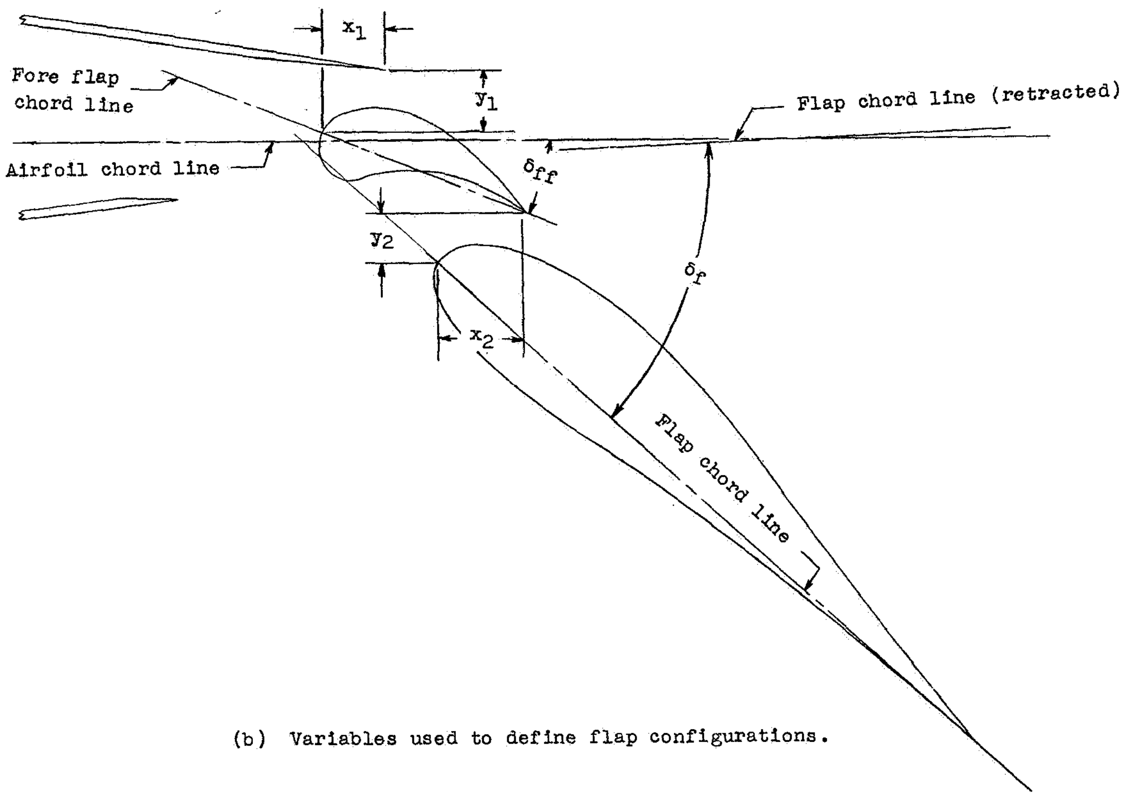

(b) Variables used to define flap configurations.

NATIONAL ADVISORY
COMMITTEE FOR AERONAUTICS

Figure 2 .- Typical airfoil and flap configuration.

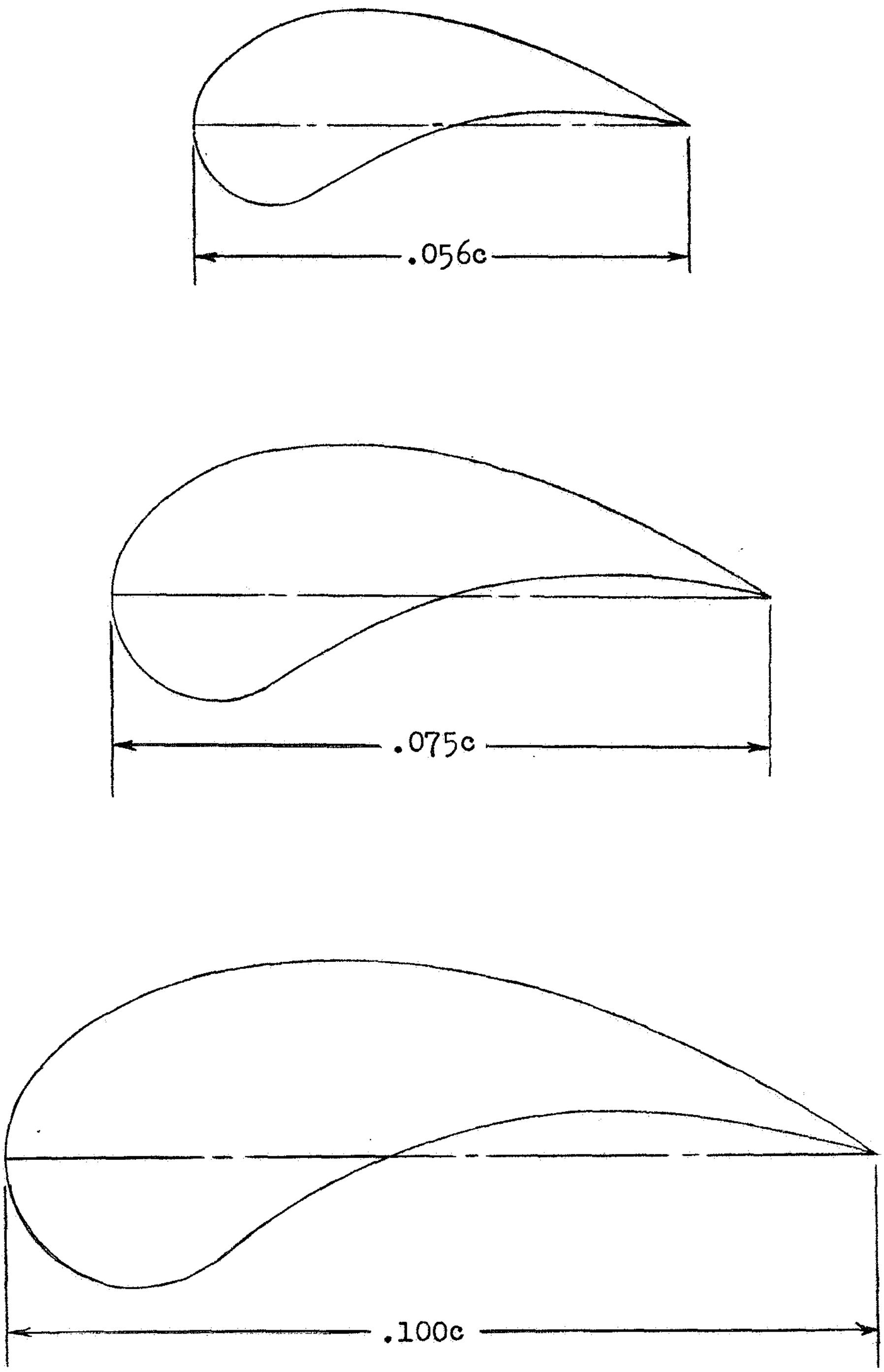

NATIONAL ADVISORY
COMMITTEE FOR AERONAUTICS

Figure 3 .- Profiles of the three fore flaps tested in combination with 0.250c slotted flaps.

NACA 63-210

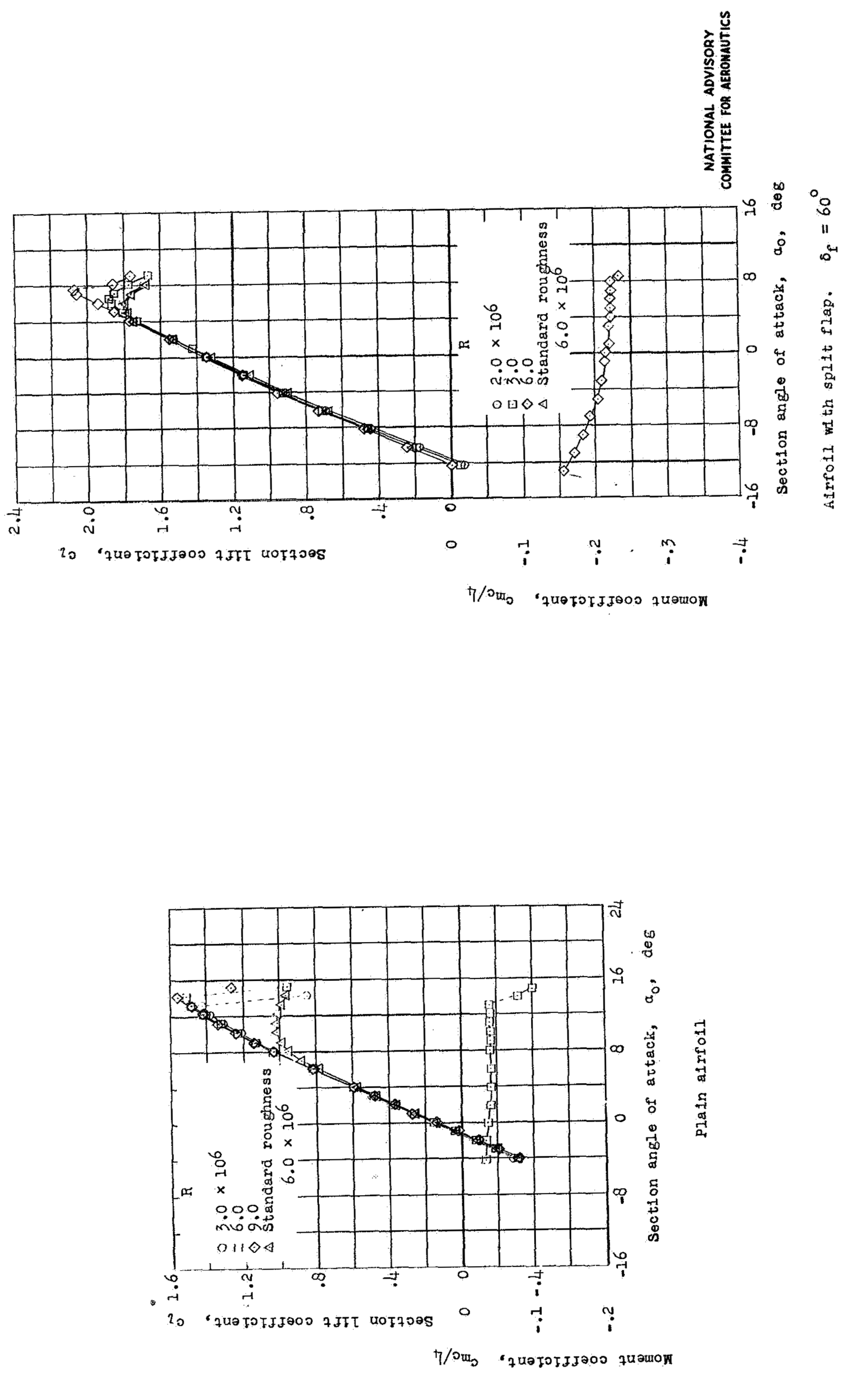

Figure 4 .- Section lift and pitching-moment characteristics of the NACA 63-210 airfoil section with and without a 0.20c split flap.

NACA 63-210

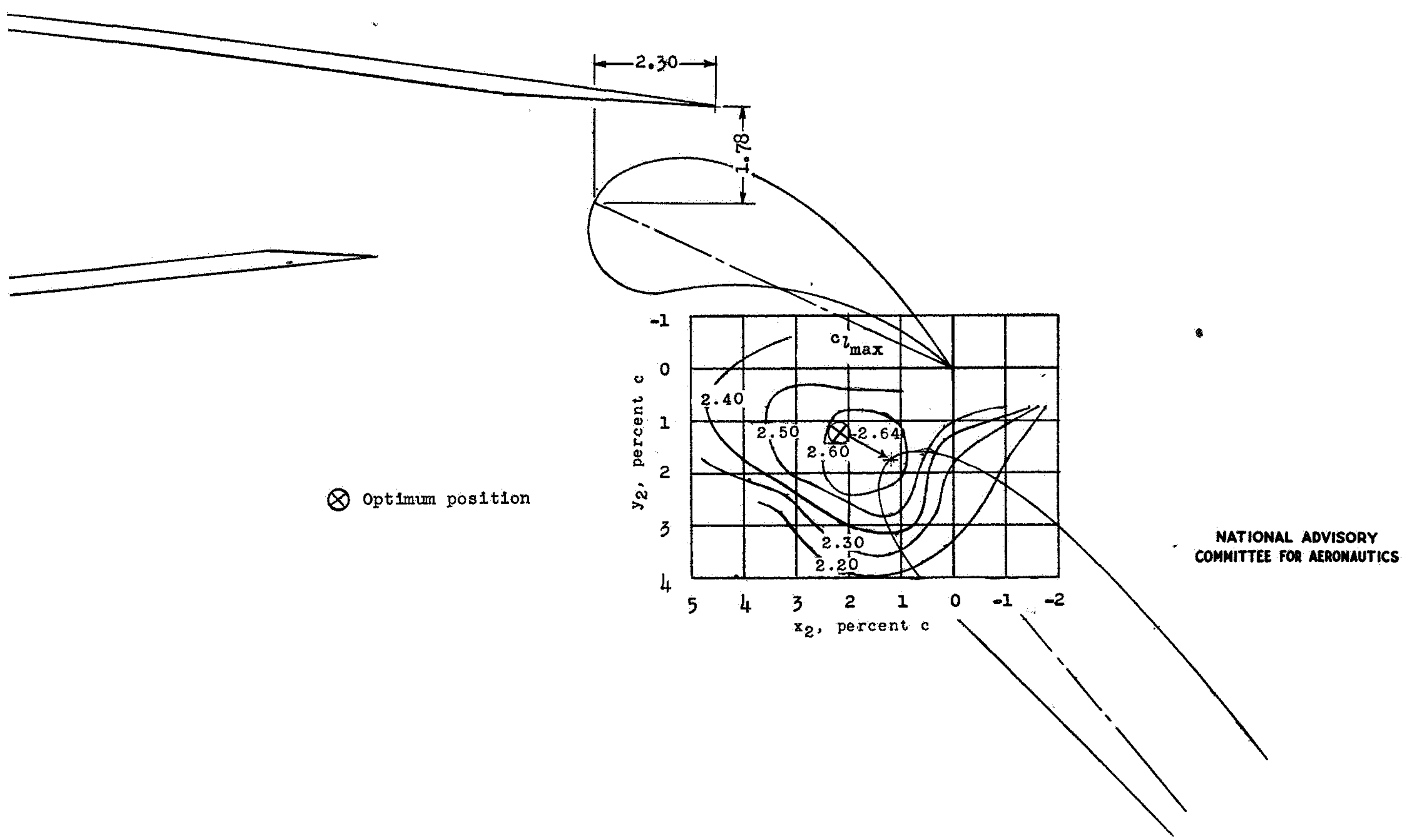

(a) $\delta_f = 50^\circ$; $\delta_{ff} = 25^\circ$.

Figure 5.- Contours of flap location for maximum lift of the NACA 63-210 airfoil section with a double slotted flap; 0.075c fore flap; 0.250c flap. $R = 2.4 \times 10^6$.

NACA 63-210

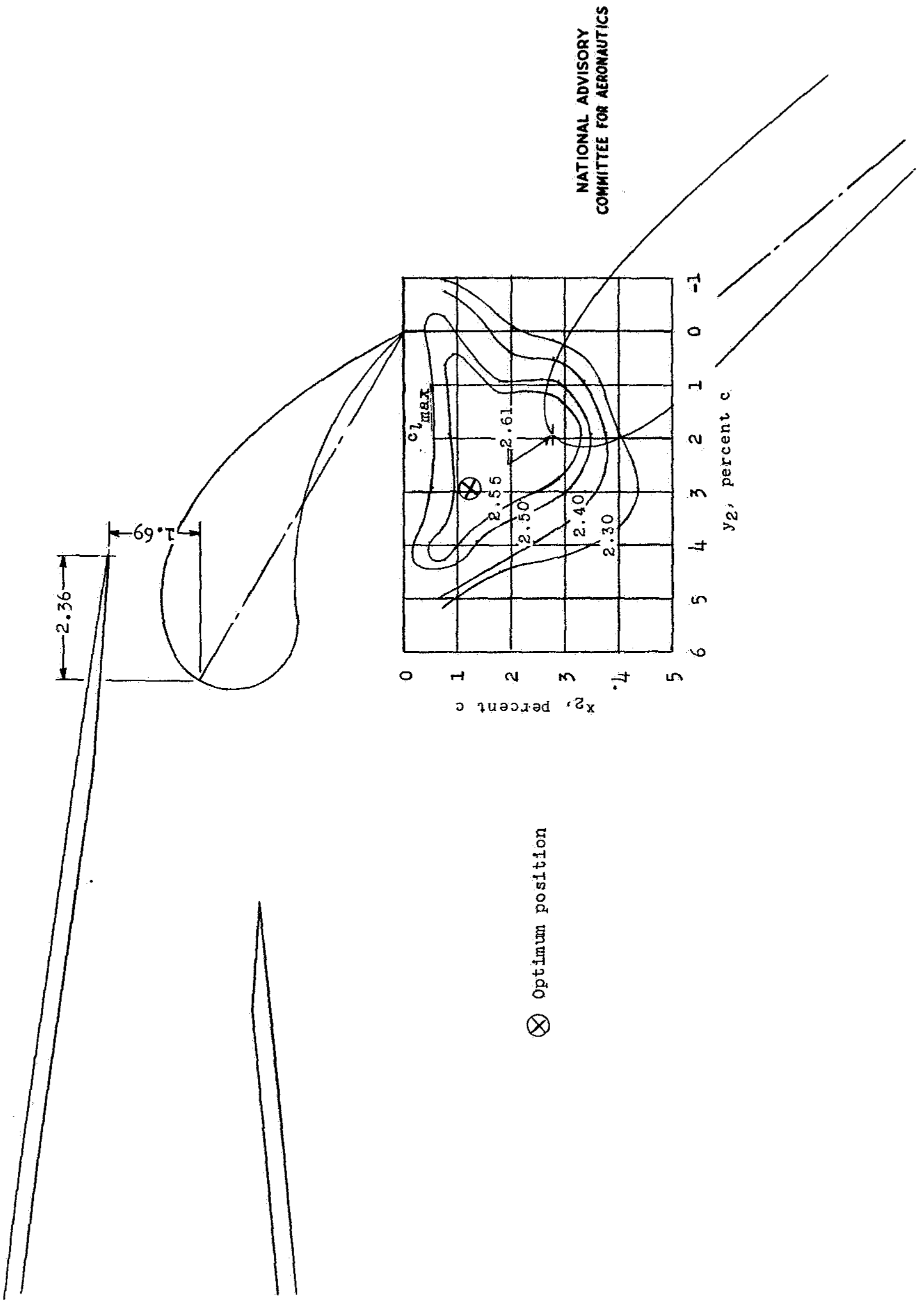

(b) $\delta_f = 50^\circ$; $\delta_{ff} = 30^\circ$.
Figure 5 .- Continued.

NACA 63-210

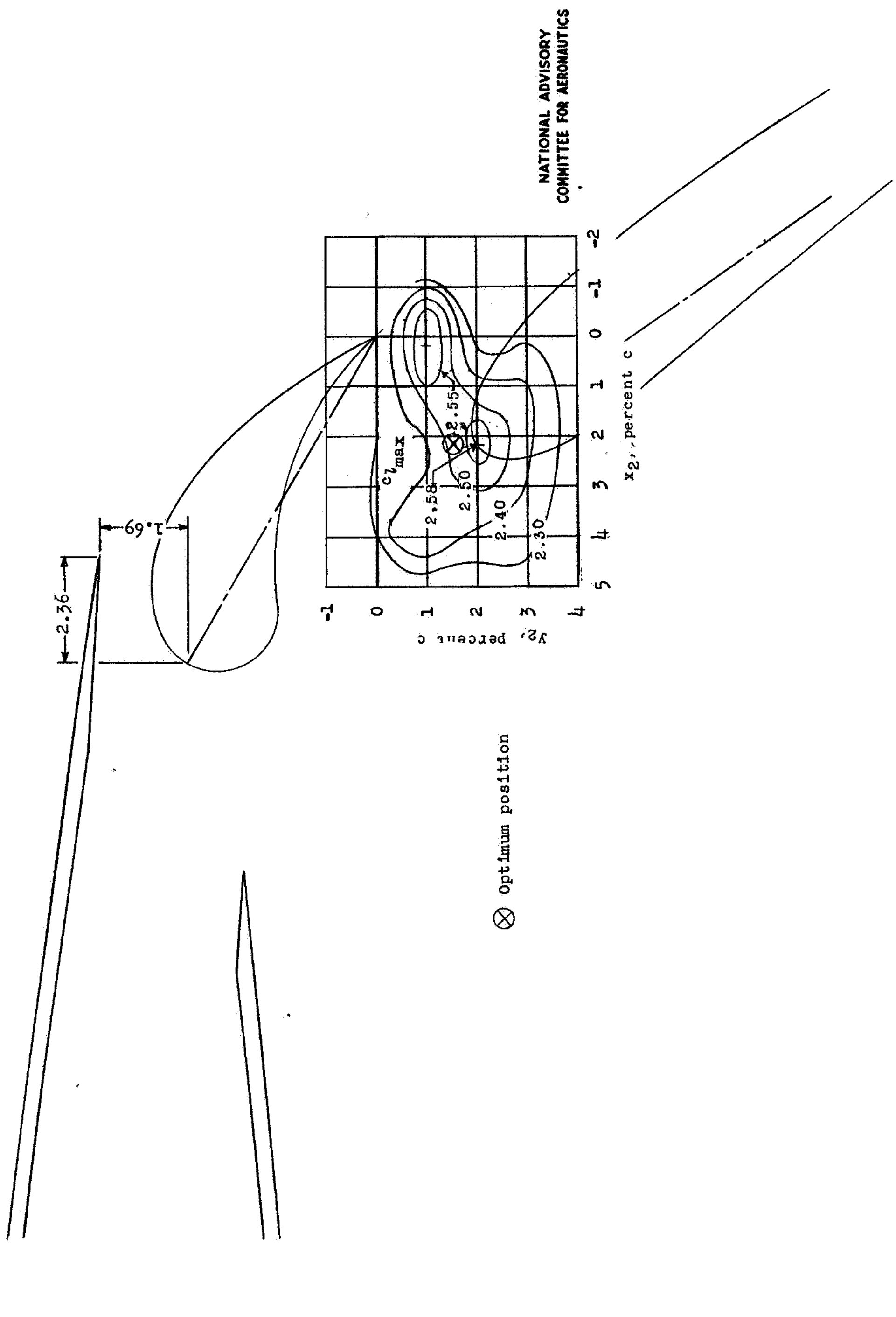

(c) $\delta_f = 55^\circ$; $\delta_{ff} = 30^\circ$.

Figure 5 .- Concluded.

NACA 63-210

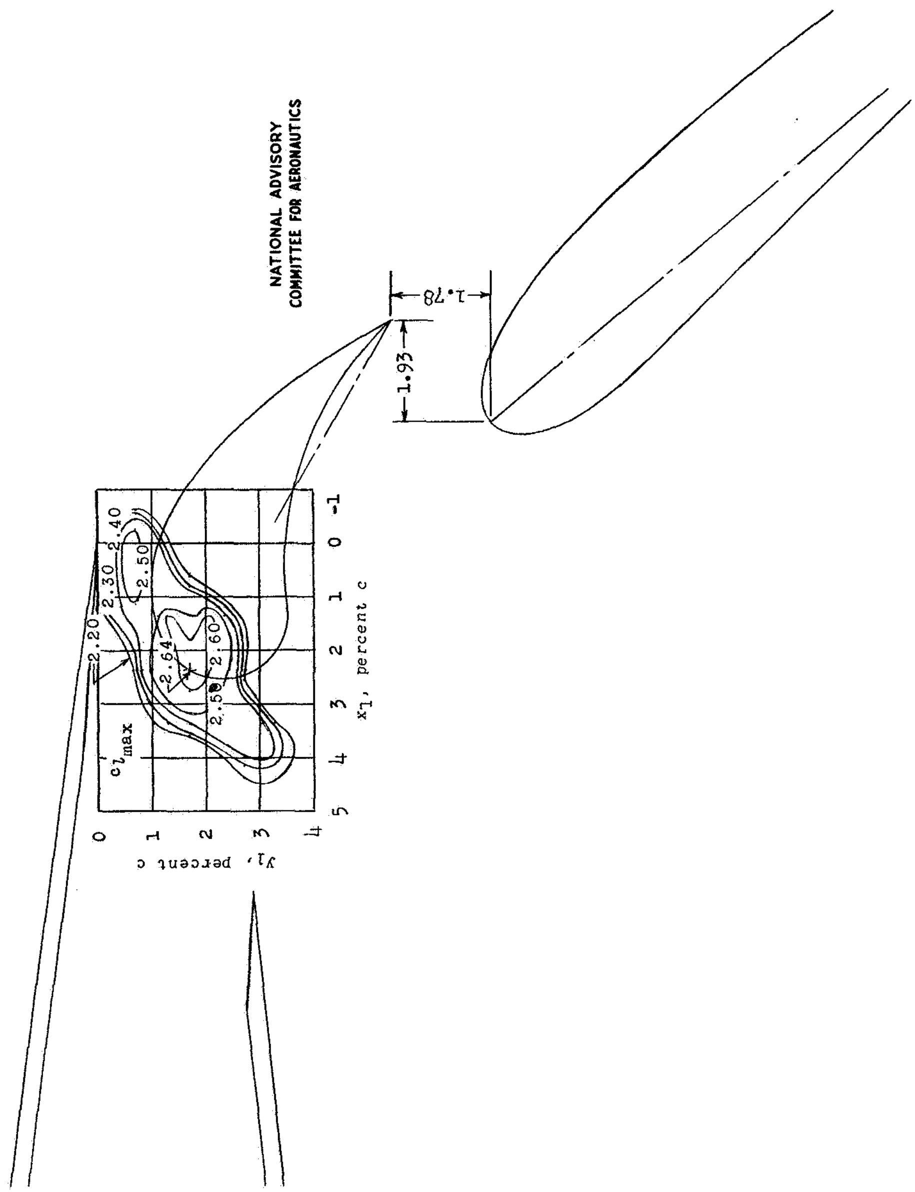

Figure 6.- Contours of flap and fore flap location for maximum lift of the NACA 63-210 airfoil section with a double slotted flap; 0.075c fore flap; 0.250c flap. $\delta_f = 50^\circ$; $\delta_{ff} = 30^\circ$; $R = 2.4 \times 10^6$.

NACA 63-210

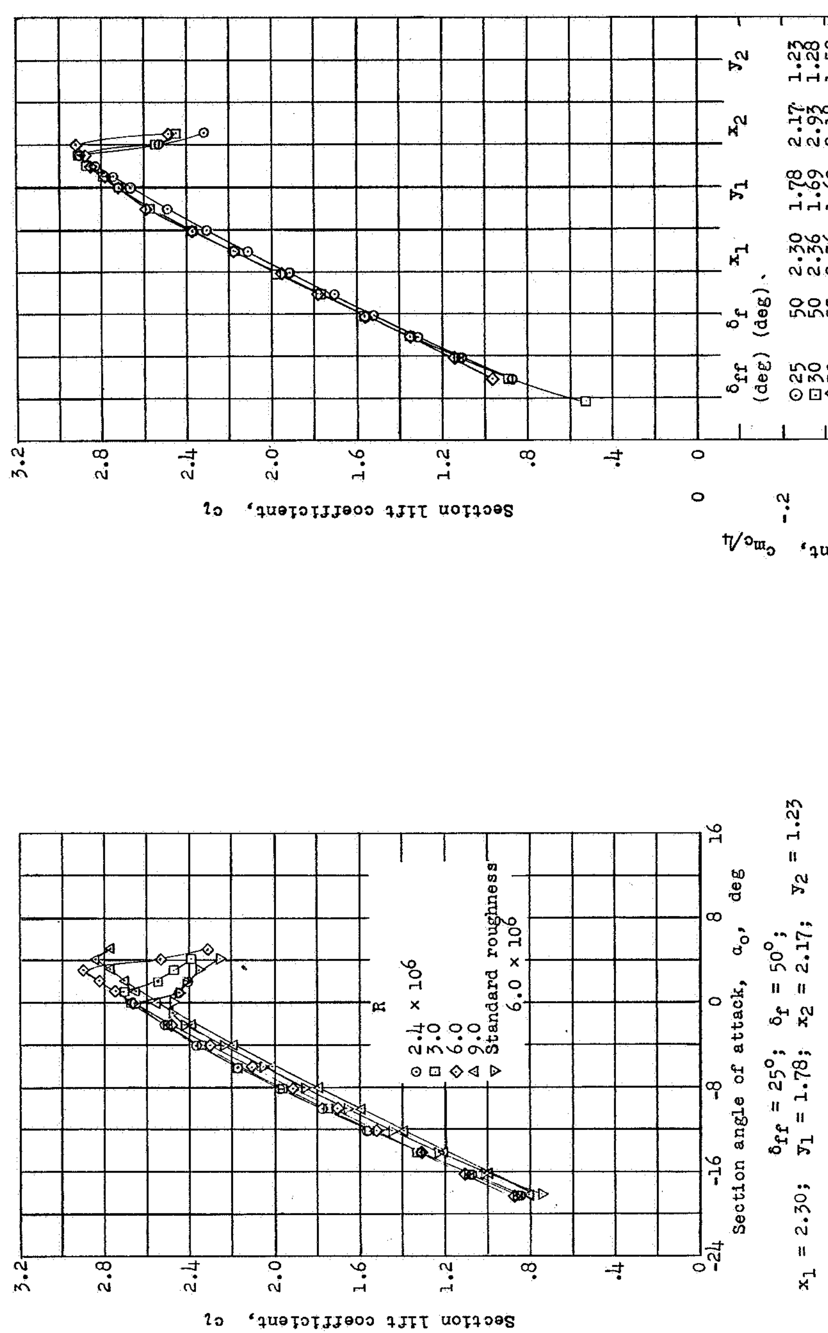

Figure 7.- Section lift and pitching-moment characteristics of the NACA 63-210 airfoil section with a double slotted flap. 0.075c fore flap; 0.250c flap.

NACA 64-208

NATIONAL ADVISORY
COMMITTEE FOR AERONAUTICS

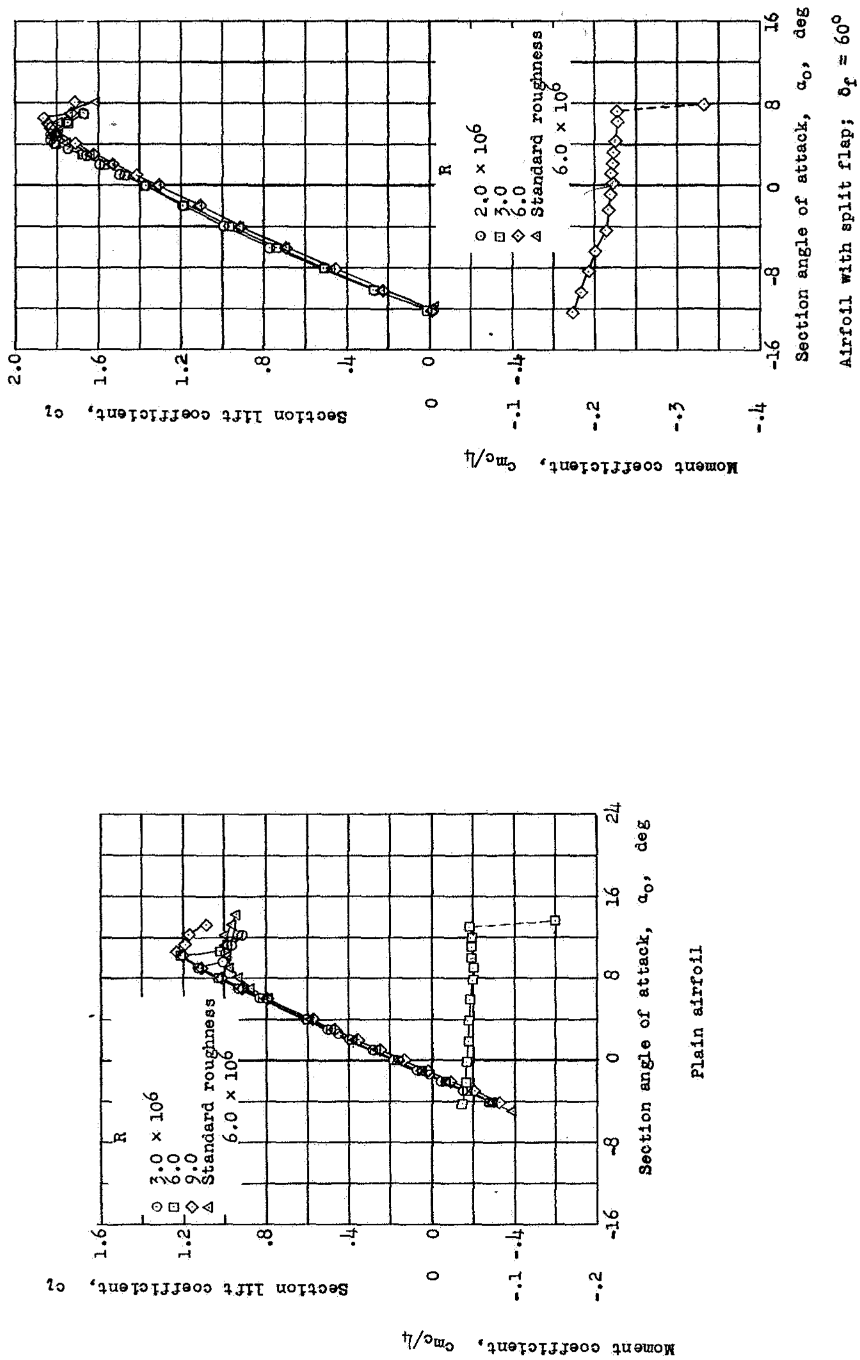

Figure 8.- Section lift and pitching-moment characteristics of the NACA 64-208 airfoil section with and without a 0.20c split flap.

NACA 64-208

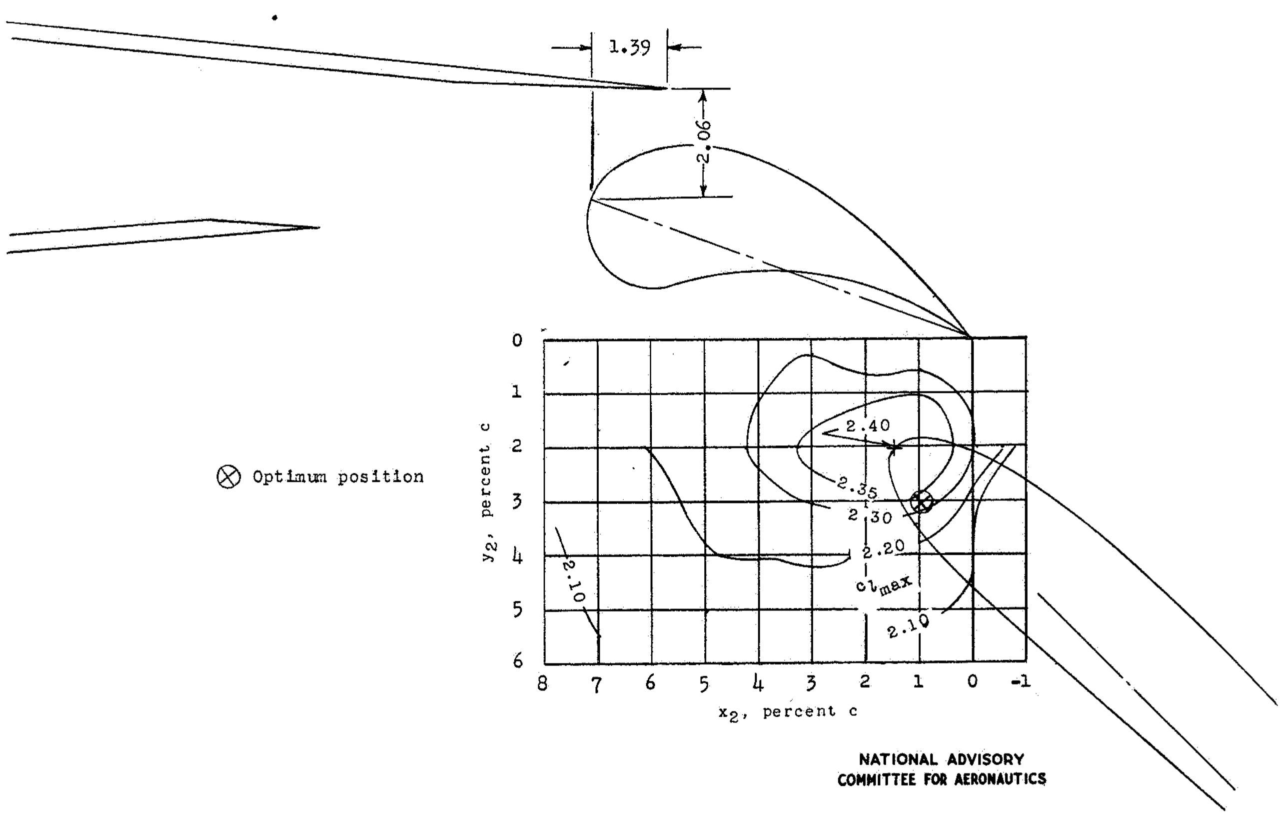

(a) $\delta_f = 45^{\circ}$; $\delta_{ff} = 20^{\circ}$.

Figure 9.- Contours of flap location for maximum lift of the NACA 64-208 airfoil section with a double slotted flap; 0.075c fore flap; 0.250c flap. $R = 2.4 \times 10^6$.

NACA 64-208

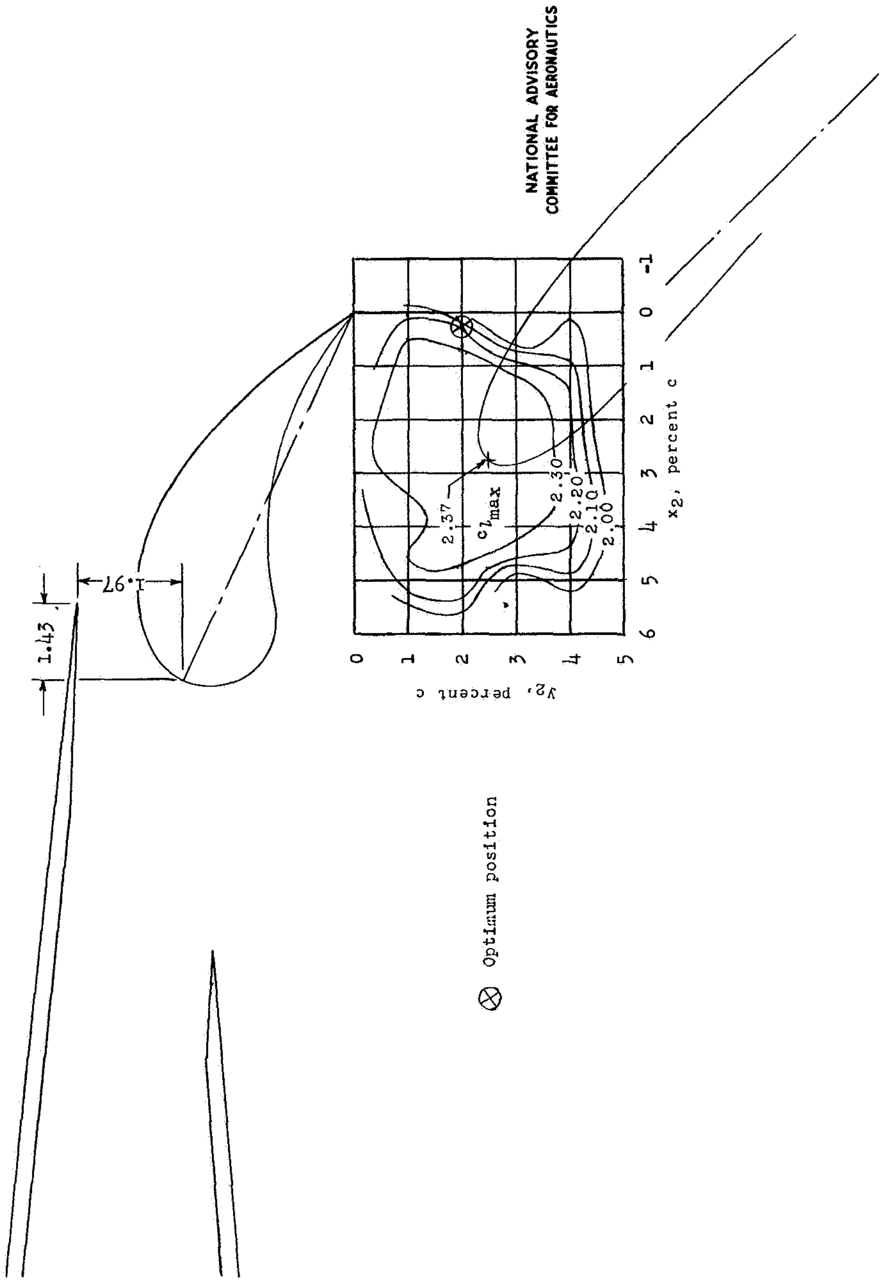

(b) $\delta_f = 45^\circ$; $\delta_{ff} = 25^\circ$.
Figure 9 .- Continued.

NACA 64-208

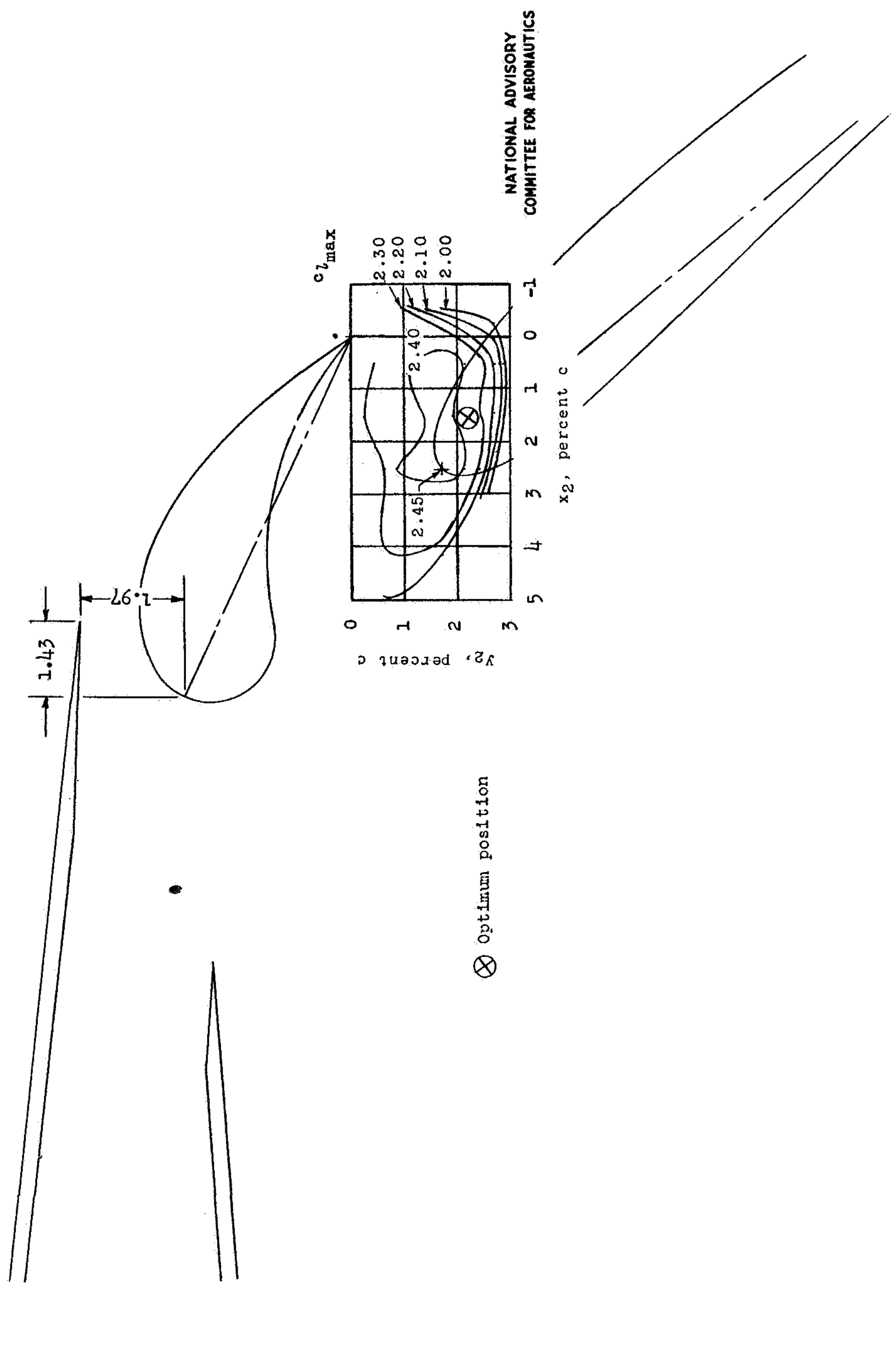

(c) $\delta_f = 50^\circ$; $\delta_{ff} = 25^\circ$.
Figure 7 .- Continued.

NACA 64-208

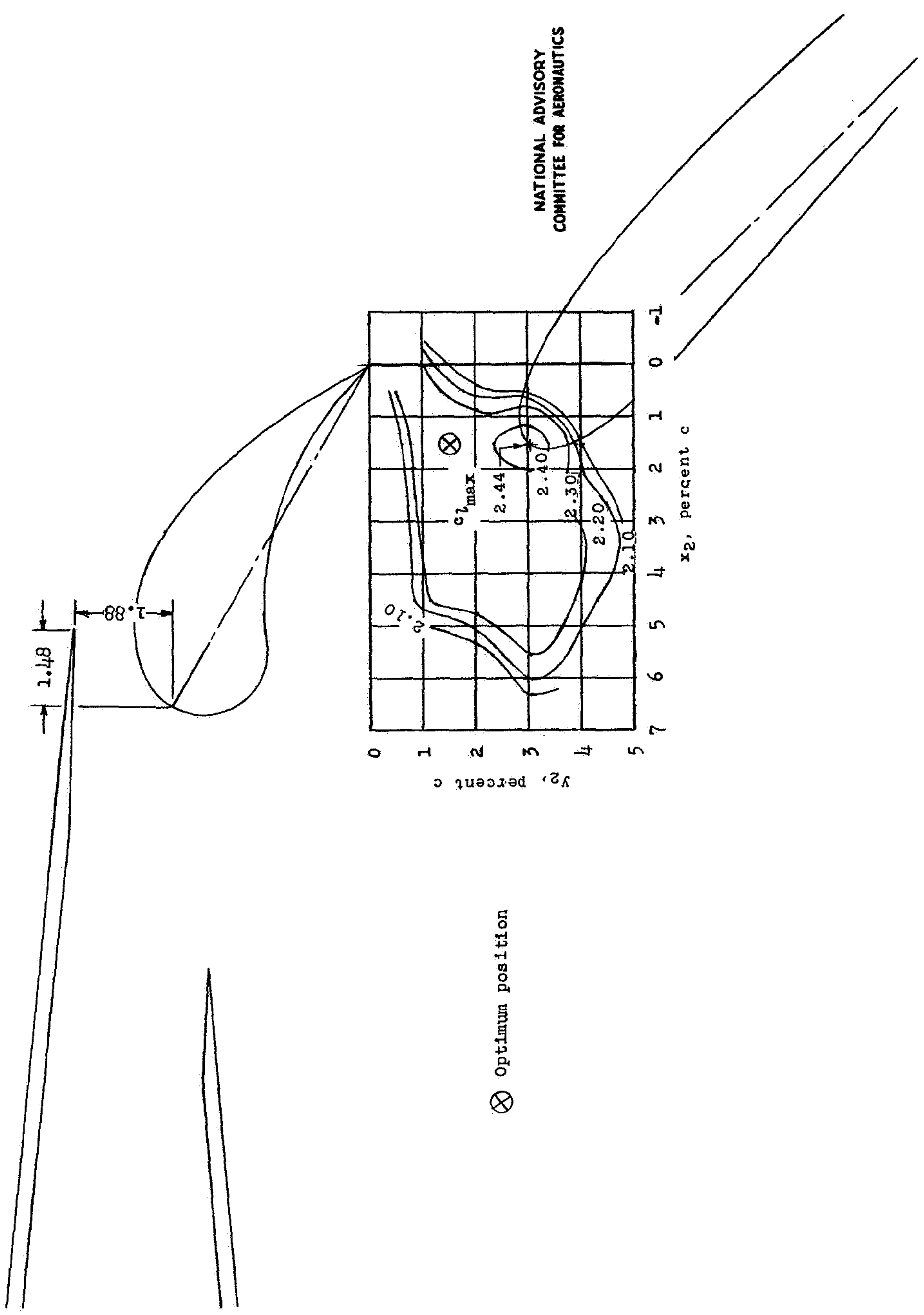

(d) $\delta_f = 45^{\circ}$; $\delta_{ff} = 30^{\circ}$.
Figure 9 .- Continued.

NACA 64-208

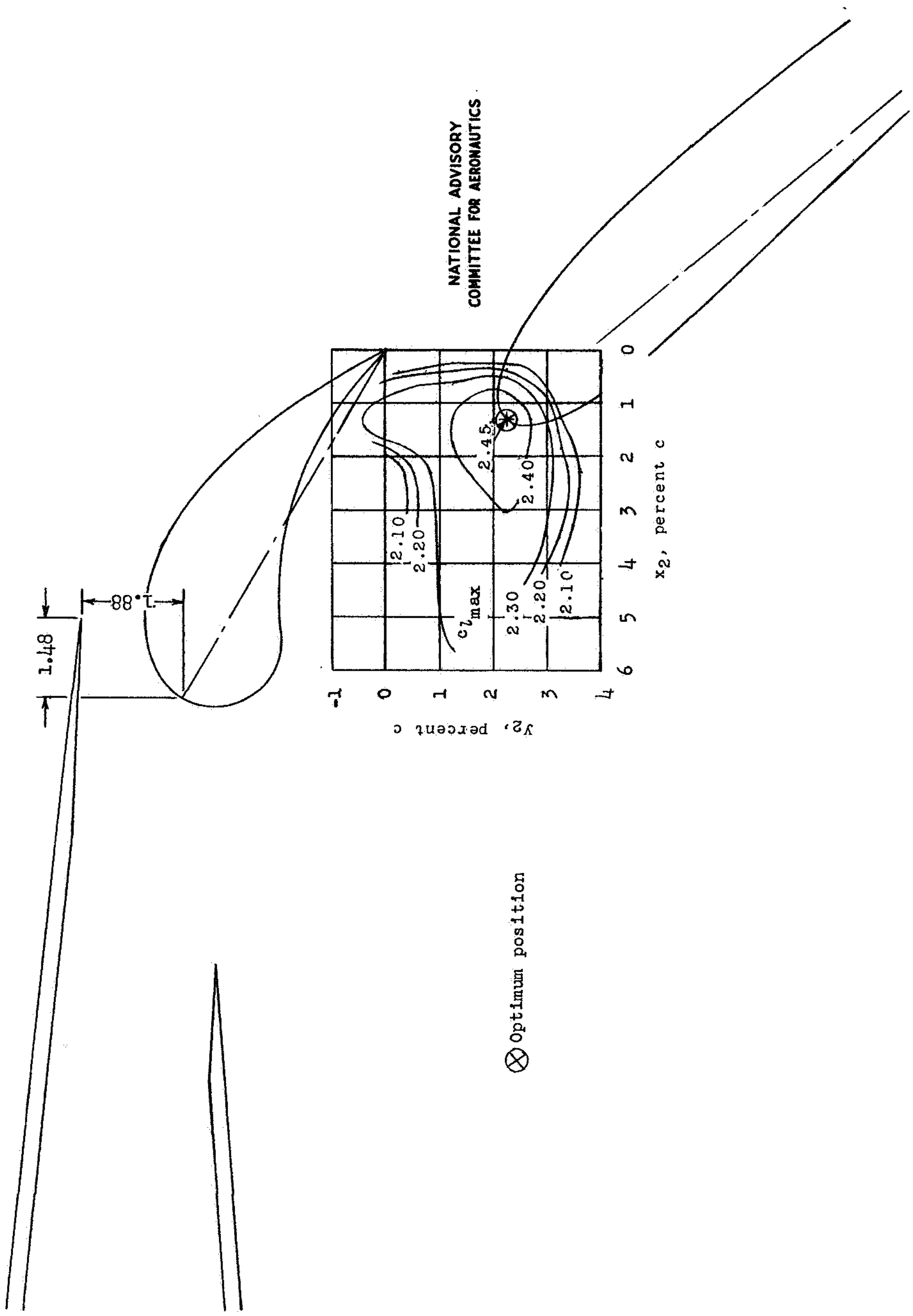

(e) $\delta_f = 50^\circ$; $\delta_{ff} = 30^\circ$.
Figure 9 .- Continued.

NACA 64-208

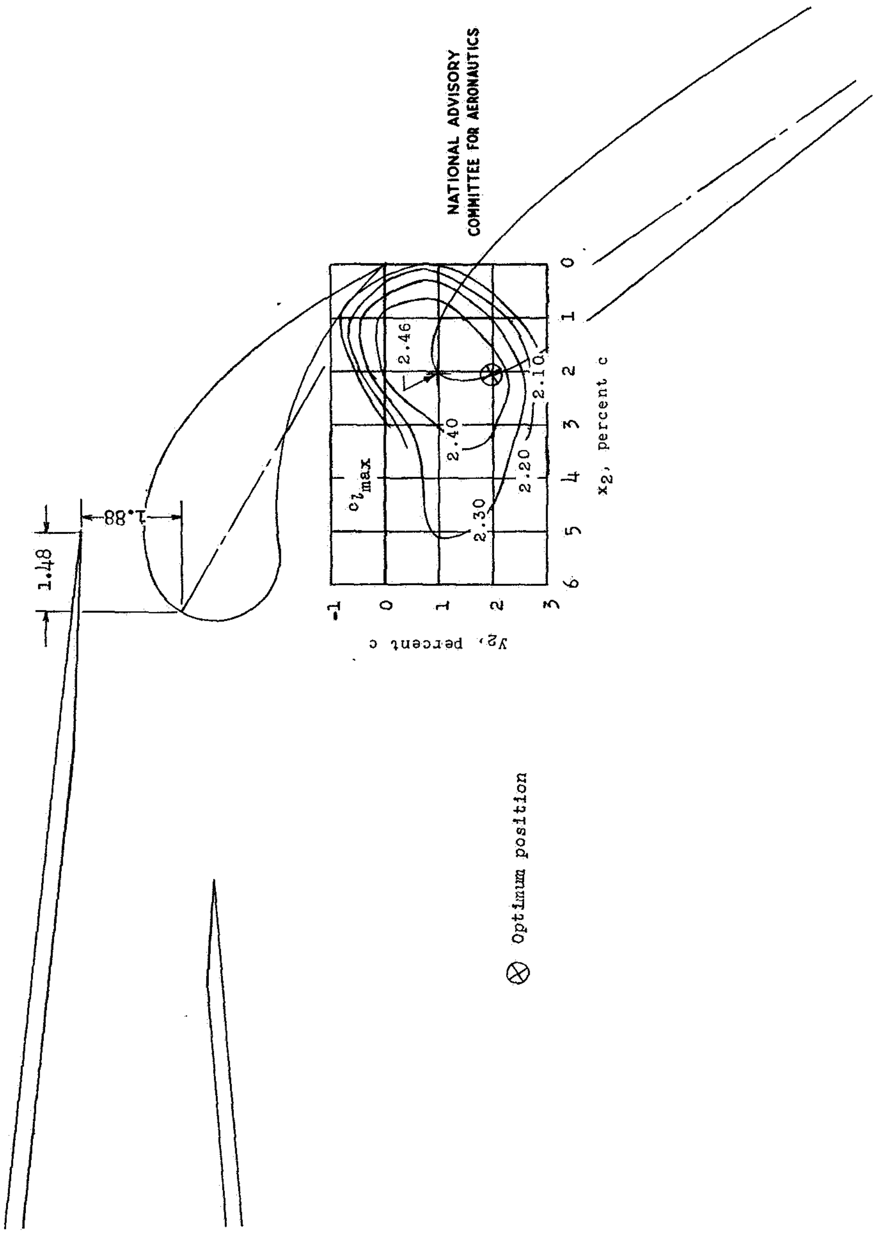

(f) $\delta_f = 55^\circ$; $\delta_{ff} = 30^\circ$.
Figure 9 .- Concluded.

NACA 64-208

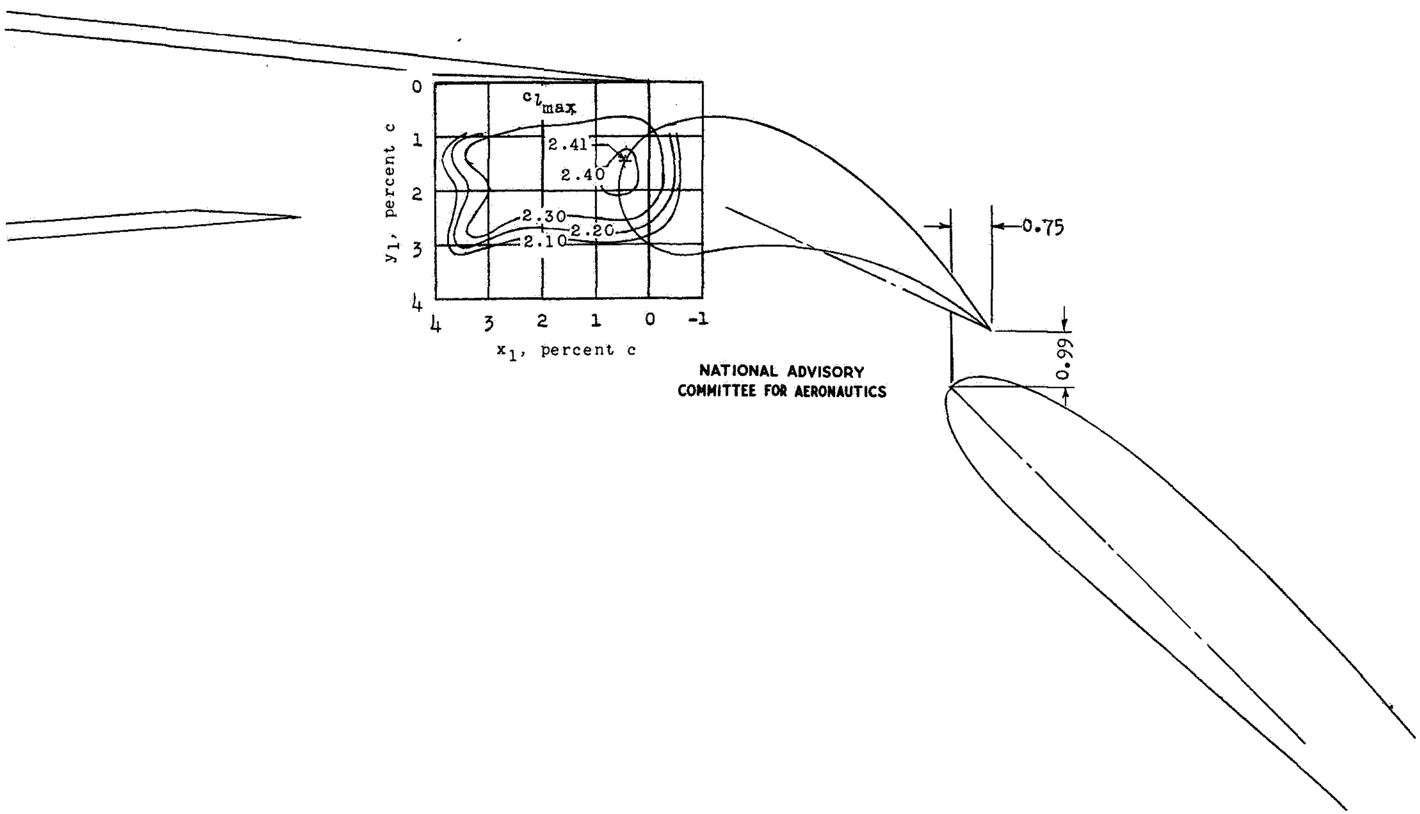

Figure 10.- Contours of flap and fore flap location for maximum lift of the NACA 64-208 airfoil section with a double slotted flap; 0.075c fore flap; 0.250c flap. $\delta_f = 45^\circ$; $\delta_{ff} = 25^\circ$; $R = 2.4 \times 10^6$.

NACA 64-208

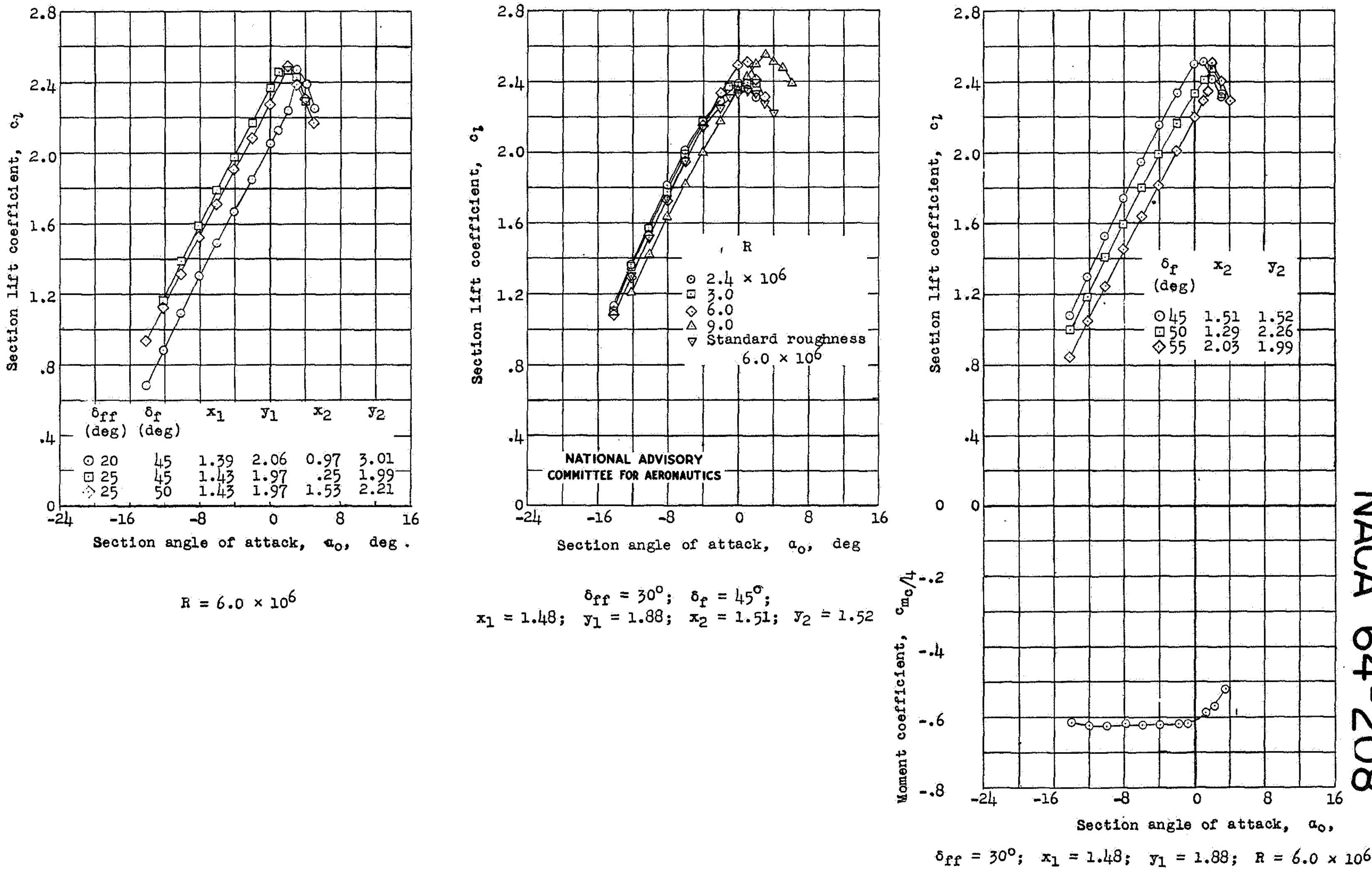

Figure 11.- Section lift and pitching-moment characteristics of the NACA 64-208 airfoil section with a double slotted flap; 0.075c fore flap; 0.250c flap.

NACA 64-208

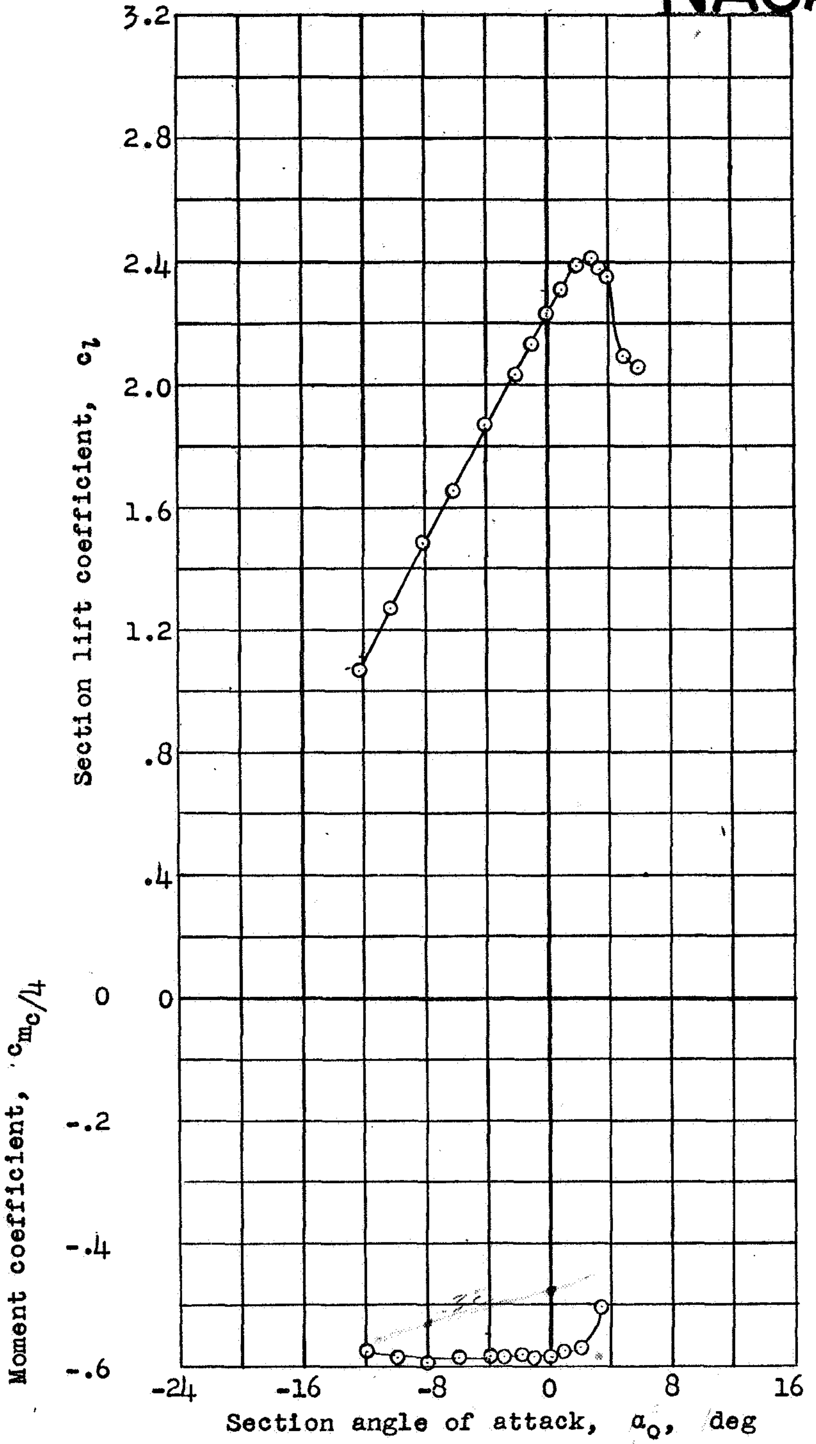

NATIONAL ADVISORY COMMITTEE FOR AERONAUTICS

Figure 12.- Section lift and pitching-moment characteristics of the NACA 64-208 airfoil section with a double slotted flap; 0.056c fore flap; 0.250c flap. $\delta_{ff} = 25^\circ$; $\delta_f = 50^\circ$; $x_1 = 1.47$; $y_1 = 2.36$; $x_2 = 1.78$; $y_2 = 1.41$; $R = 6.0 \times 10^6$.

NACA 64-210

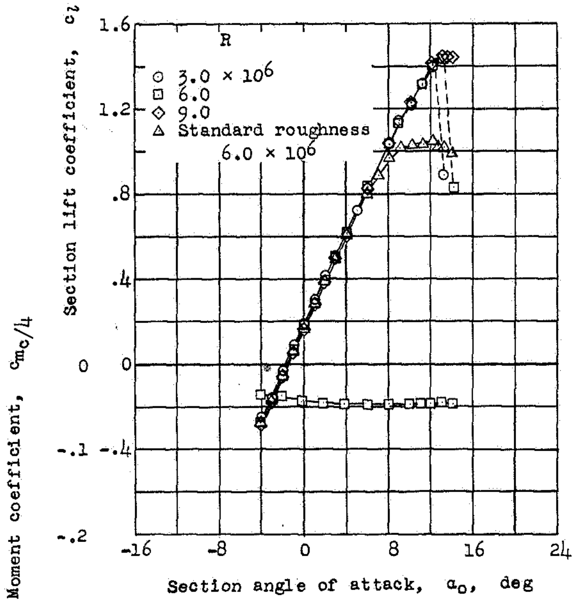

Plain airfoil

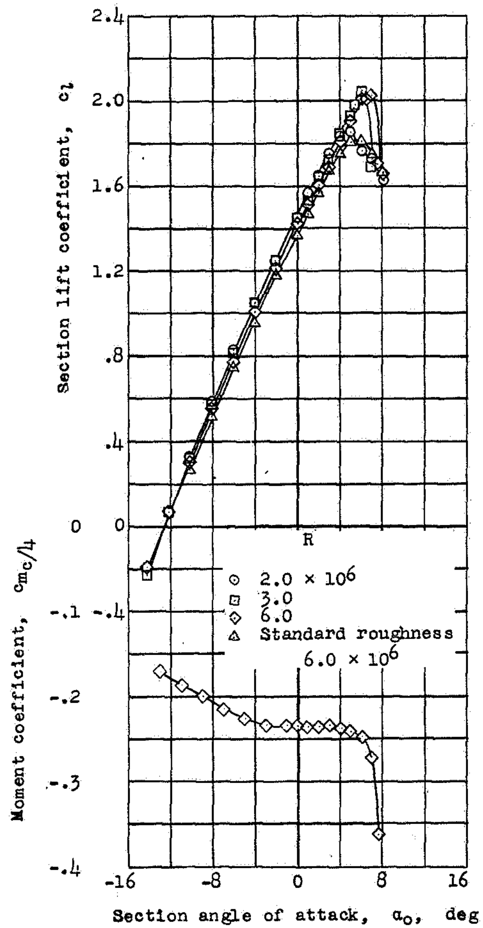

Airfoil with split flap. $\delta_f = 60°$

NATIONAL ADVISORY
COMMITTEE FOR AERONAUTICS

Figure 13.- Section lift and pitching-moment characteristics of the NACA 64-210 airfoil section with and without a 0.20c split flap.

NACA 64-210

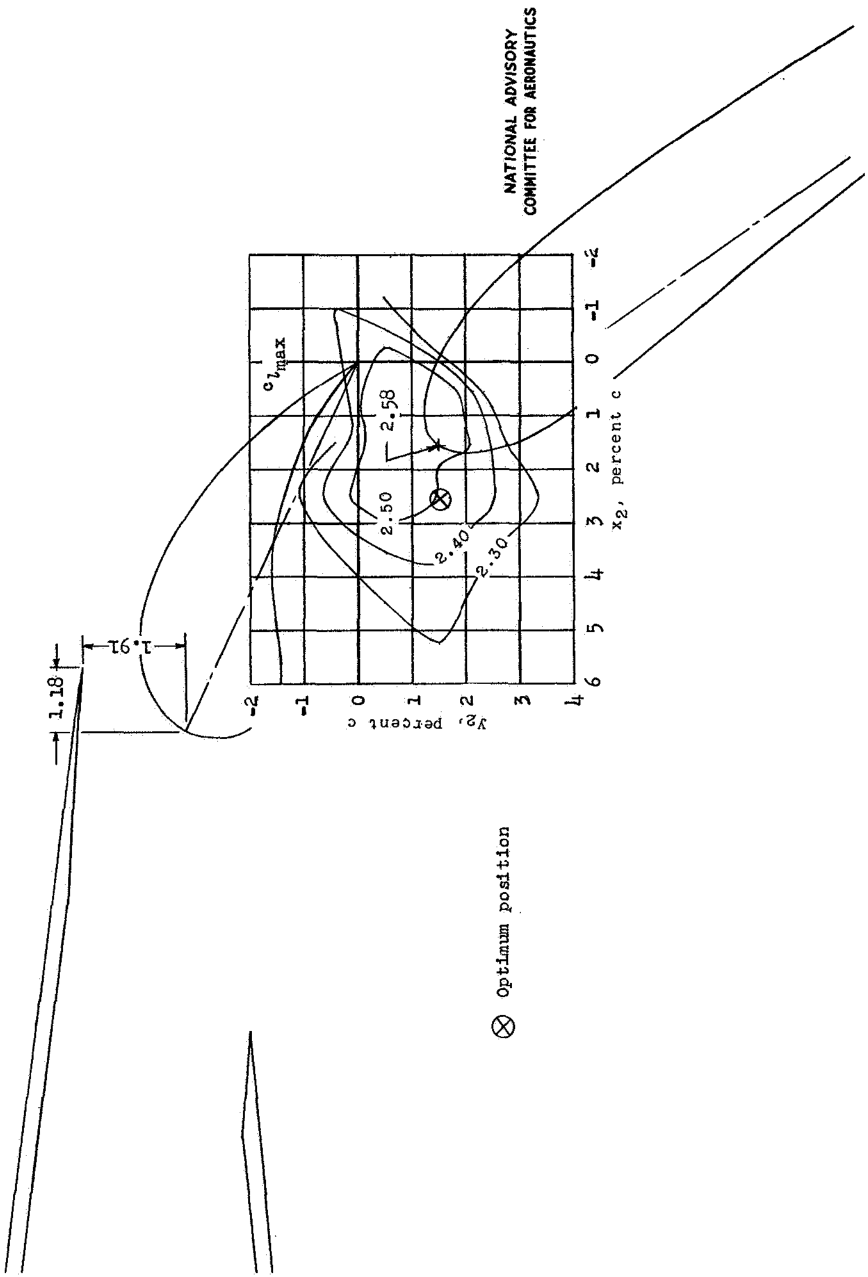

(a) $\delta_f = 55^{\circ}$; $\delta_{ff} = 25^{\circ}$.

Figure 14.- Contours of flap location for maximum lift of the NACA 64-210 airfoil section with a double slotted flap; 0.075c fore flap; 0.250c flap. $R = 2.4 \times 10^6$.

NACA 64-210

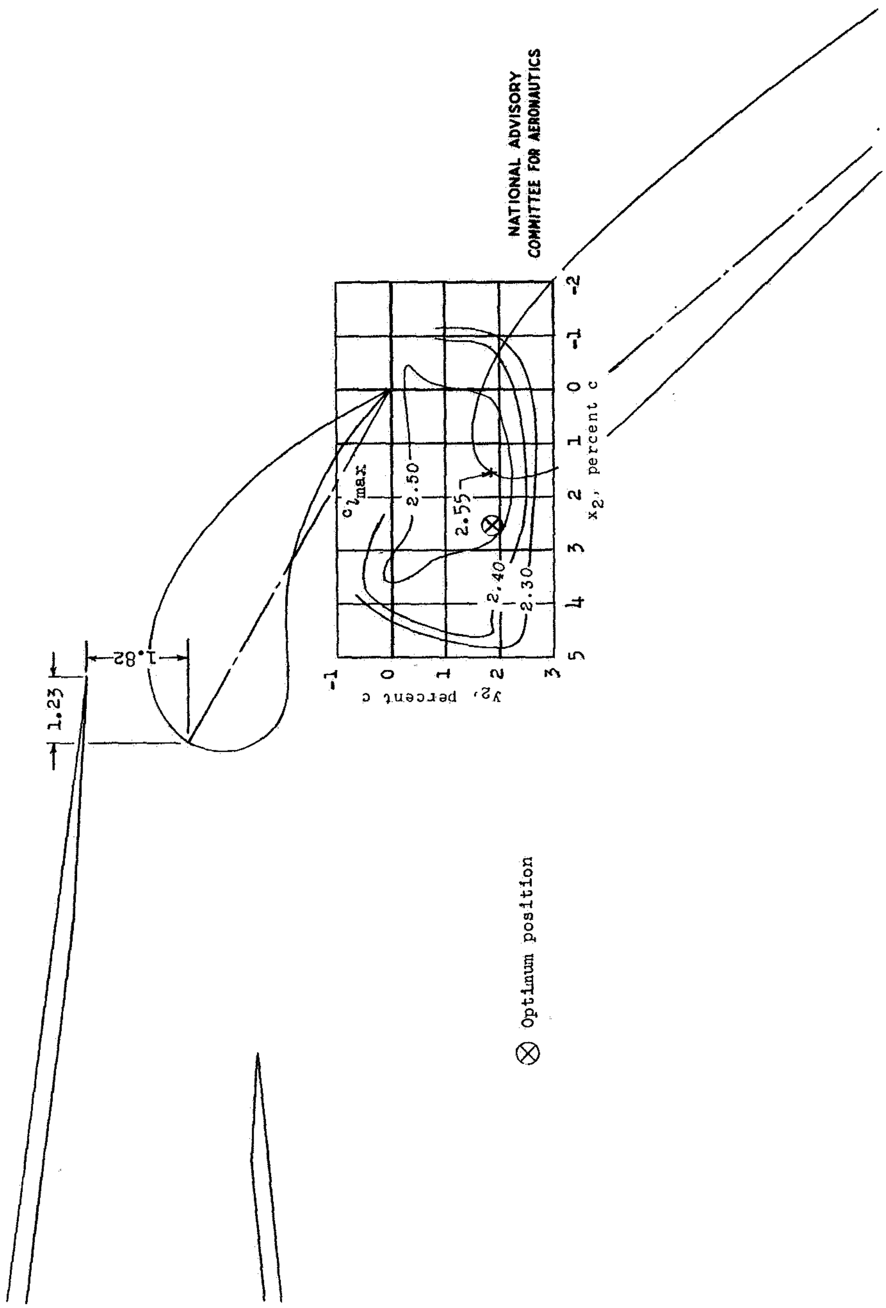

(b) $\delta_f = 50^\circ$; $\delta_{ff} = 30^\circ$.

Figure 14.- Continued.

NACA 64-210

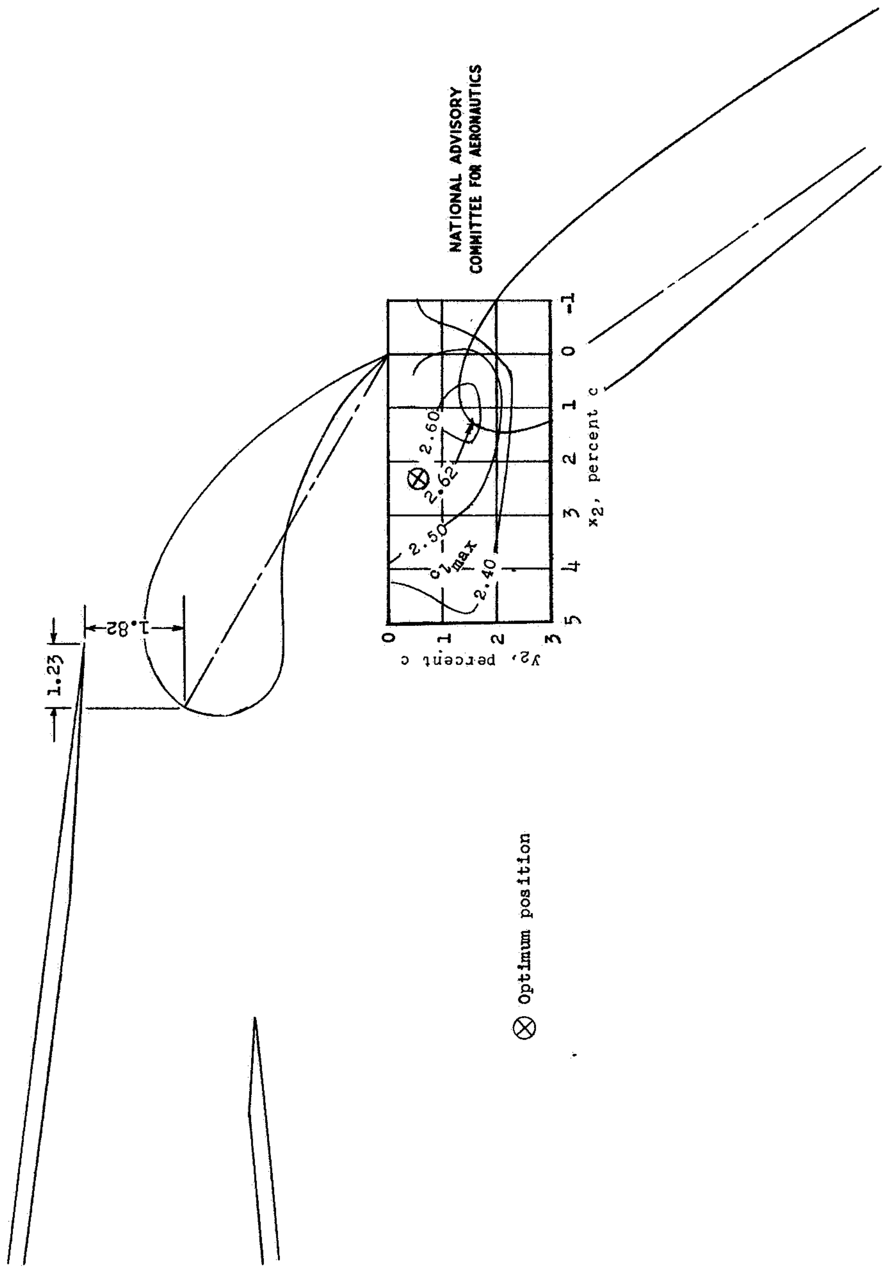

(c) $\delta_f = 55^{\circ}$; $\delta_{ff} = 30^{\circ}$.

Figure 14.- Concluded.

NACA 64-210

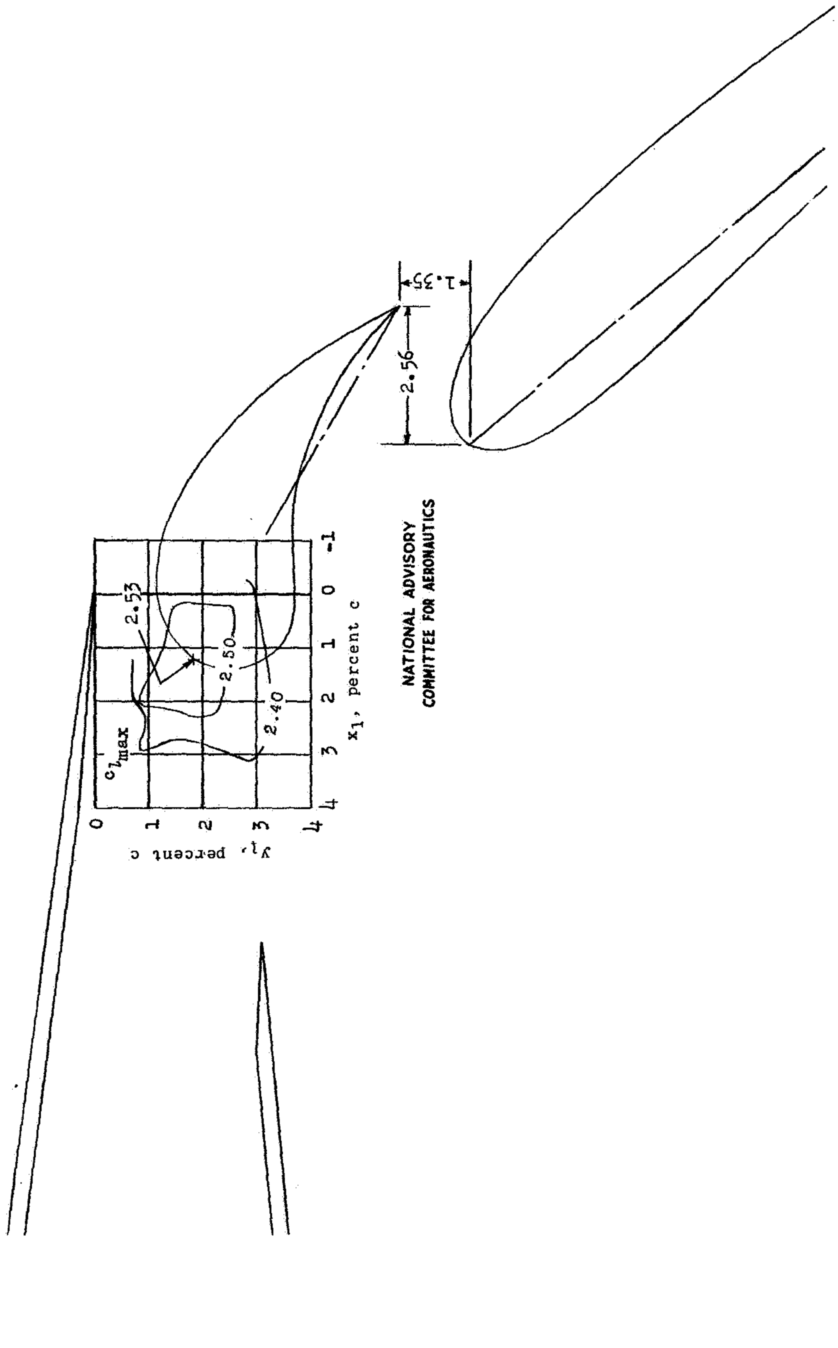

Figure 15.- Contours of flap and fore flap location for maximum lift of the NACA 64-210 airfoil section with a double slotted flap; 0.075c fore flap; 0.250c flap. $\delta_f = 50^\circ$; $\delta_{ff} = 30^\circ$; $R = 2.4 \times 10^6$.

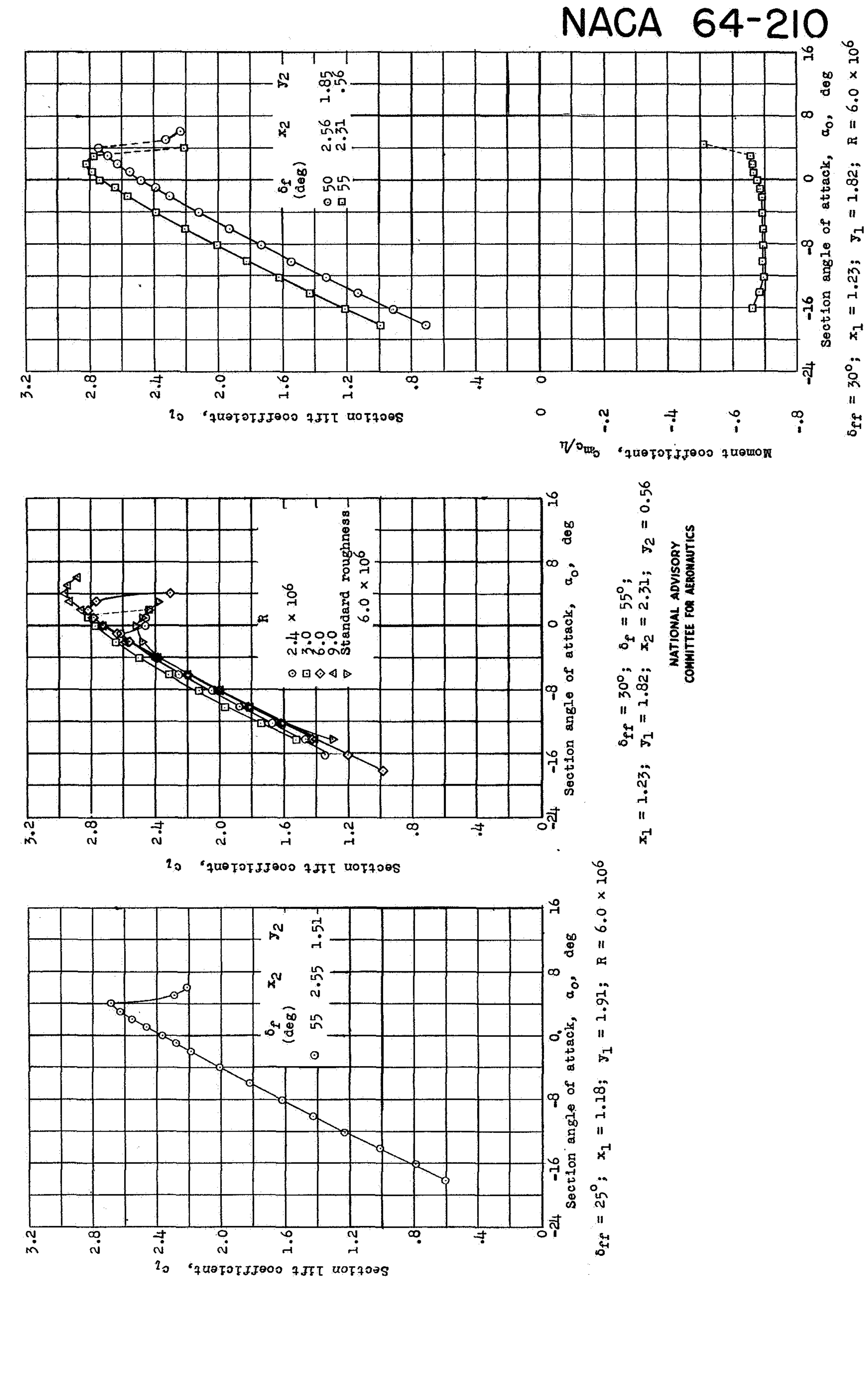

Figure 16.- Section lift and pitching-moment characteristics of the NACA 64-210 airfoil section with a double slotted flap; 0.075c fore flap; 0.250c flap.

NACA 65-210

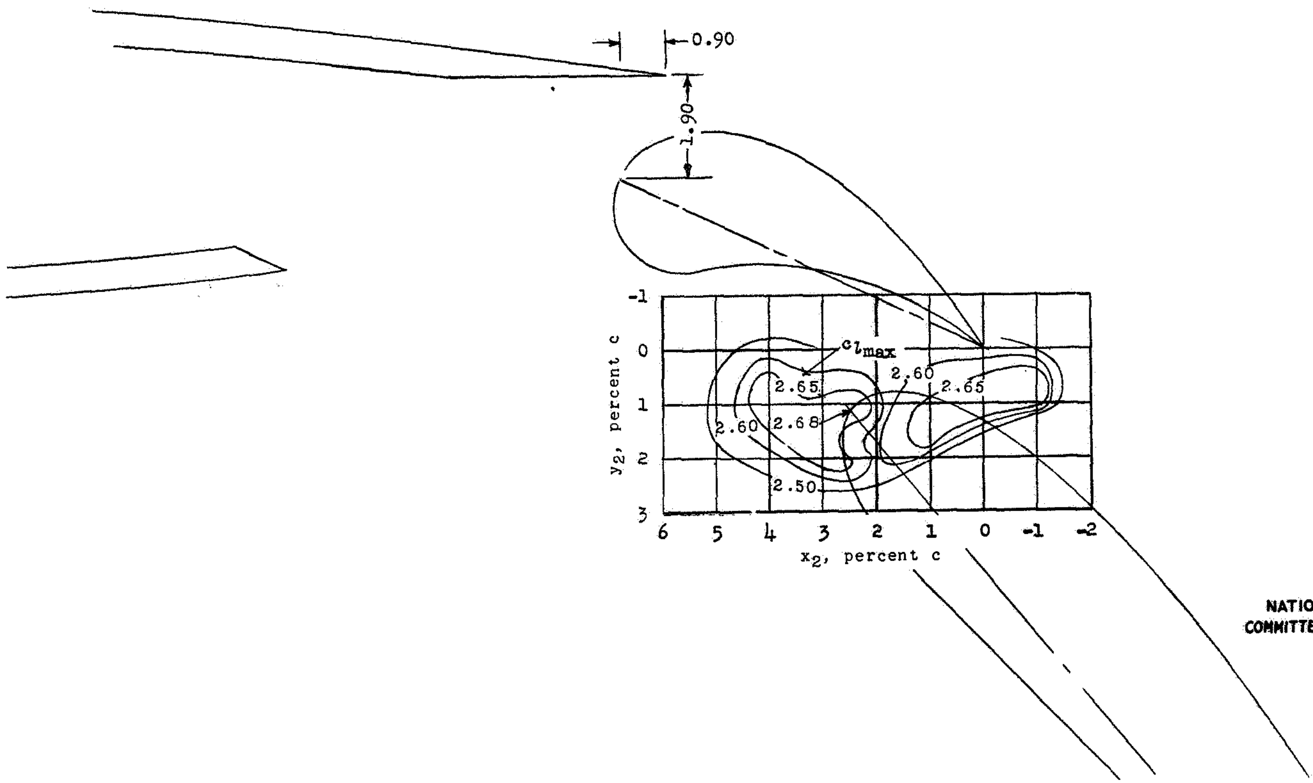

NATIONAL ADVISORY COMMITTEE FOR AERONAUTICS

Figure 17.- Contours of flap location for maximum lift of the NACA 65-210 airfoil section with a double slotted flap; 0.075c fore flap; 0.250c flap. $\delta_f = 50^\circ$; $\delta_{ff} = 25^\circ$; $R = 2.4 \times 10^6$.

NACA 65-210

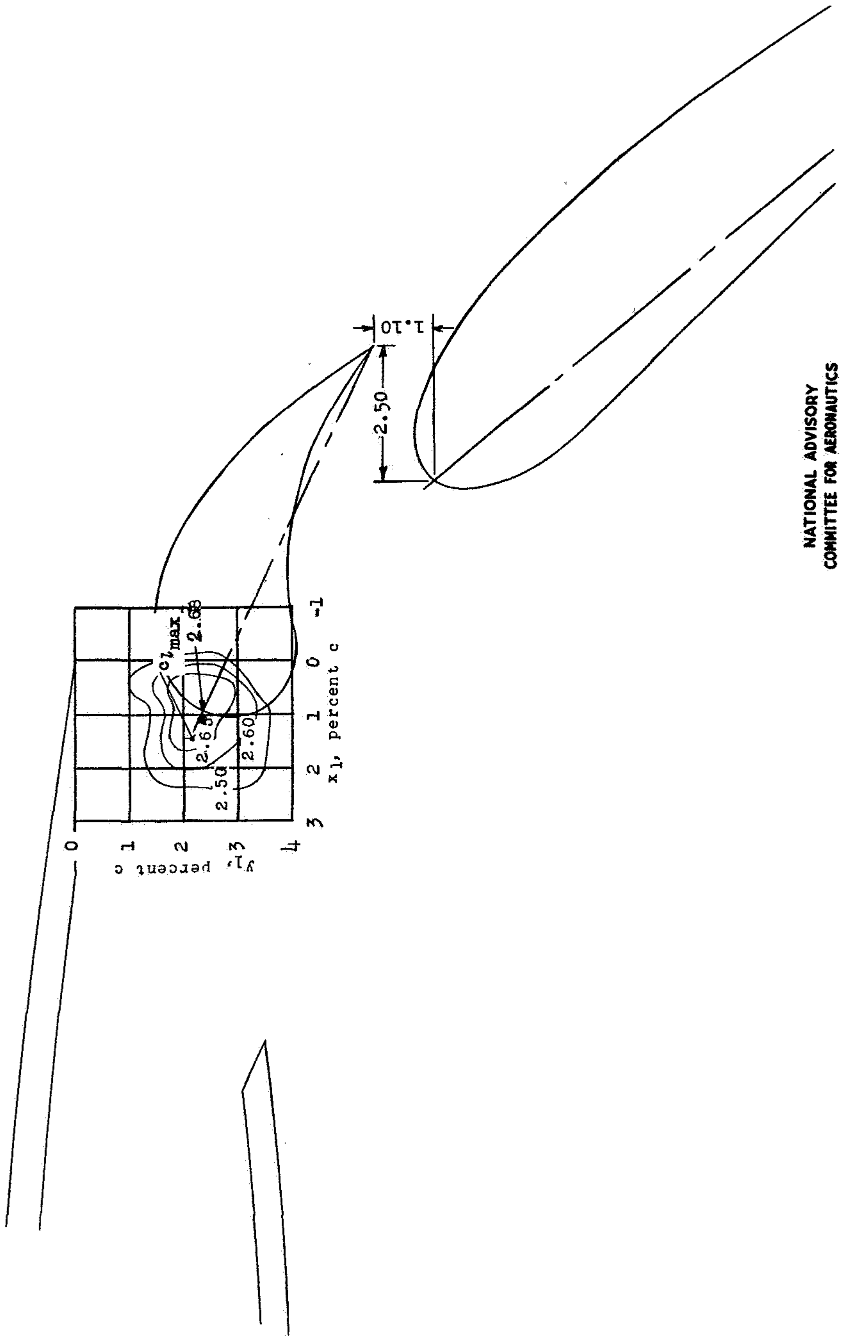

Figure 18.- Contours of flap and fore flap location for maximum lift of the NACA 65-210 airfoil section with a double slotted flap; 0.075c fore flap; 0.250c flap. $\delta_f = 50^\circ$; $\delta_{ff} = 25^\circ$; $R = 2.4 \times 10^6$.

NACA 65-210

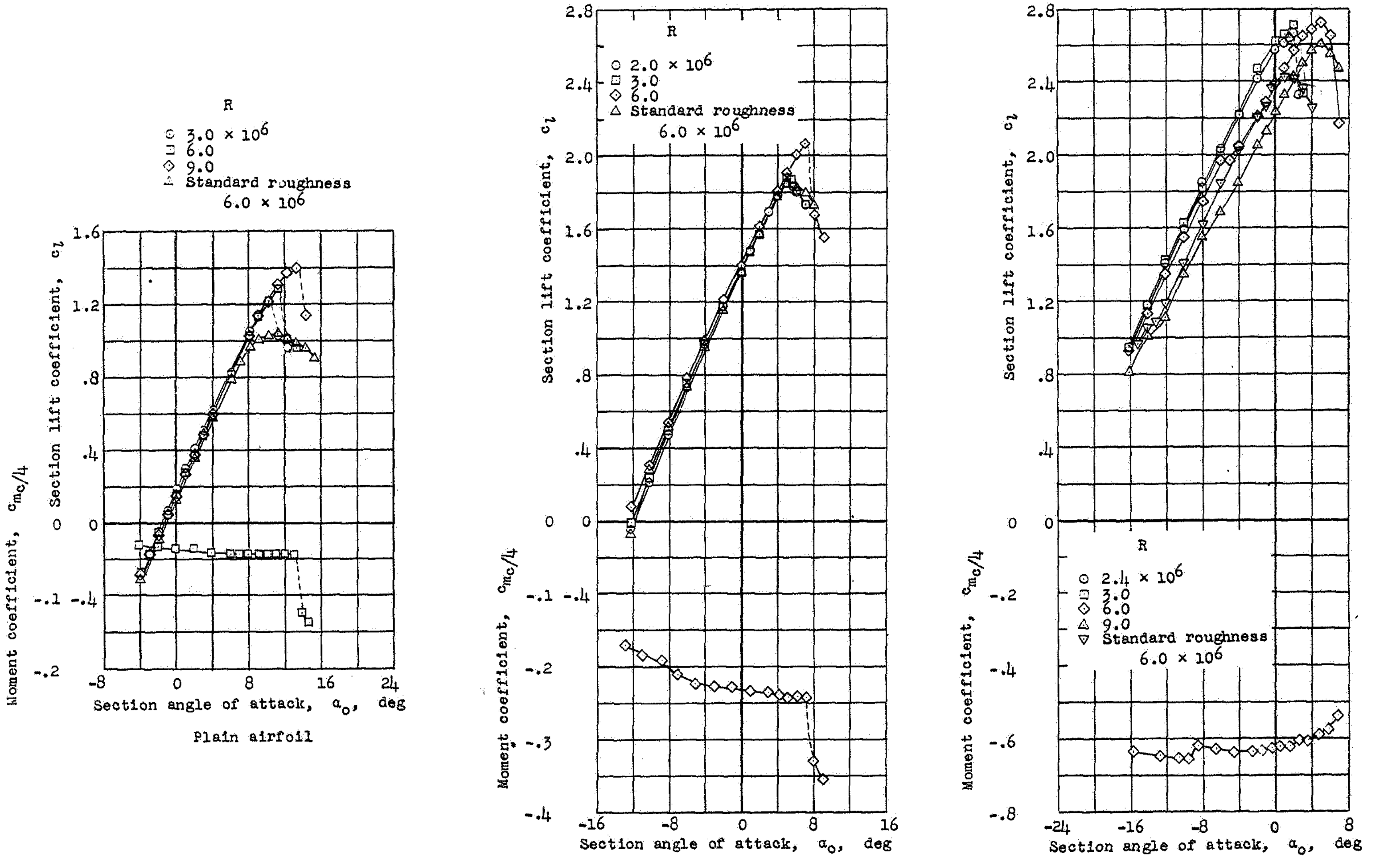

Airfoil with 0.20c split flap; $\delta_f = 60^\circ$

Airfoil with double slotted flap; 0.250c flap; 0.075c fore flap; $\delta_{ff} = 25^\circ$; $\delta_f = 50^\circ$; $x_1 = 0.92$; $y_1 = 2.36$; $x_2 = 2.50$; $y_2 = 1.10$

NATIONAL ADVISORY COMMITTEE FOR AERONAUTICS

Figure 19.- Section lift and pitching-moment characteristics of the NACA 65-210 airfoil section with and without flap.

NACA 66-210

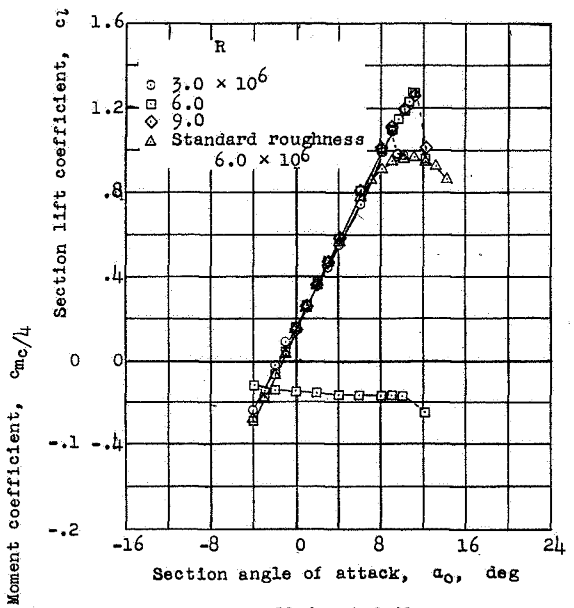

Plain airfoil

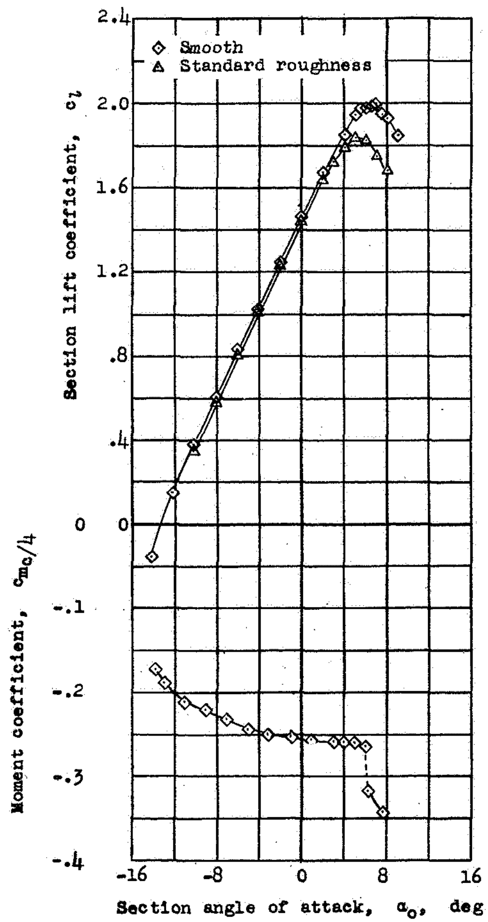

Airfoil with split flap; $\delta_f = 60^o$; $R = 6.0 \times 10^6$

NATIONAL ADVISORY COMMITTEE FOR AERONAUTICS

Figure 20.- Section lift and pitching-moment characteristics of the NACA 66-210 airfoil section with and without a 0.20c split flap.

NACA 66-210

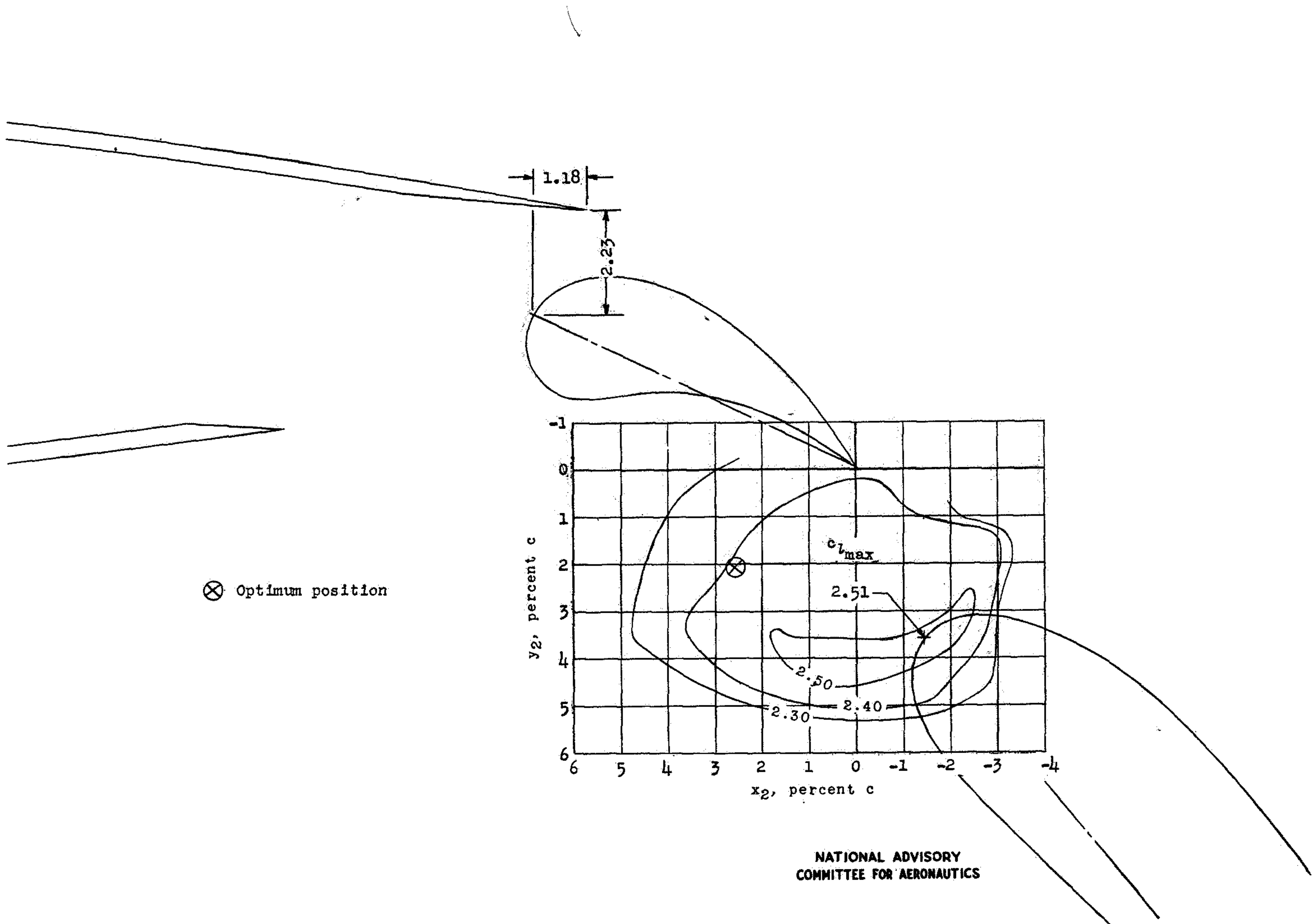

(a) $\delta_f = 50^{\circ}$; $\delta_{ff} = 25^{\circ}$.

Figure 21.- Contours of flap location for maximum lift of the NACA 66-210 airfoil section with a double slotted flap; 0.075c fore flap; 0.250c flap. $R = 2.4 \times 10^6$.

NACA 66-210

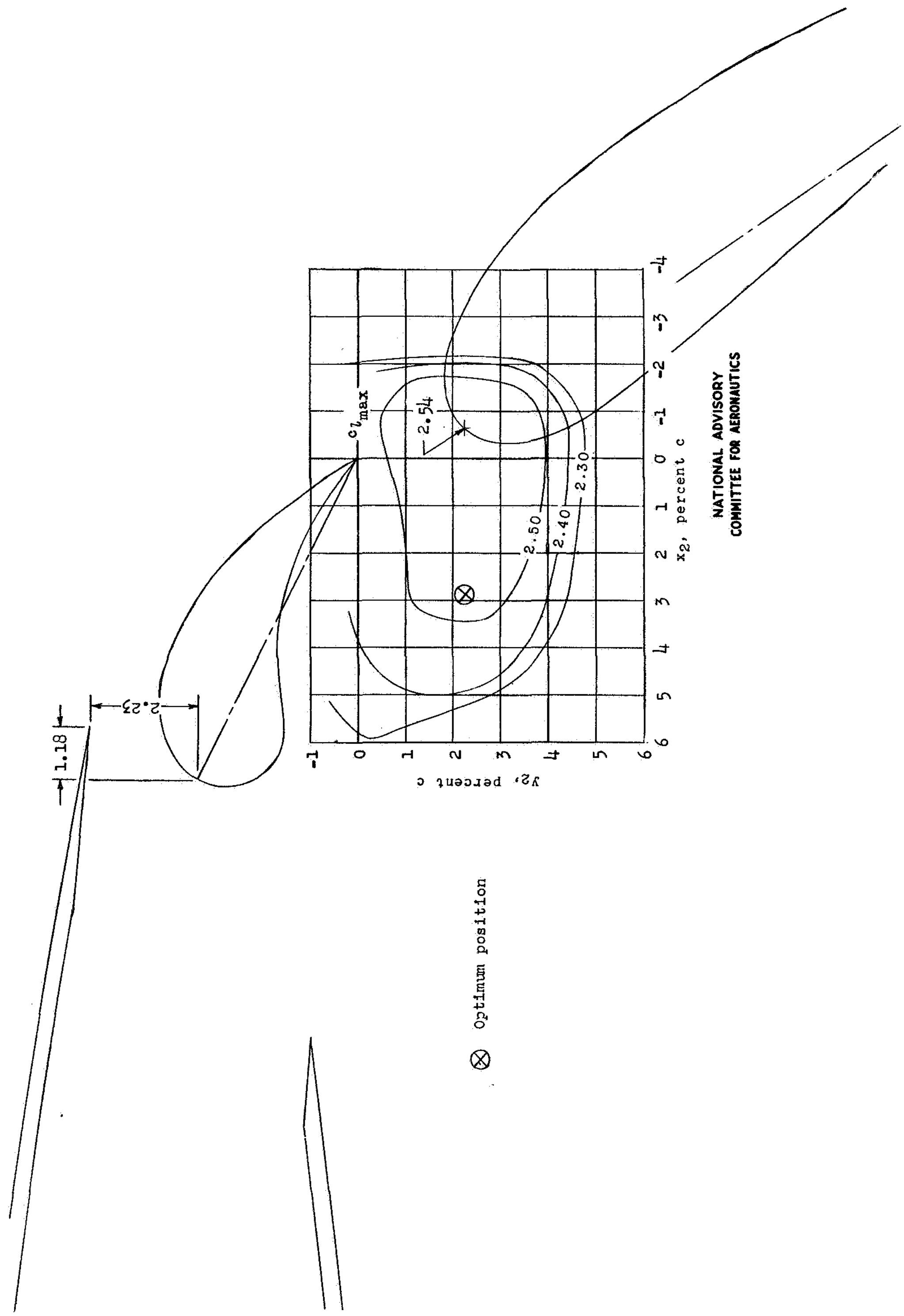

(b) $\delta_f = 55^{\circ}$; $\delta_{ff} = 25^{\circ}$.
Figure 21.- Continued.

NACA 66-210

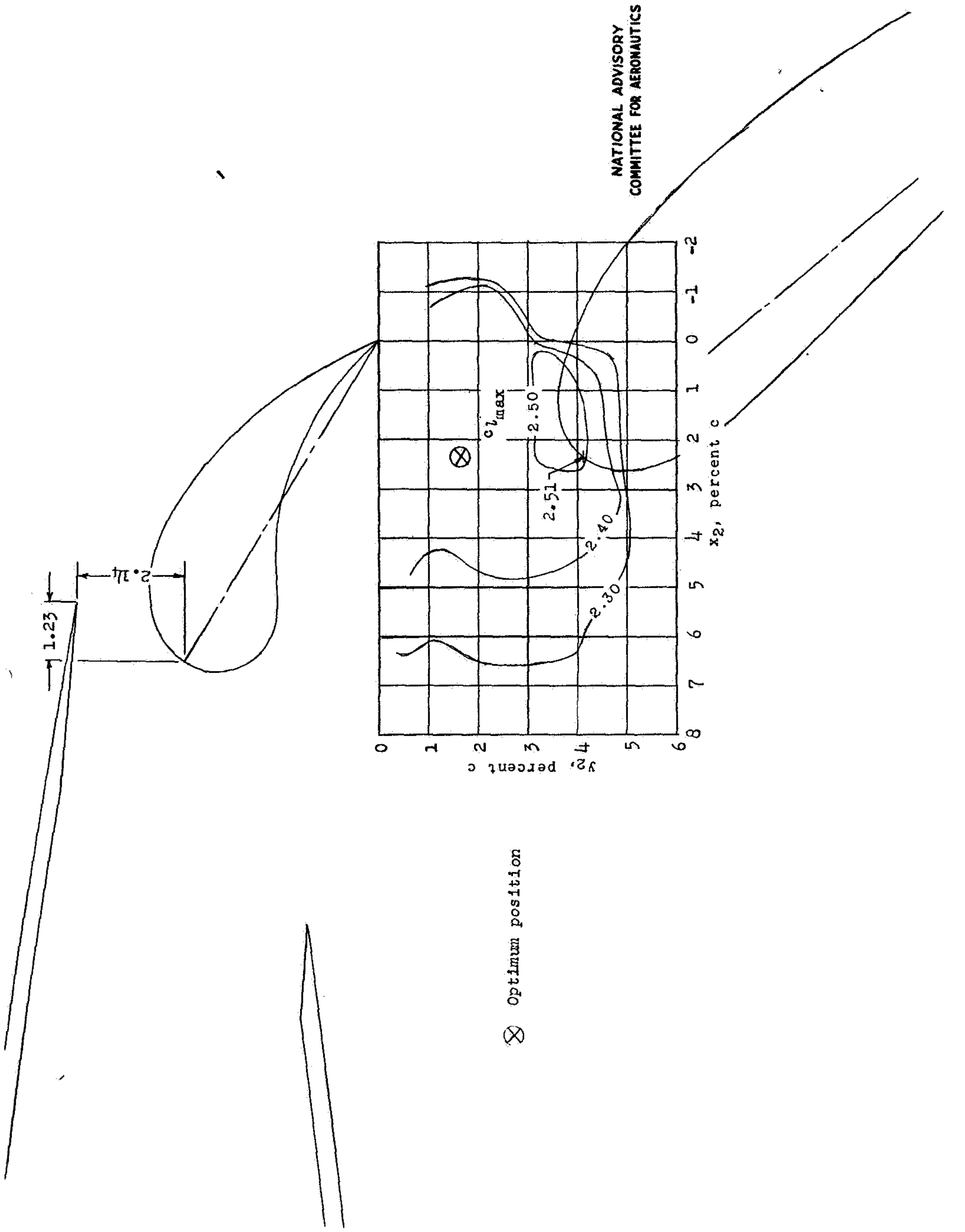

(c) $\delta_f = 50^{\circ}$; $\delta_{ff} = 30^{\circ}$.

Figure 21.- Continued.

NACA 66-210

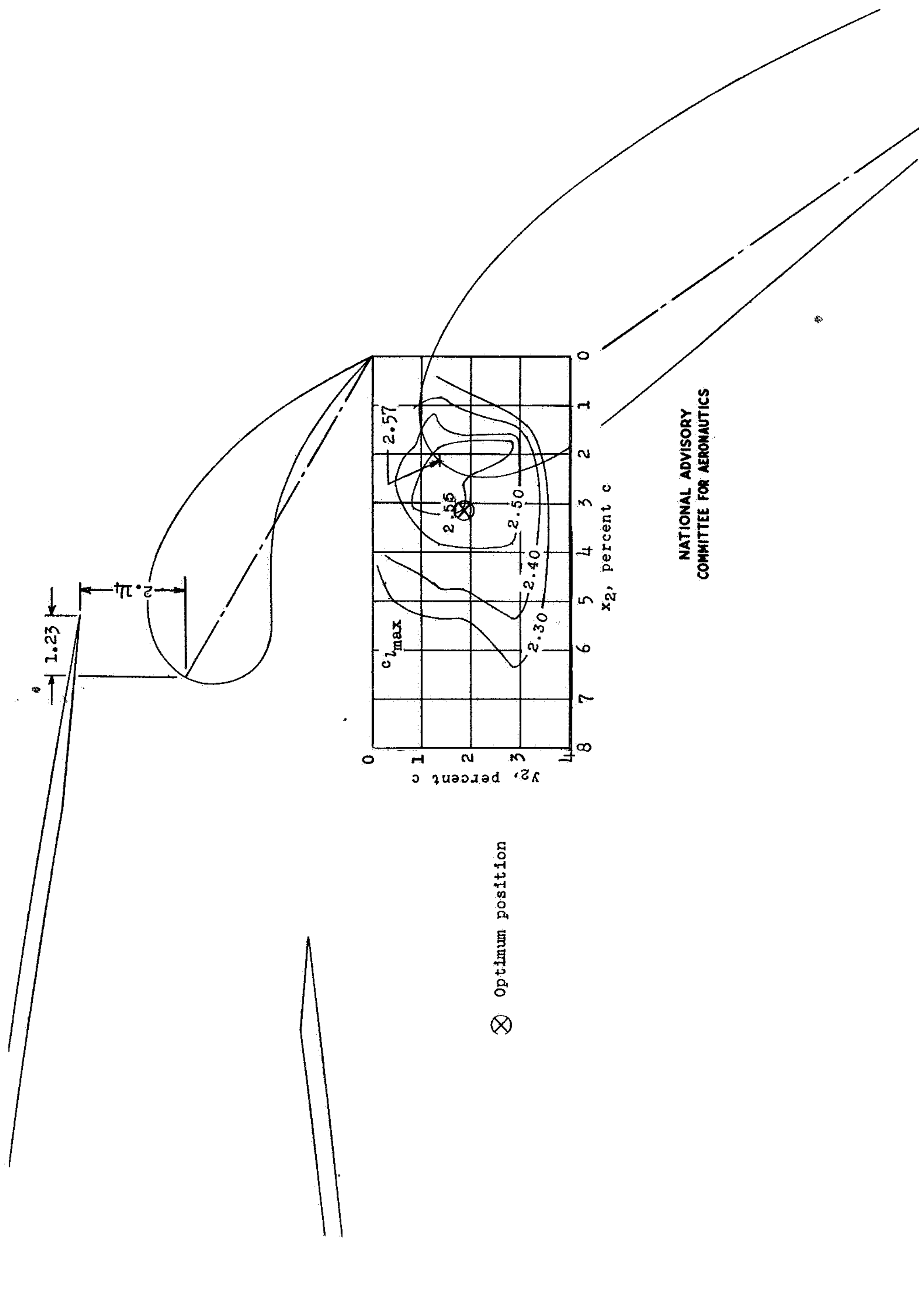

(d) $\delta_f = 55^\circ$; $\delta_{ff} = 30^\circ$

Figure 21.- Concluded.

NACA 66-210

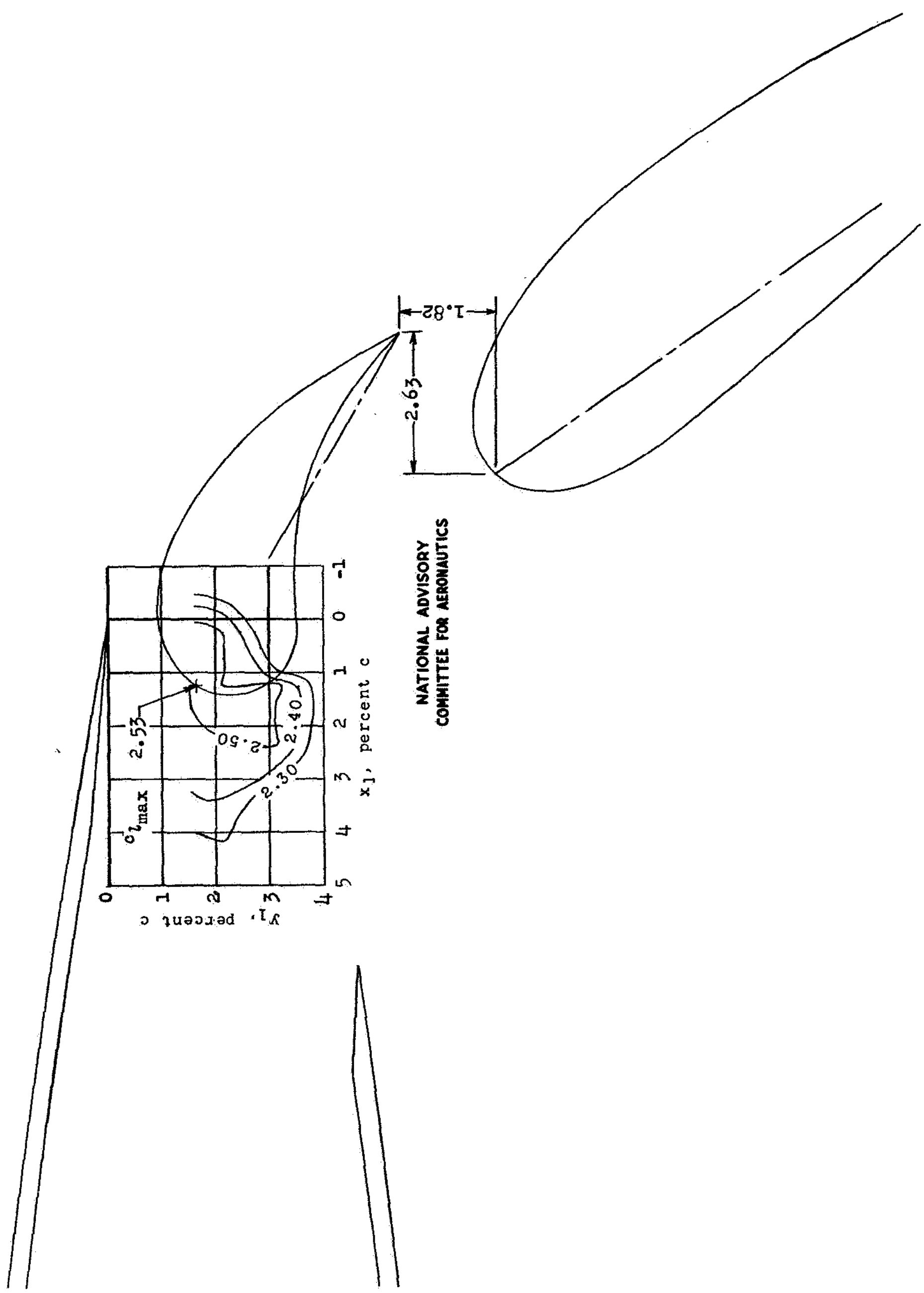

Figure 22.- Contours of flap and fore flap location for maximum lift of the NACA 66-210 airfoil section with a double slotted flap; 0.075c fore flap; 0.250c flap. $\delta_f = 55^\circ$; $\delta_{ff} = 30^\circ$; $R = 2.4 \times 10^6$.

NACA 66-210

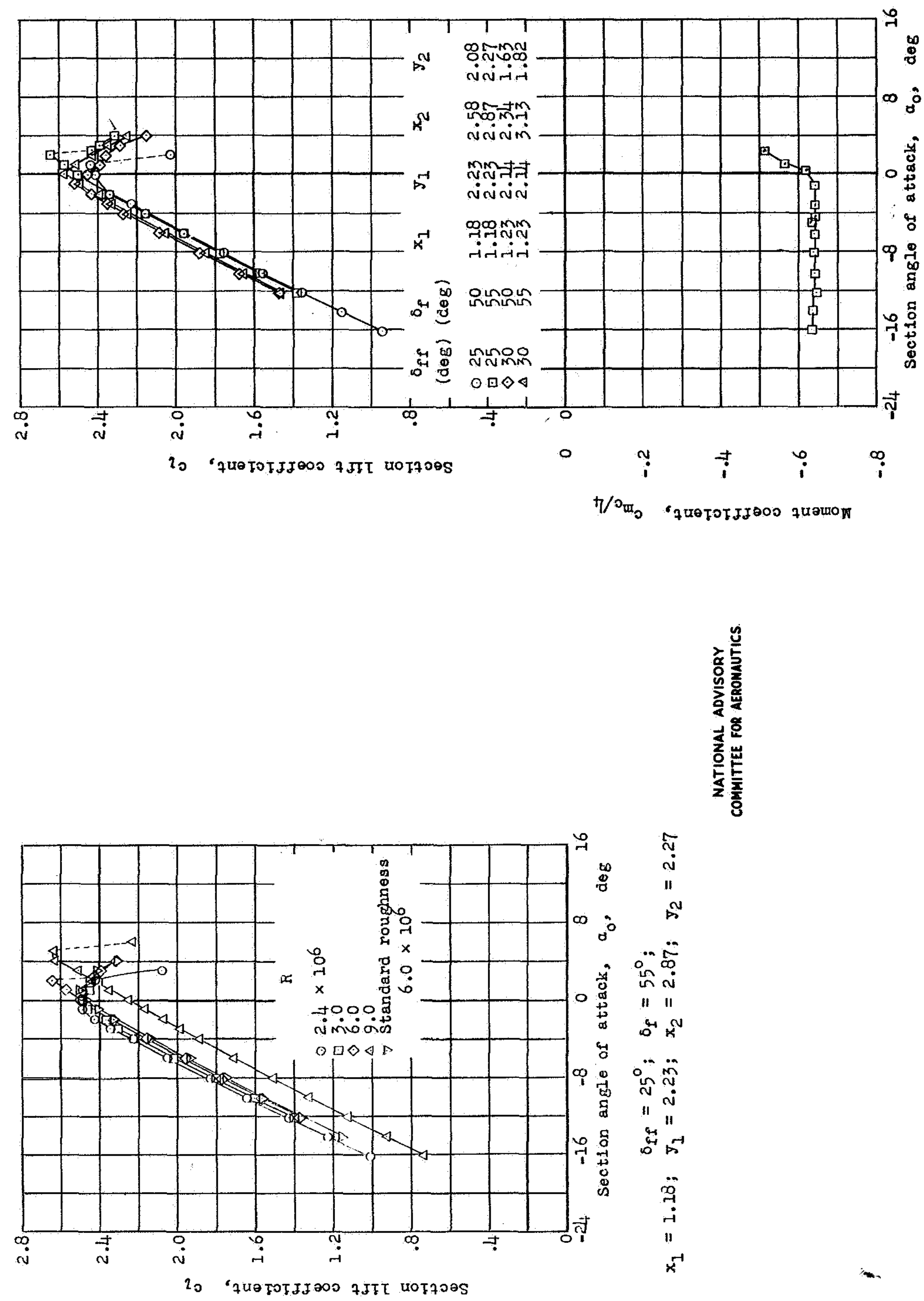

Figure 23.- Section lift and pitching-moment characteristics of the NACA 66-210 airfoil section with a double slotted flap; 0.075c fore flap; 0.250c flap.

NACA 66-210

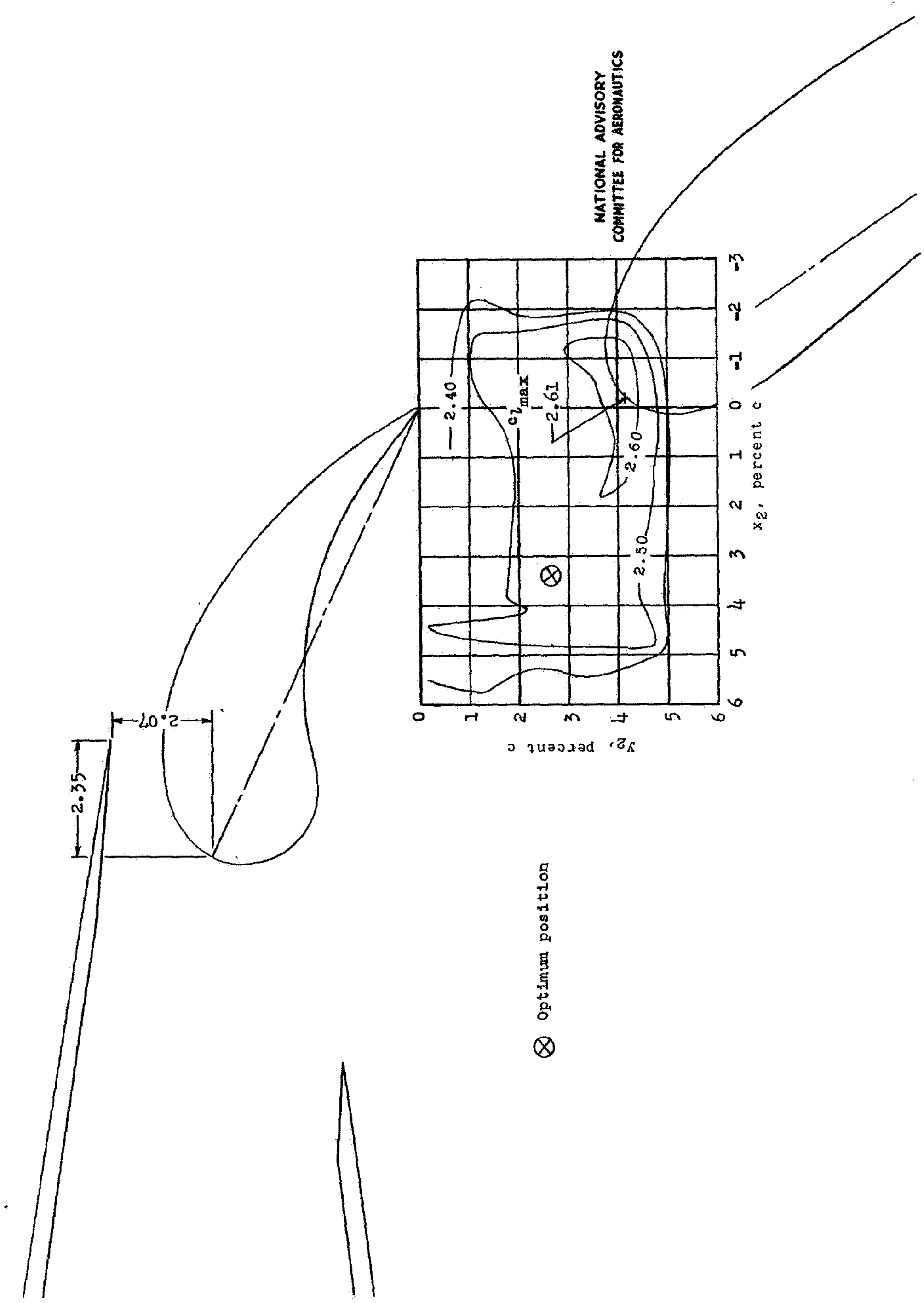

(a) $\delta_f = 55^{\circ}$; $\delta_{ff} = 25^{\circ}$.

Figure 24.- Contours of flap location for maximum lift of the NACA 66-210 airfoil section with a double slotted flap; 0.100c fore flap; 0.250c flap. $R = 2.4 \times 10^6$.

NACA 66-210

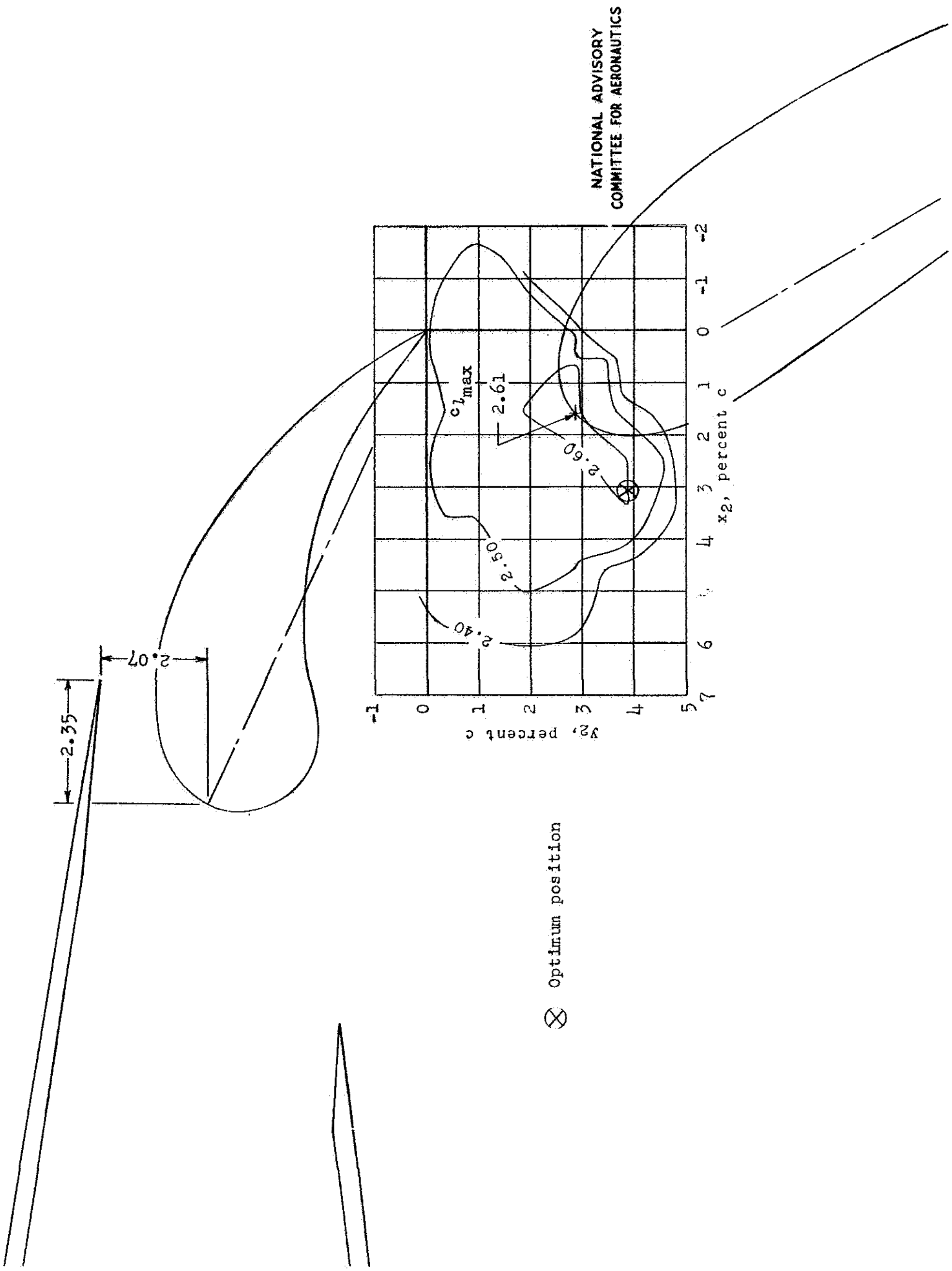

(b) $\delta_f = 60^{\circ}$; $\delta_{ff} = 25^{\circ}$

Figure 24.- Continued.

NACA 66-210

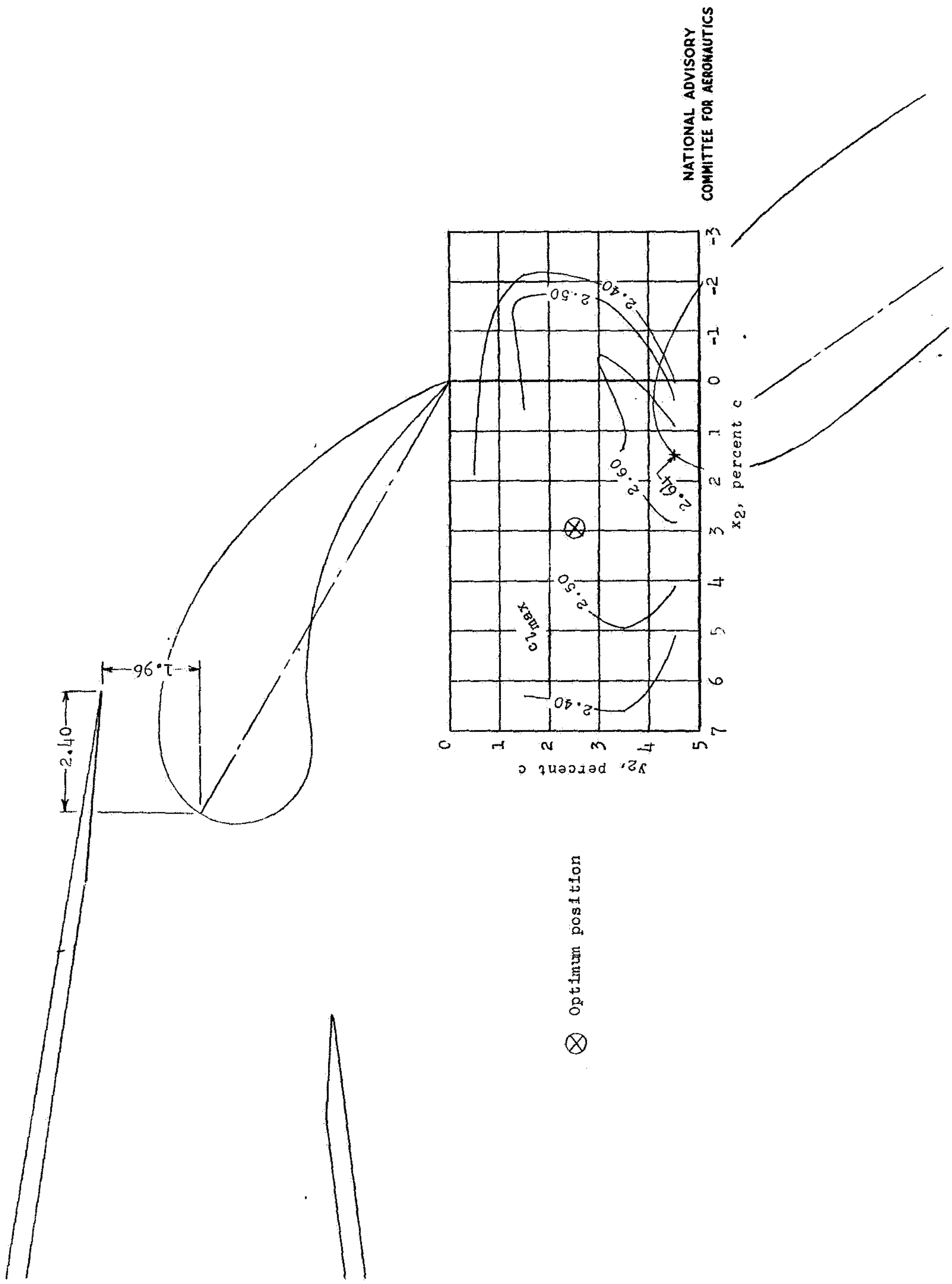

(c) $\delta_f = 55^\circ$; $\delta_{ff} = 30^\circ$.

Figure 24.- Concluded.

NACA 66-210

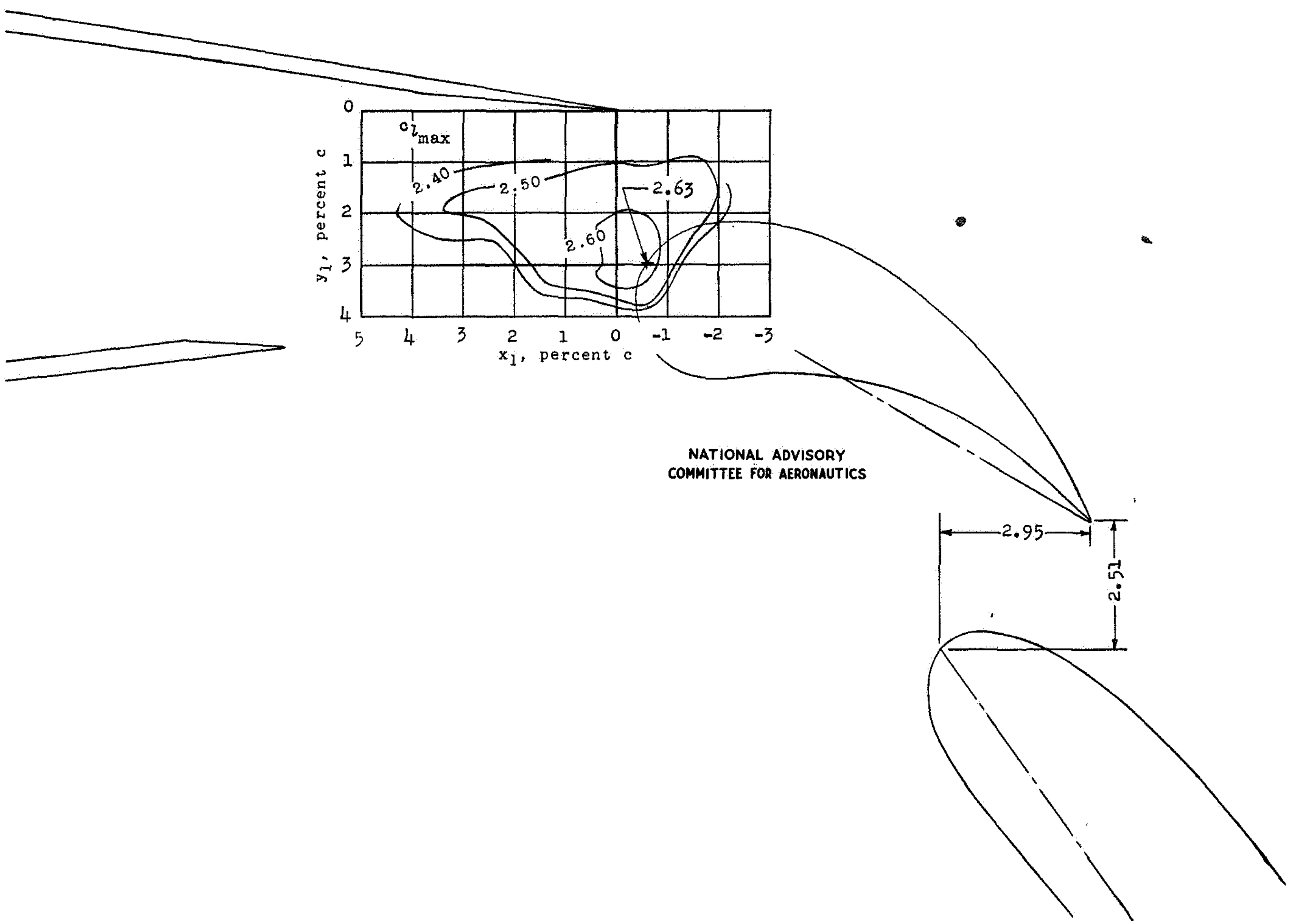

Figure 25.- Contours of flap and fore flap location for maximum lift of the NACA 66-210 airfoil section with a double slotted flap; 0.100c fore flap; 0.250c flap. $\delta_f = 55^{\circ}$; $\delta_{ff} = 30^{\circ}$; $R = 2.4 \times 10^6$.

NACA 66-210

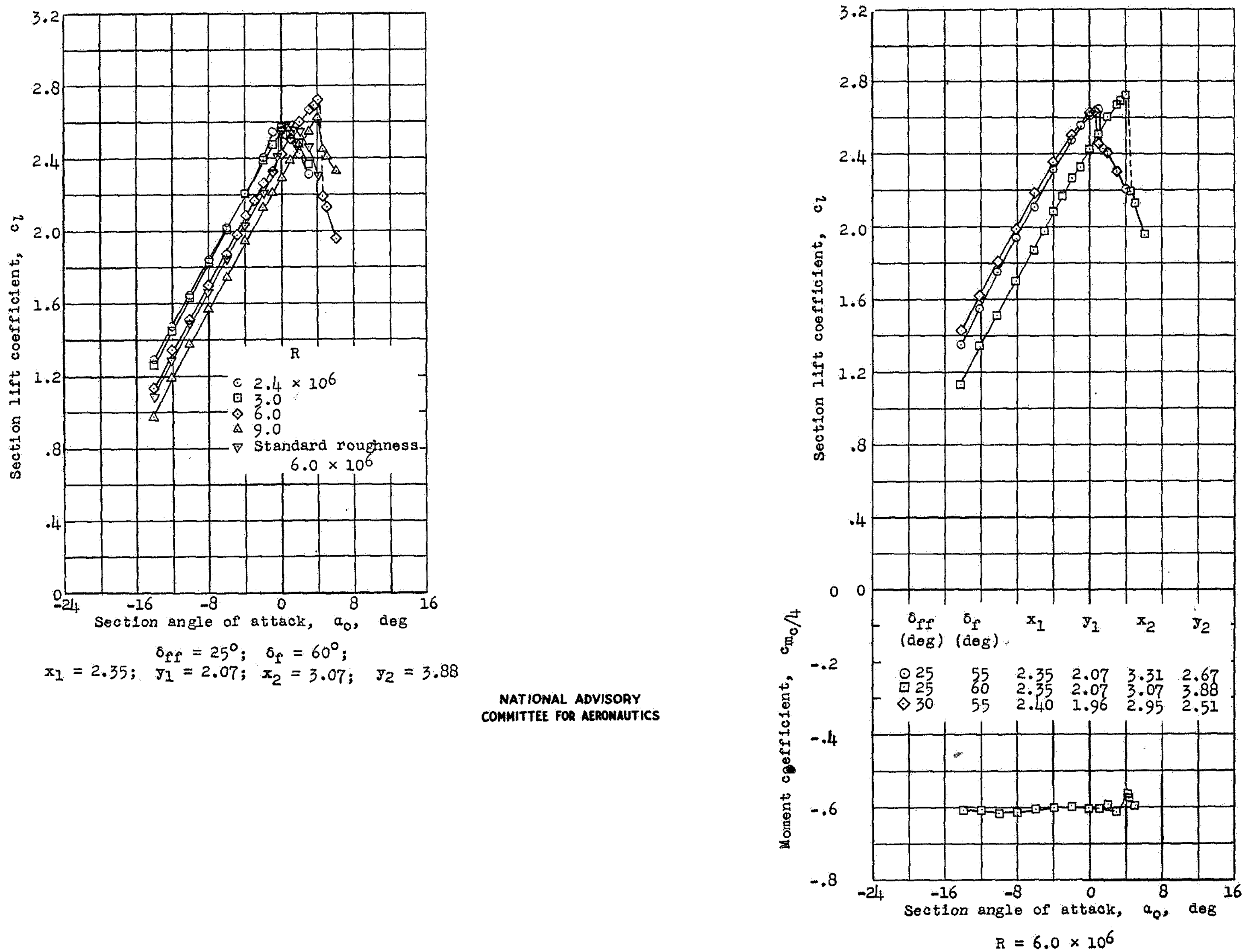

NATIONAL ADVISORY
COMMITTEE FOR AERONAUTICS

Figure 26.- Section lift and pitching-moment characteristics of the NACA 66-210 airfoil section with a double slotted flap; 0.100c fore flap; 0.250c flap.

NACA 1410

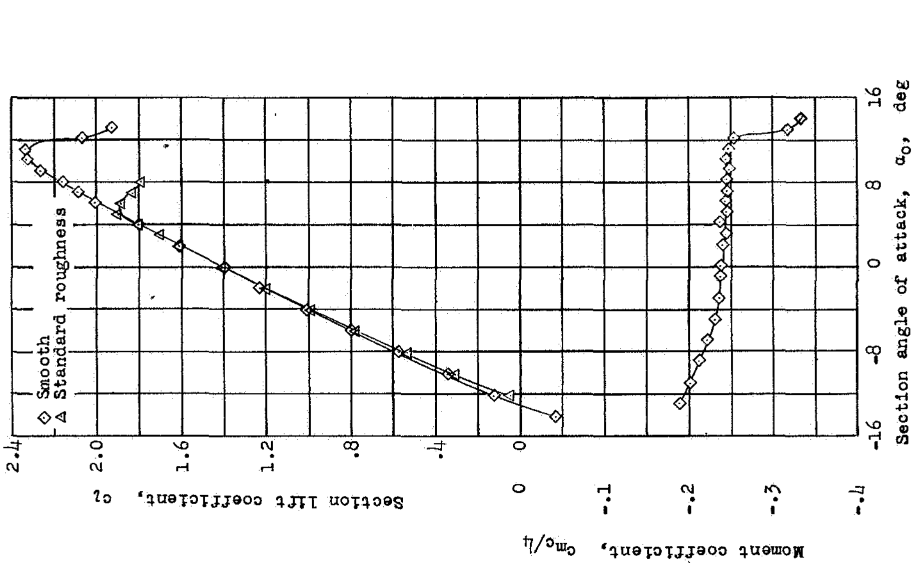

Airfoil with split flap. $\delta_f = 60°$; $R = 6 \times 10^6$

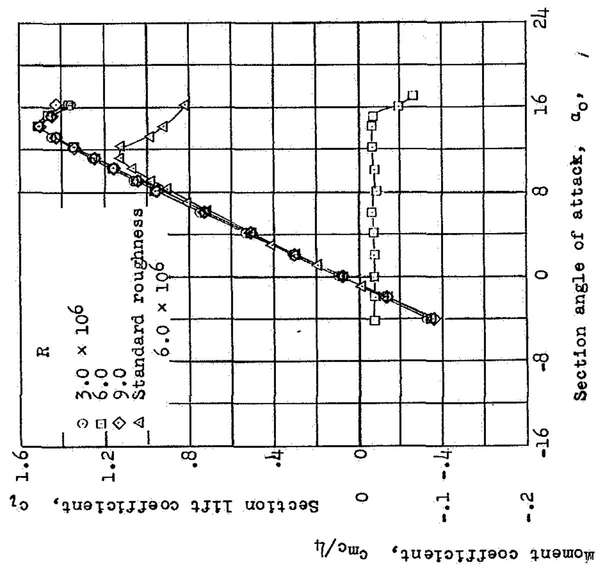

Plain airfoil

Figure 27.- Section lift and pitching-moment characteristics of the NACA 1410 airfoil section with and without a 0.20c split flap.

NACA 1410

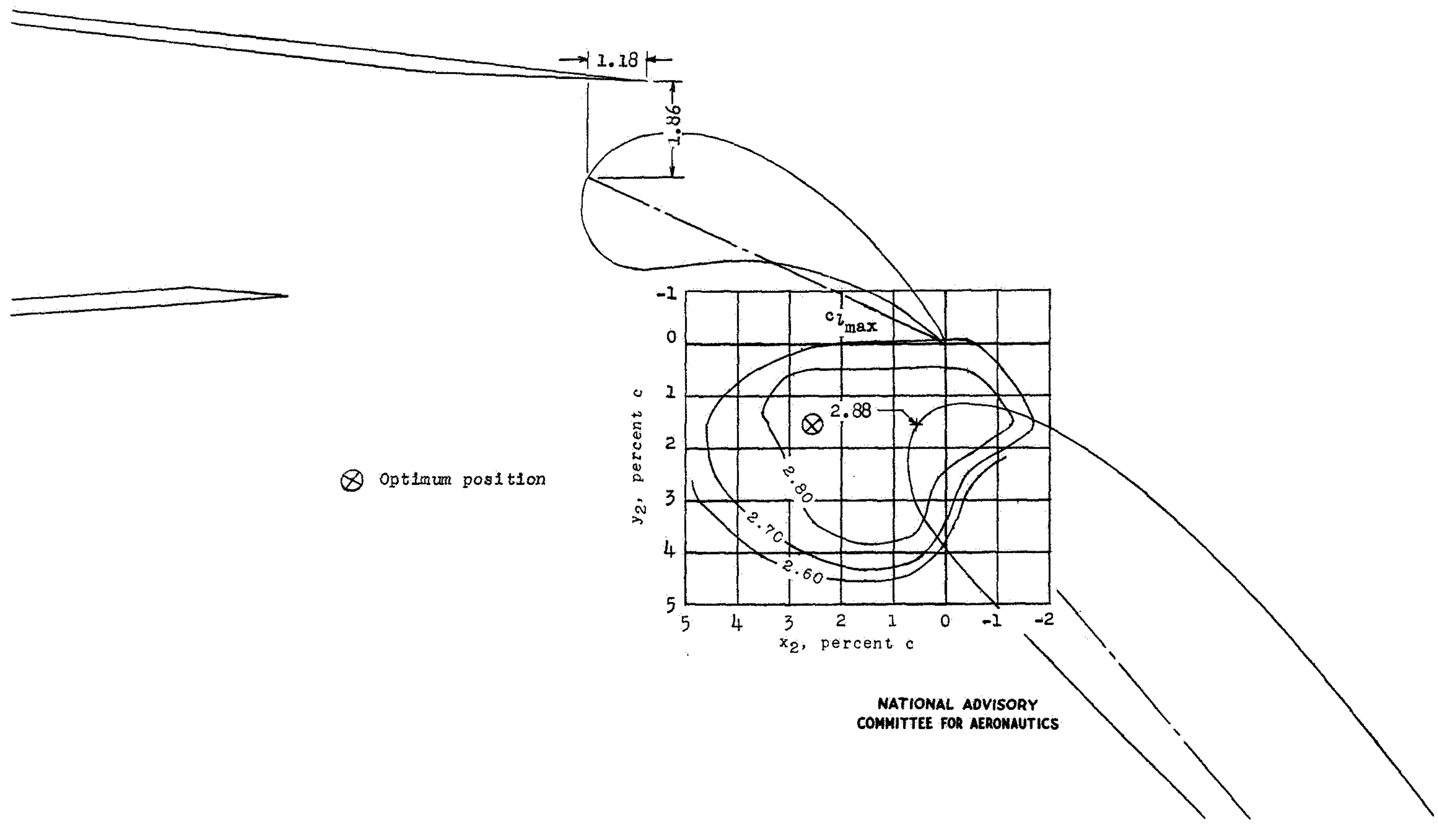

(a) $\delta_f = 50^{\circ}$; $\delta_{ff} = 25^{\circ}$.

Figure 28.- Contours of flap location for maximum lift of the NACA 1410 airfoil section with a double slotted flap; 0.075c fore flap; 0.250c flap. $R = 2.4 \times 10^6$.

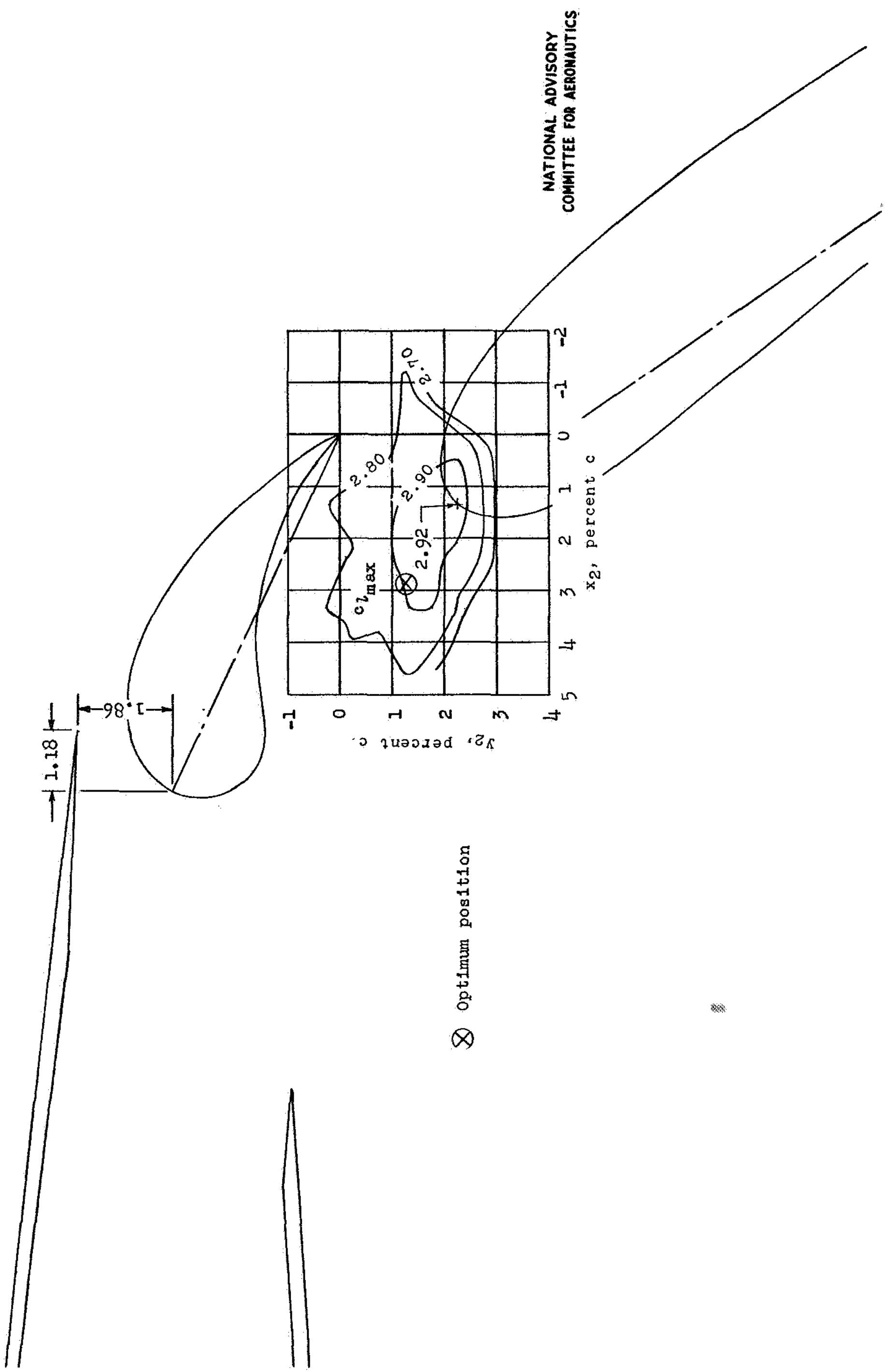

(b) $\delta_f = 55^{\circ}$; $\delta_{ff} = 25^{\circ}$.
Figure 28.- Continued.

NACA 1410

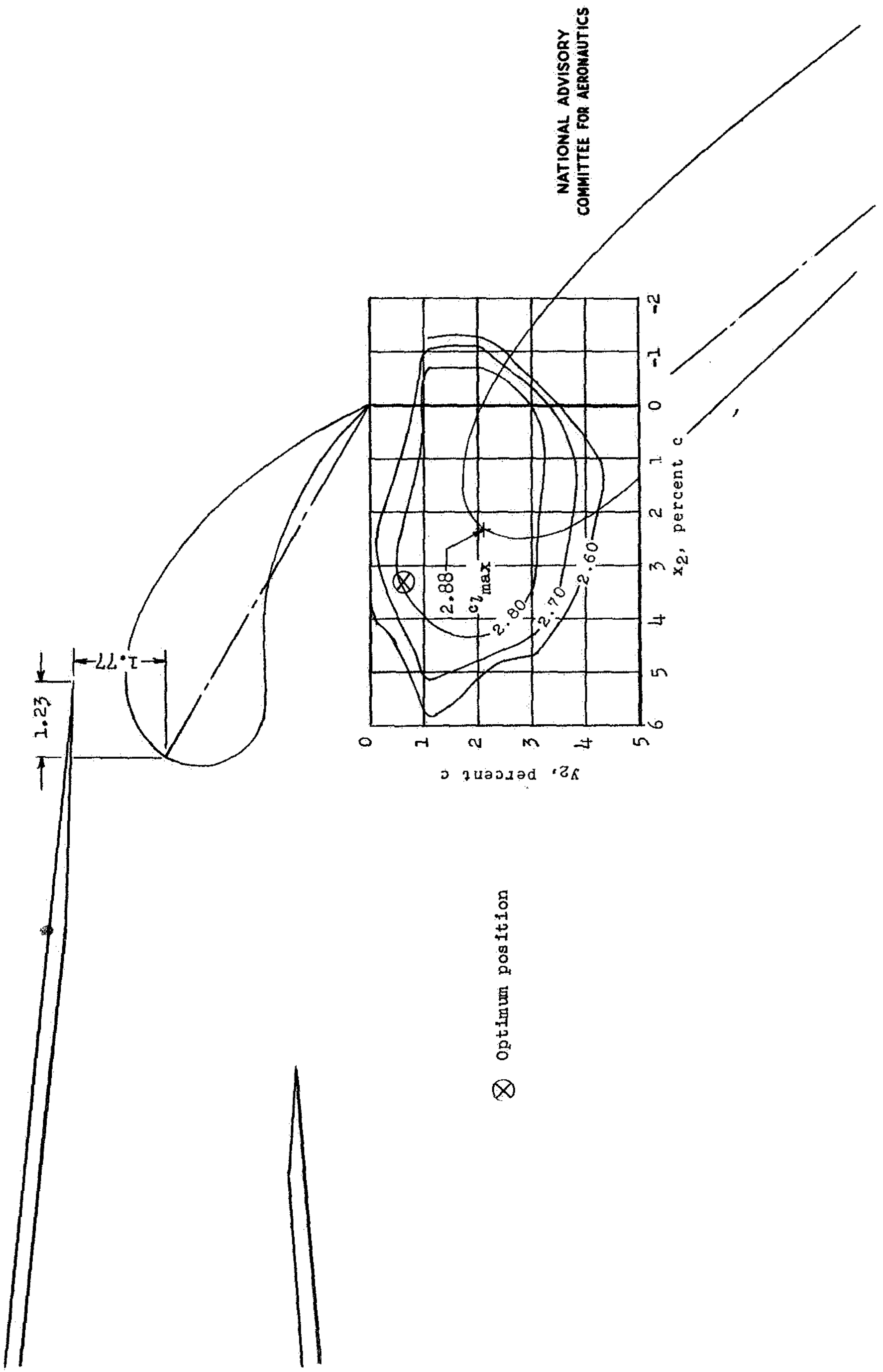

(c) $\delta_f = 50°$; $\delta_{ff} = 30°$.

Figure 28.- Concluded.

NACA 1410

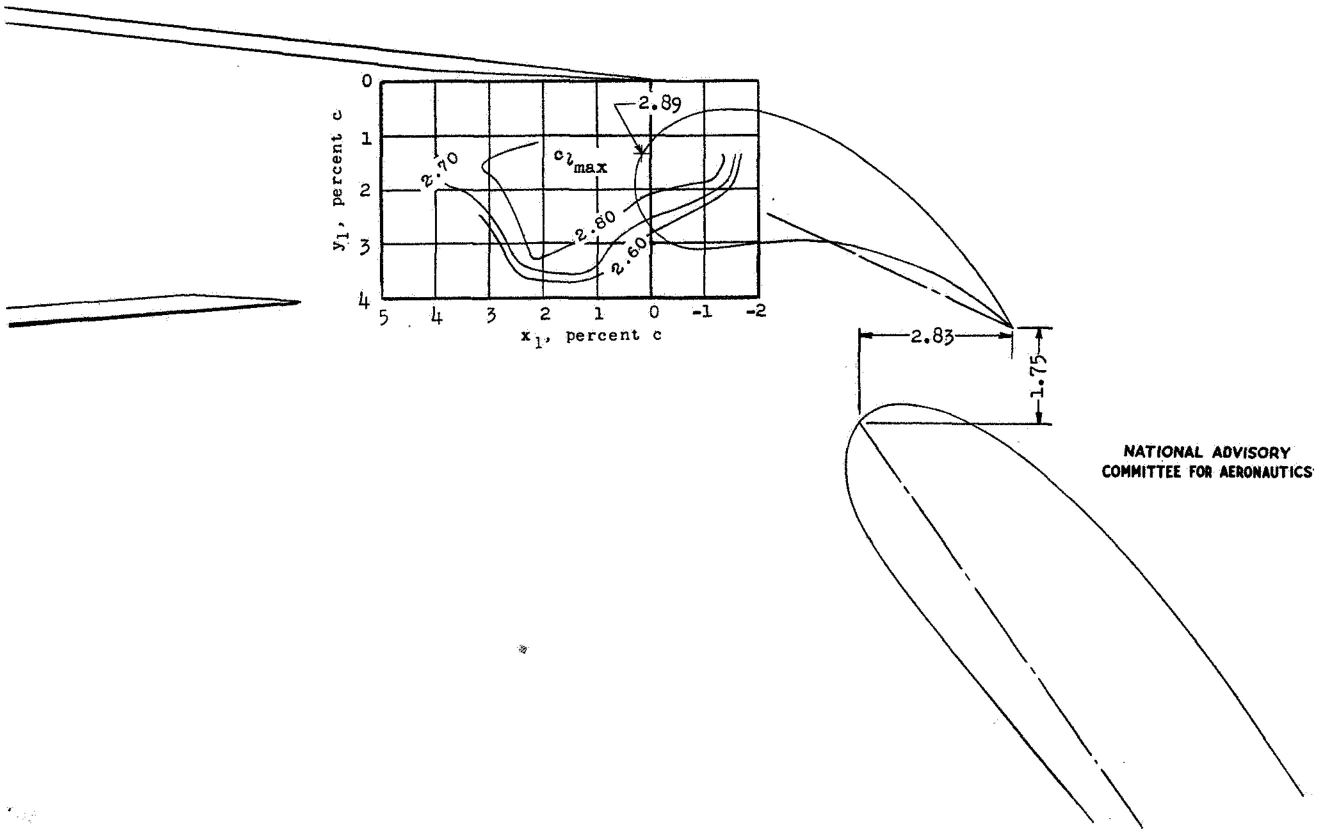

Figure 29.- Contours of flap and fore flap location for maximum lift of the NACA 1410 airfoil section with a double slotted flap; 0.075c fore flap; 0.250c flap. $\delta_f = 55^\circ$; $\delta_{ff} = 25^\circ$; $R = 2.4 \times 10^6$.

NACA 1410

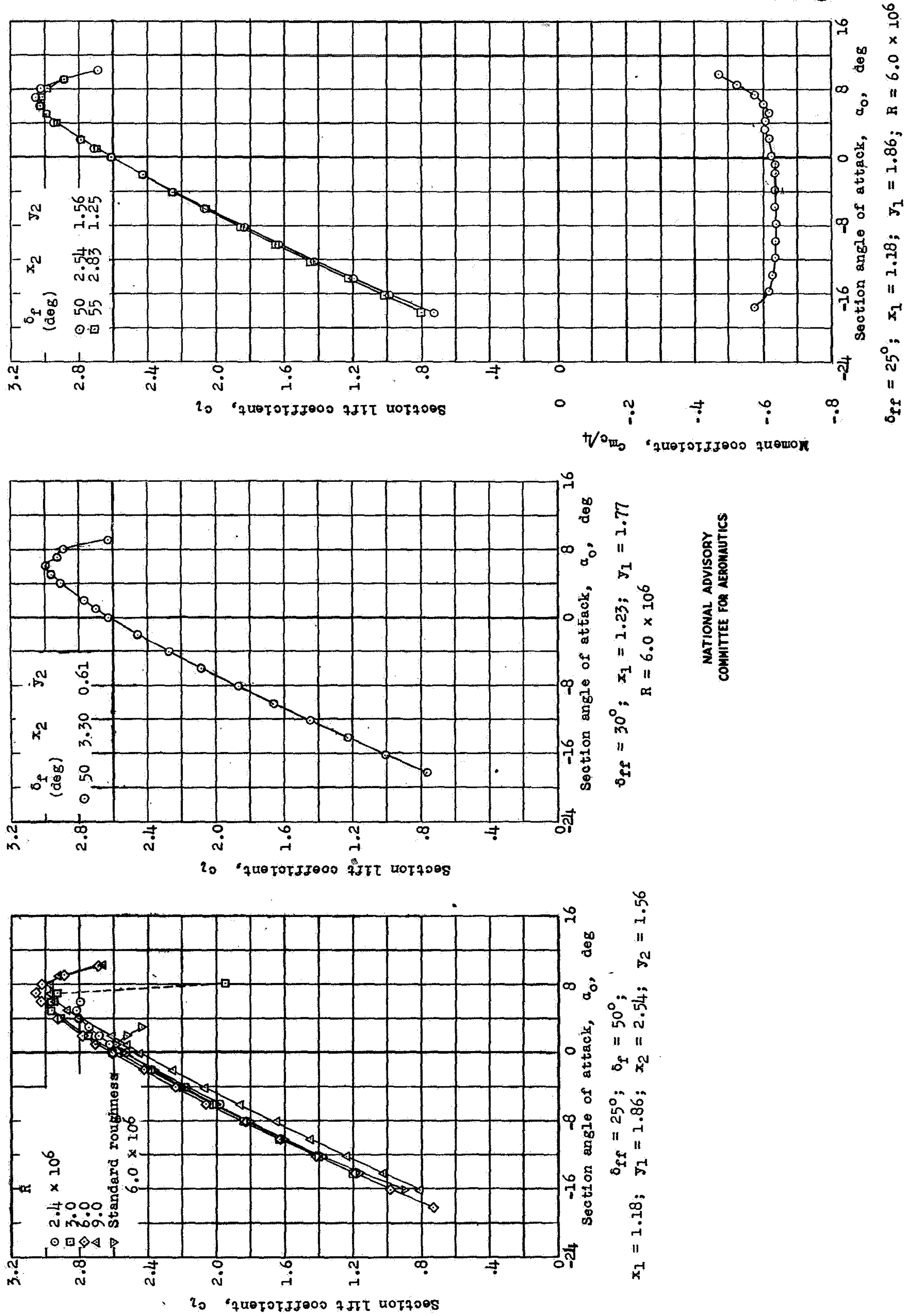

Figure 30.- Section lift and pitching-moment characteristics of the NACA 1410 airfoil section with a double slotted flap; 0.075c fore flap; 0.250c flap.

NACA 64_1-212

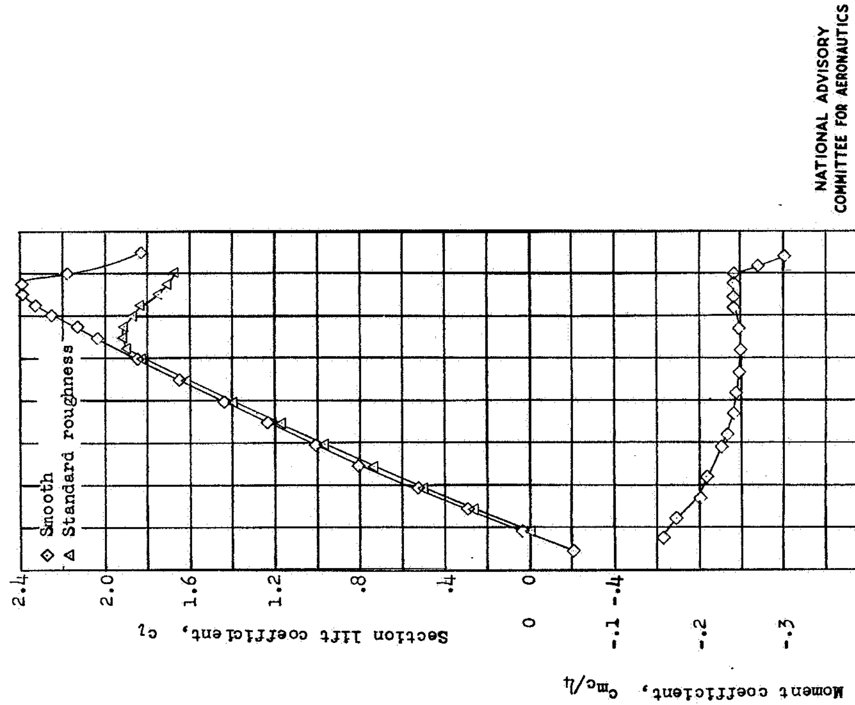

Airfoil with split flap. $\delta_f = 60^\circ$; $R = 6.0 \times 10^6$

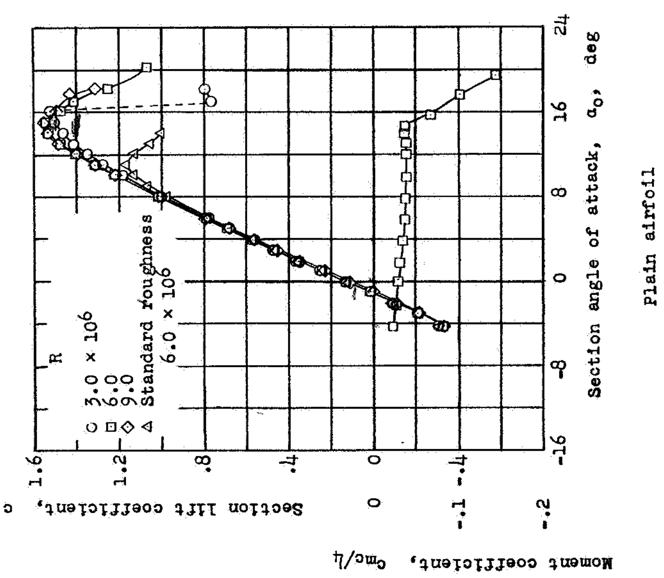

Plain airfoil

Figure 31.- Section lift and pitching-moment characteristics of the NACA 64_1-212 airfoil section with and without a 0.20c split flap.

NACA 64_1-212

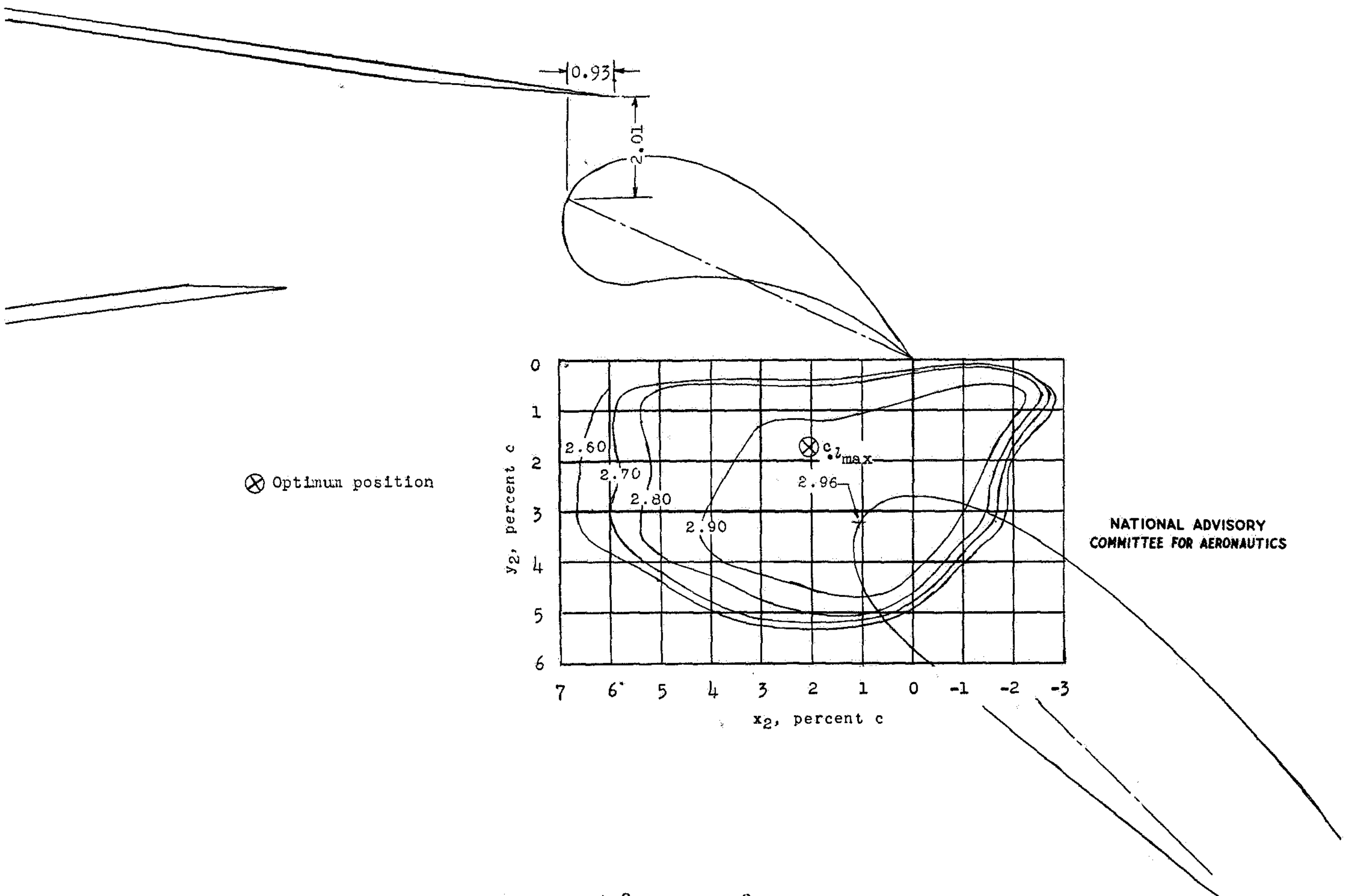

(a) $\delta_f = 45^\circ$; $\delta_{ff} = 25^\circ$.

Figure 32.- Contours of flap location for maximum lift of the NACA 64_1-212 airfoil section with a double slotted flap; 0.075c fore flap; 0.250c flap. $R = 2.4 \times 10^6$.

NACA 64_1-212

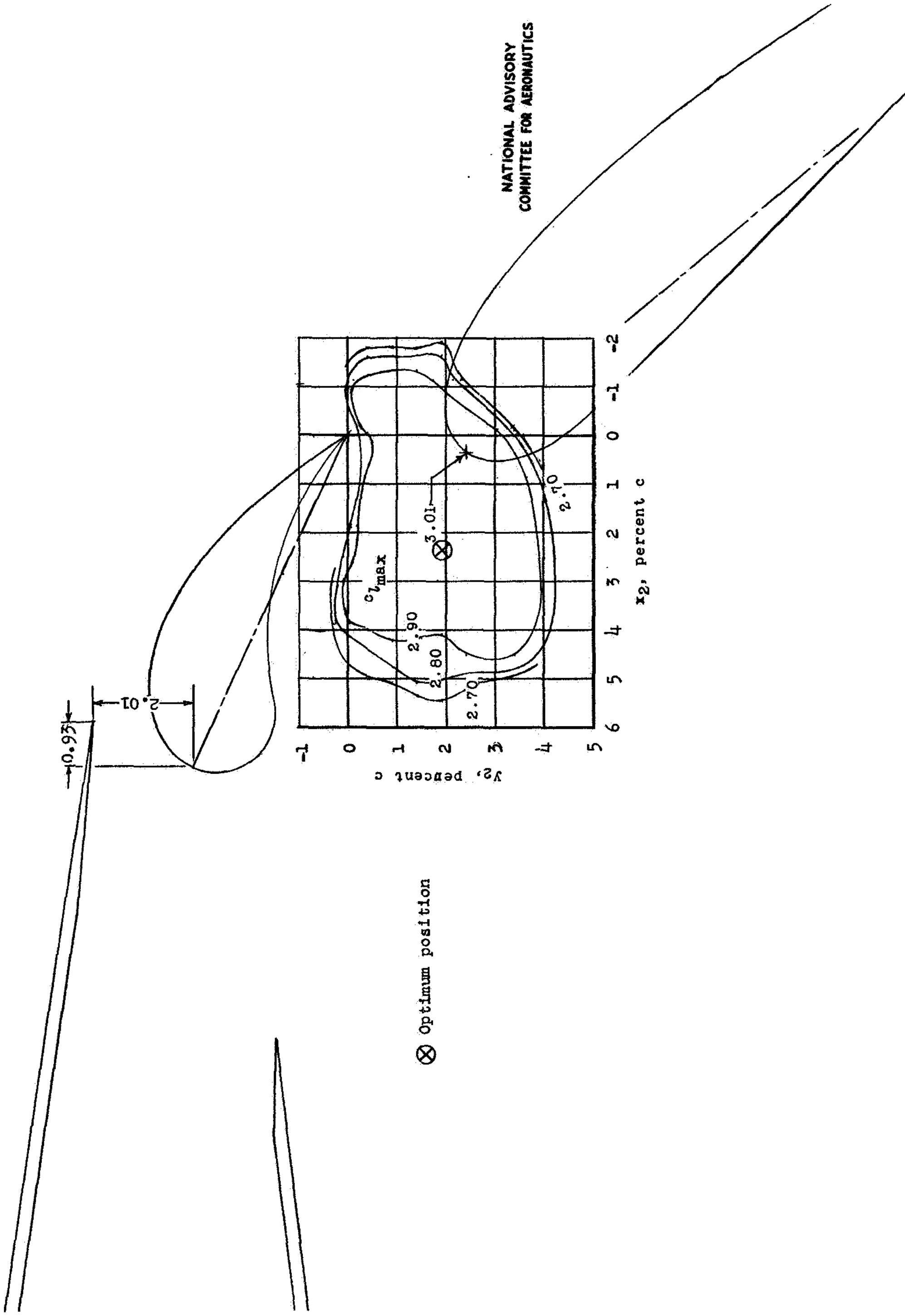

(b) $\delta_f = 50^{\circ}$; $\delta_{ff} = 25^{\circ}$.

Figure 32.- Continued.

NACA 64_1-212

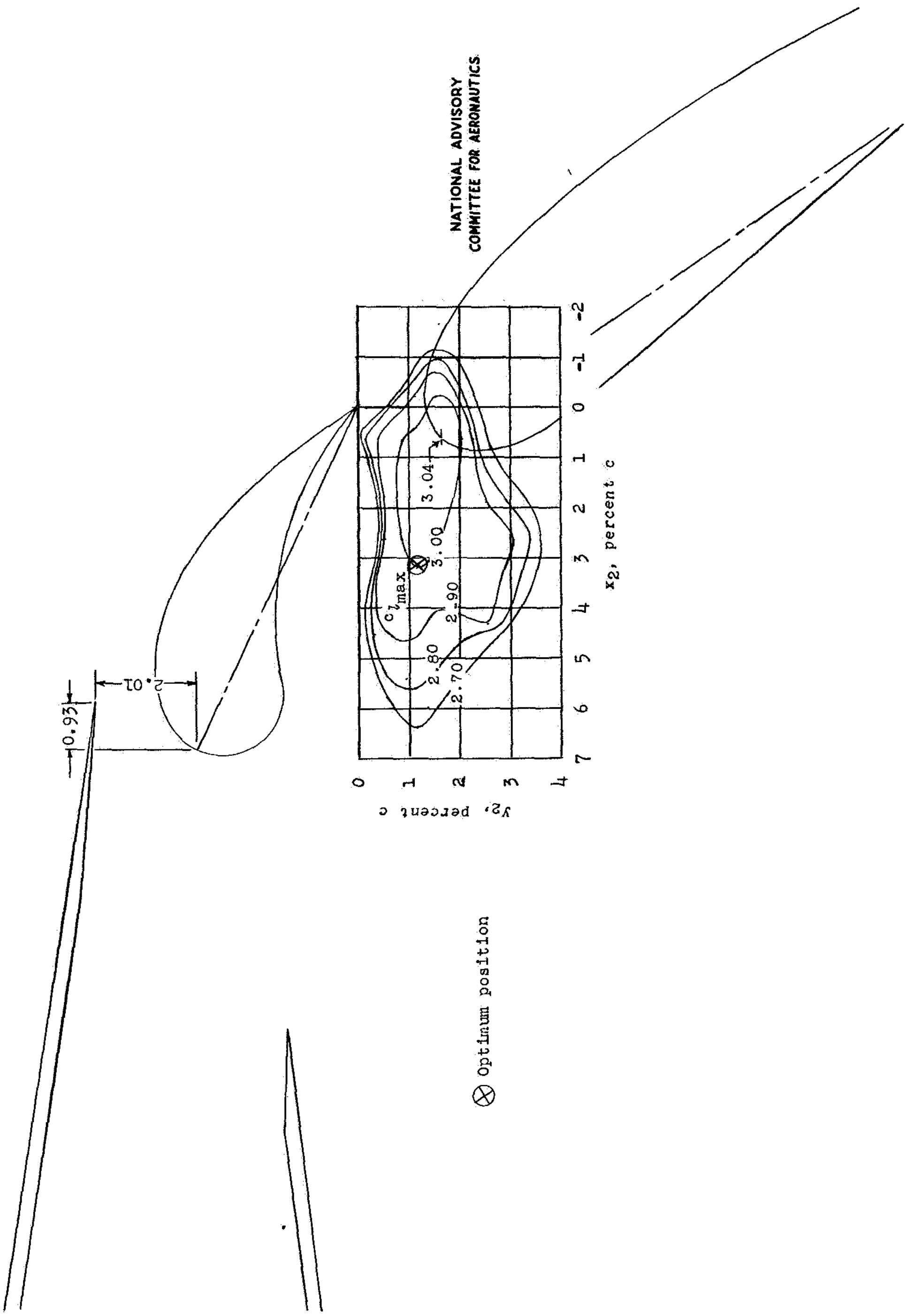

(c) $\delta_f = 55^\circ$; $\delta_{ff} = 25^\circ$.

Figure 32.- Continued.

NACA 64_1-212

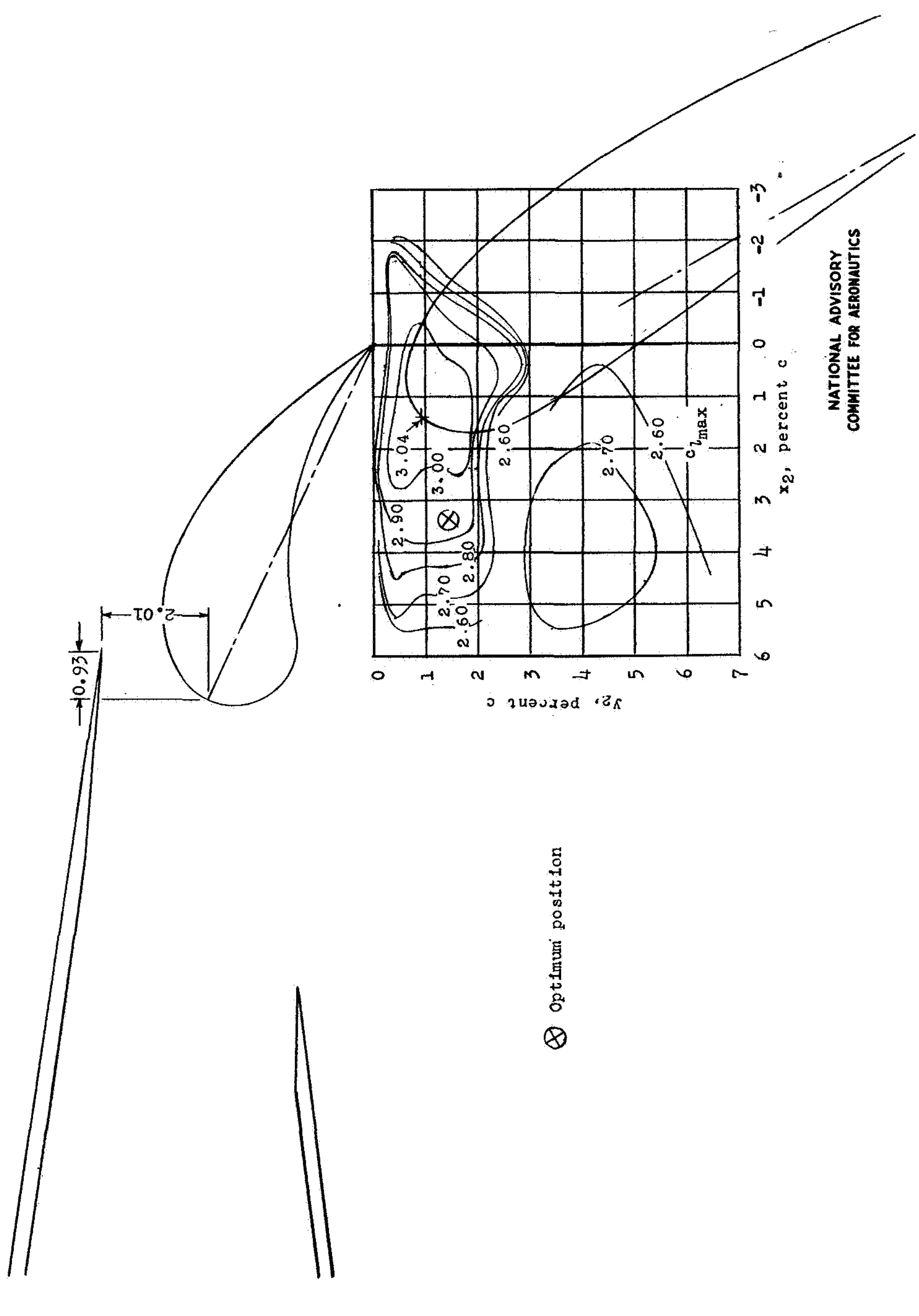

(d) $\delta_f = 60^{\circ}$; $\delta_{ff} = 25^{\circ}$

Figure 32.- Continued.

NACA 64_1-212

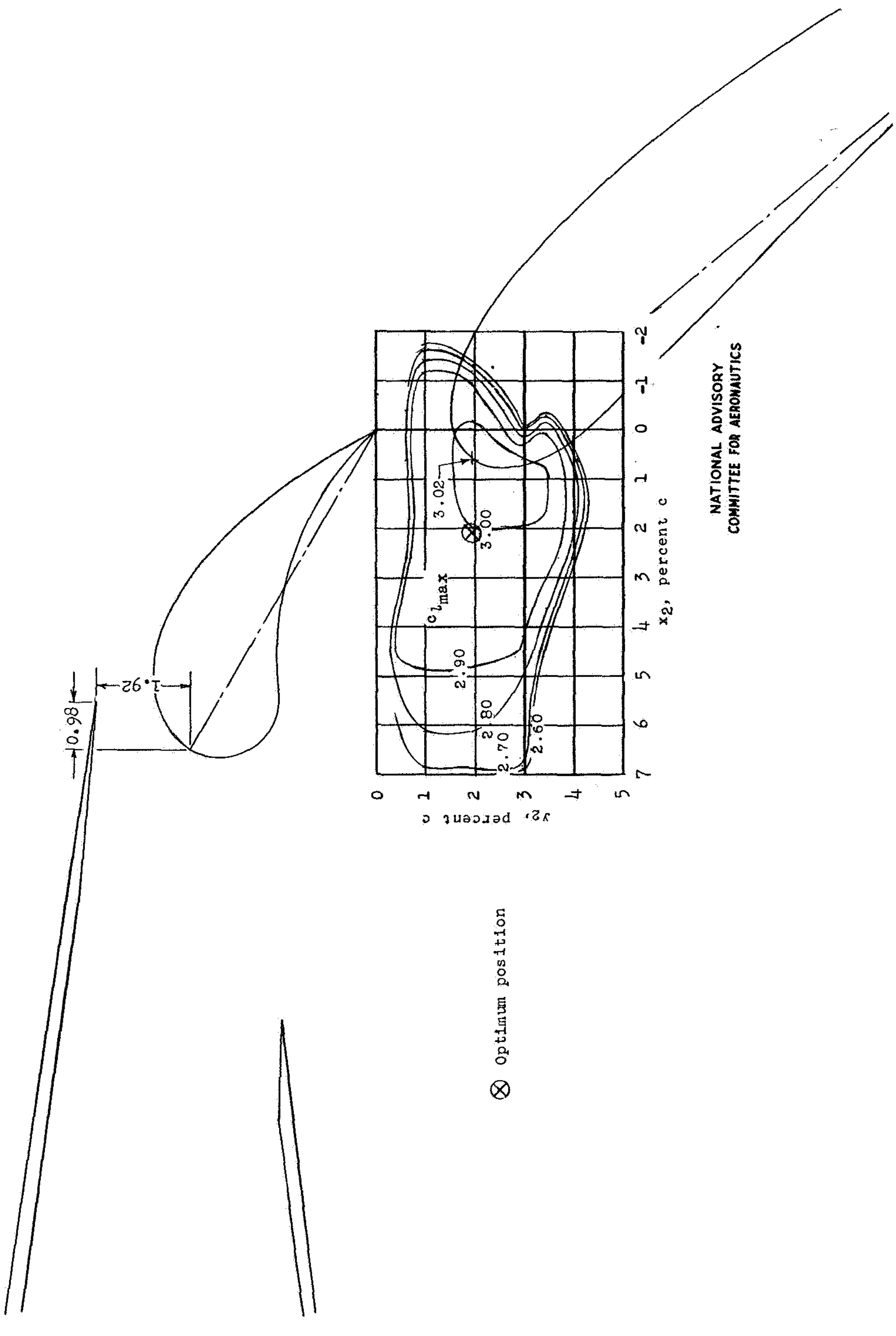

(e) $\delta_f = 50^\circ$; $\delta_{ff} = 30^\circ$

Figure 32.- Continued.

NACA 64_1-212

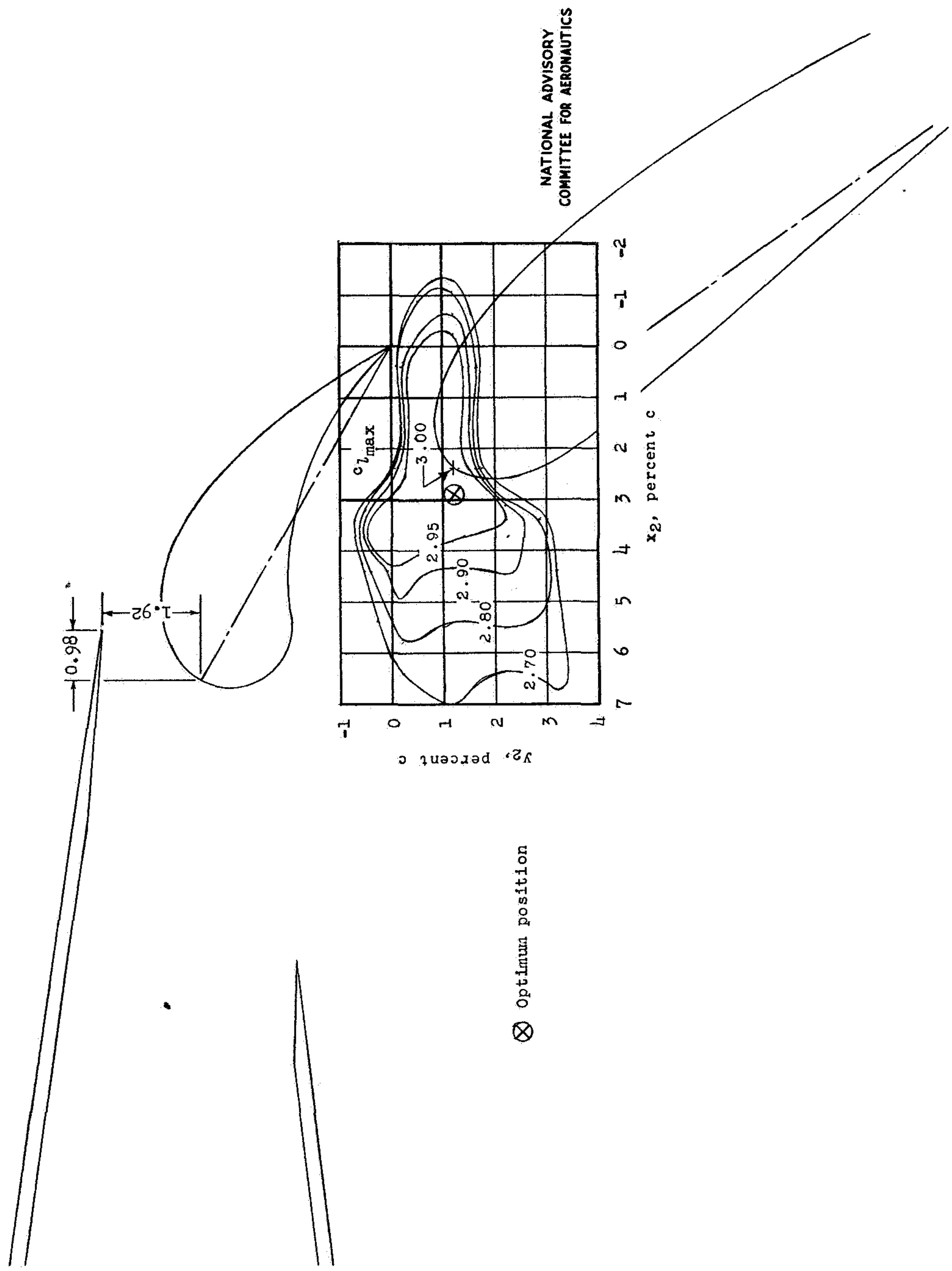

(f) $\delta_f = 55^{\circ}$; $\delta_{ff} = 30^{\circ}$
Figure 32.- Continued.

NACA 64_1-212

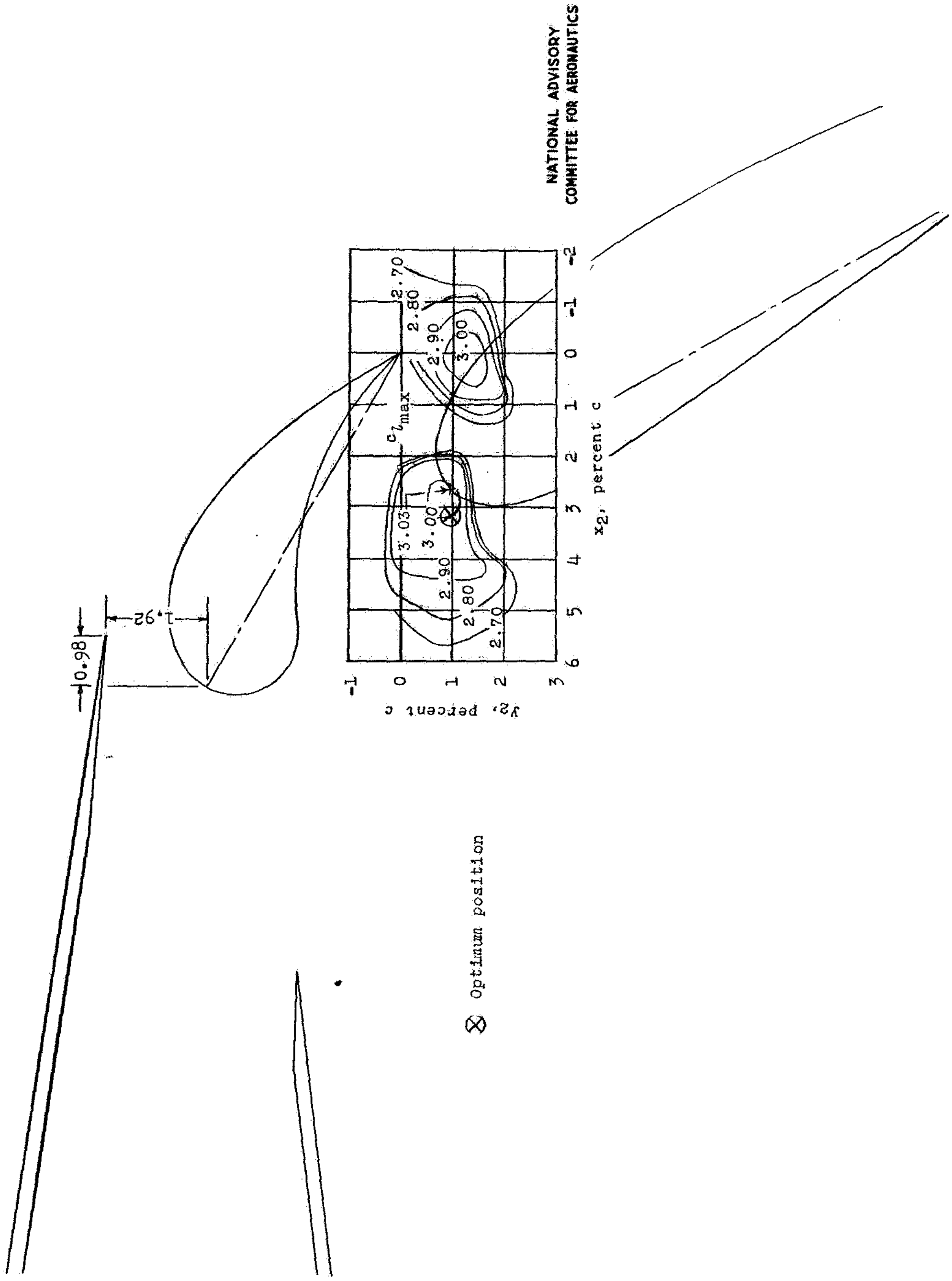

(g) $\delta_f = 60^\circ$; $\delta_{ff} = 30^\circ$.
Figure 32.- Concluded.

NACA 64_1-212

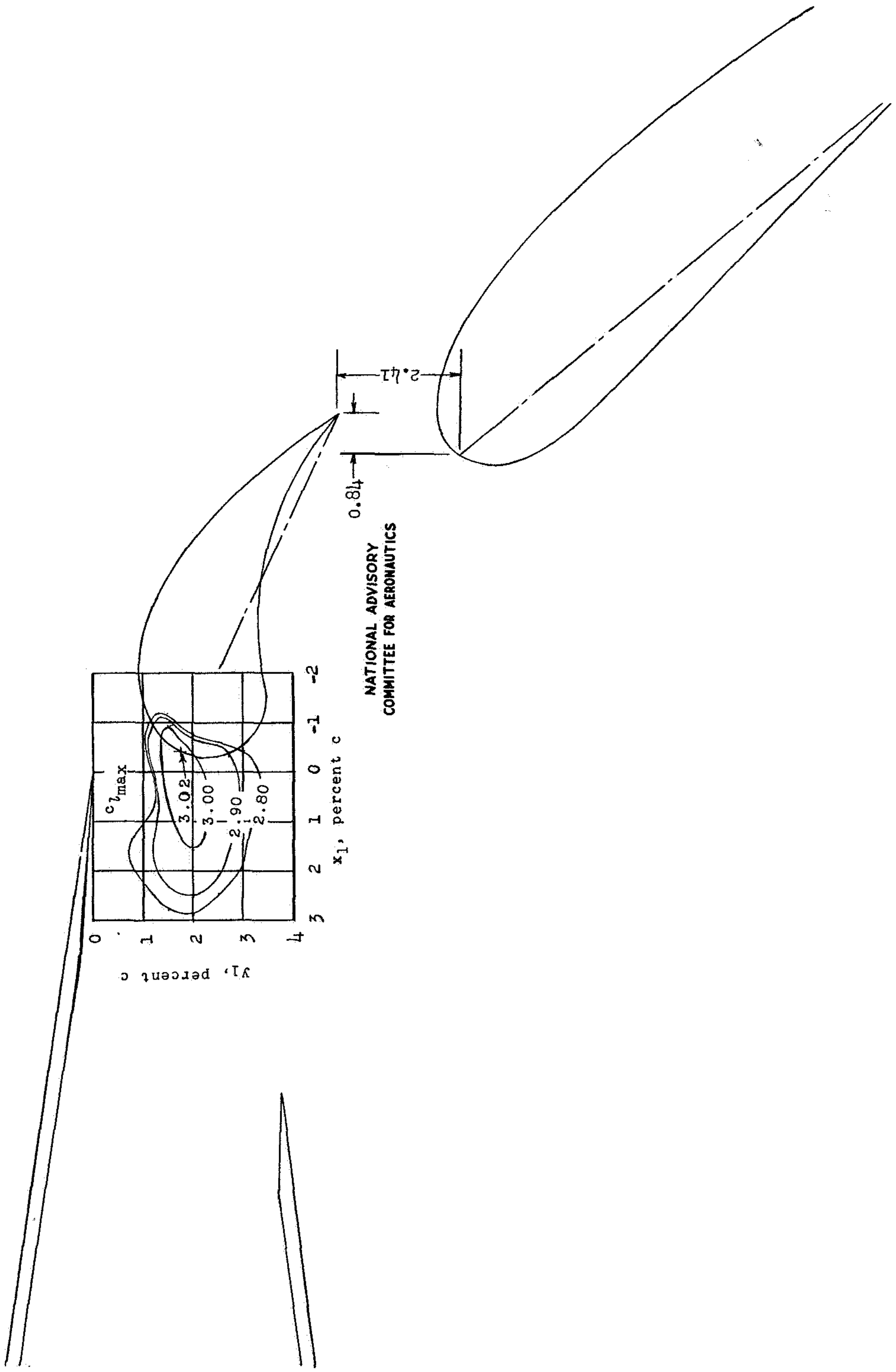

Figure 33.- Contours of flap and fore flap location for maximum lift of the NACA 64_1-212 airfoil section with a double slotted flap; 0.075c fore flap; 0.250c flap. $\delta_f = 50^\circ$; $\delta_{ff} = 25^\circ$; $R = 2.4 \times 10^6$.

NACA 64_1-212

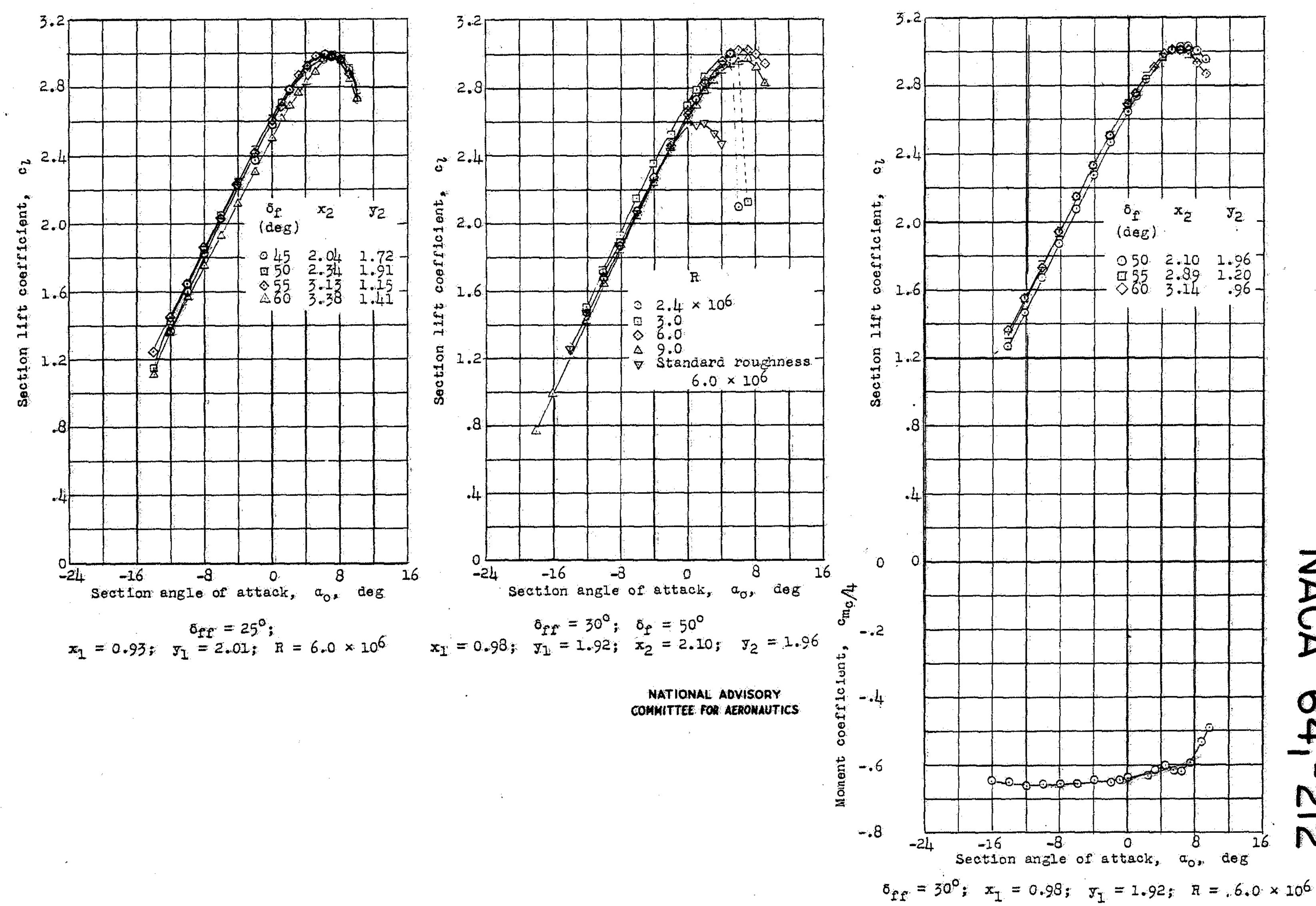

Figure 34.- Section lift and pitching-moment characteristics of the NACA 64_1-212 airfoil section with a double slotted flap; 0.075c fore flap; 0.250c flap.

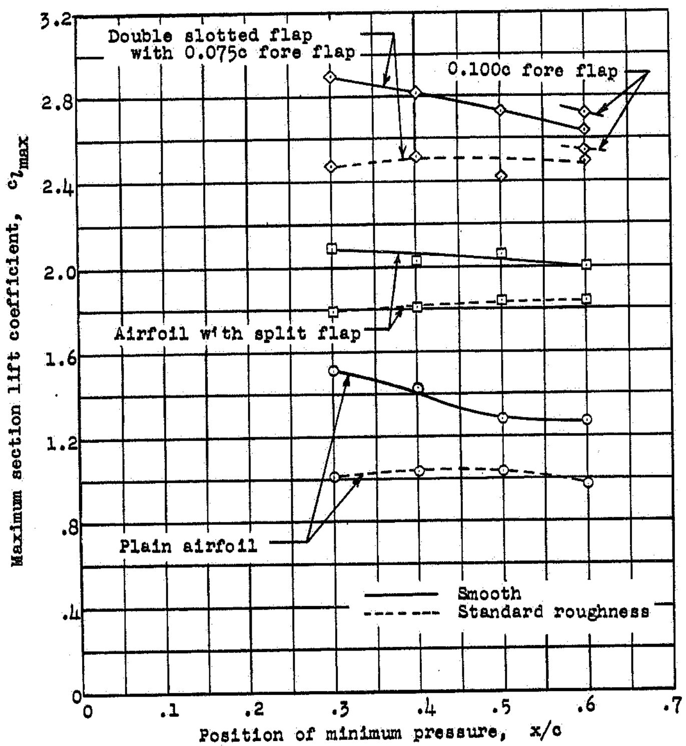

Variation of $c_{l_{max}}$ with position of minimum pressure; $t/c = 0.10$

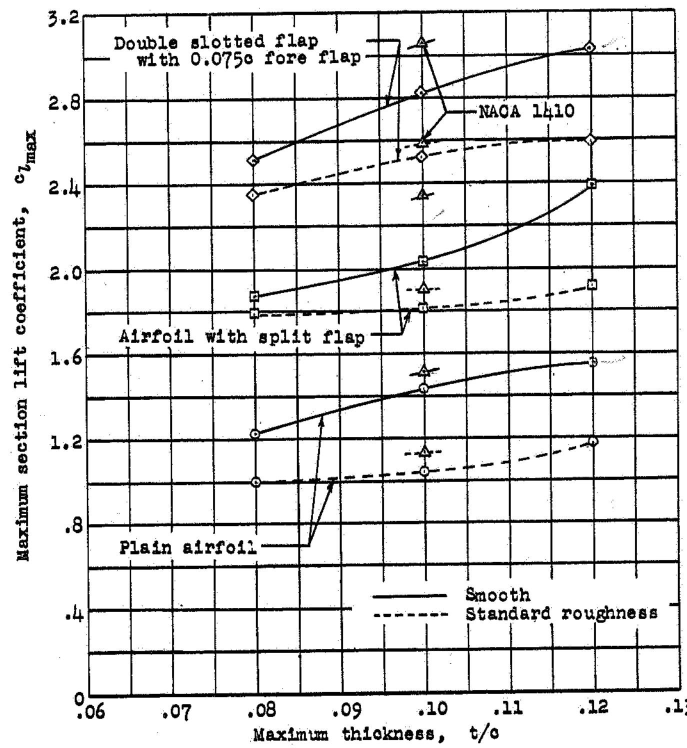

Variation of $c_{l_{max}}$ with t/c; minimum pressure at $x/c = 0.40$

NATIONAL ADVISORY
COMMITTEE FOR AERONAUTICS

Figure 35.- Variation of maximum section lift coefficient with position of minimum pressure and maximum thickness for some NACA 6-series airfoil sections cambered for ideal lift coefficients of 0.2. $R = 6.0 \times 10^6$.

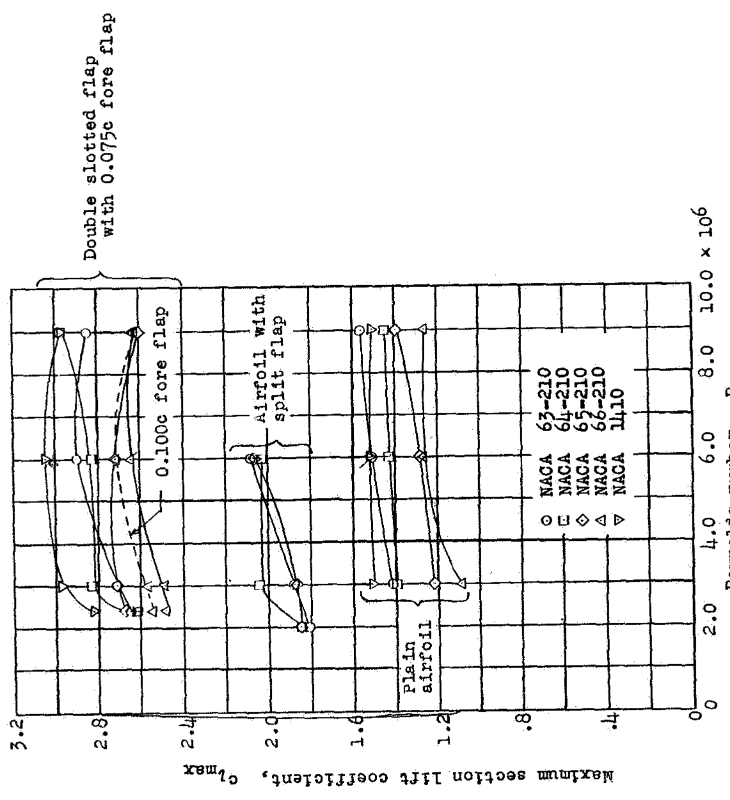

Figure 36.- Effect of Reynolds number on the maximum section lift coefficient of some NACA airfoil sections.

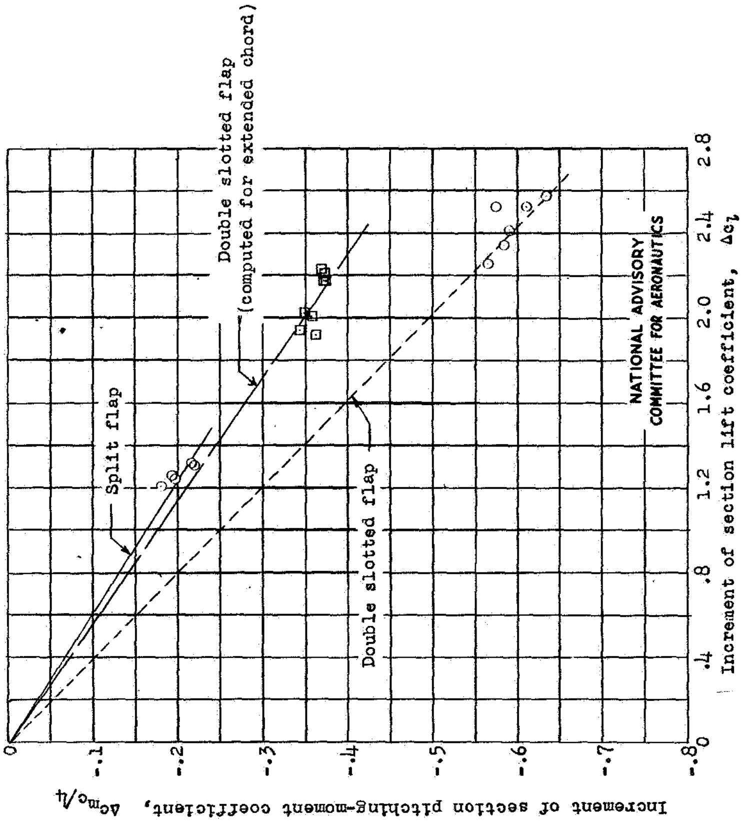

Figure 37.- Variation of increment of section lift coefficient with increment of section pitching-moment coefficient caused by addition of flaps on some thin NACA 6-series airfoil sections. $\alpha_o = 0°$